Soil-Structure Interaction For Nonslender, Large-Diameter Offshore Monopiles

Sørensen, Søren Peder Hyldal

Publication date:
2012

Document Version
Publisher's PDF, also known as Version of record

Soil-structure interaction for non-slender, large-diameter offshore monopiles

VOL. 1

PhD Thesis
Defended in public at Aalborg University
17th December 2012

Søren Peder Hyldal Sørensen

ISSN 1901-7294
DCE Thesis No. 37

AALBORG UNIVERSITY
Department of Civil Engineering

Aalborg University
Department of Civil Engineering
Group Name

DCE Thesis No. 37

Soil-structure interaction for non-slender, large-diameter offshore monopiles

PhD Thesis defended in public at Aalborg University
17th December 2012

by

Søren Peder Hyldal Sørensen

December 2012

Scientific Publications at the Department of Civil Engineering

Technical Reports are published for timely dissemination of research results and scientific work carried out at the Department of Civil Engineering (DCE) at Aalborg University. This medium allows publication of more detailed explanations and results than typically allowed in scientific journals.

Technical Memoranda are produced to enable the preliminary dissemination of scientific work by the personnel of the DCE where such release is deemed to be appropriate. Documents of this kind may be incomplete or temporary versions of papers—or part of continuing work. This should be kept in mind when references are given to publications of this kind.

Contract Reports are produced to report scientific work carried out under contract. Publications of this kind contain confidential matter and are reserved for the sponsors and the DCE. Therefore, Contract Reports are generally not available for public circulation.

Lecture Notes contain material produced by the lecturers at the DCE for educational purposes. This may be scientific notes, lecture books, example problems or manuals for laboratory work, or computer programs developed at the DCE.

Theses are monograms or collections of papers published to report the scientific work carried out at the DCE to obtain a degree as either PhD or Doctor of Technology. The thesis is publicly available after the defence of the degree.

Latest News is published to enable rapid communication of information about scientific work carried out at the DCE. This includes the status of research projects, developments in the laboratories, information about collaborative work and recent research results.

Published 2012 by
Aalborg University
Department of Civil Engineering
Sohngaardsholmsvej 57,
DK-9000 Aalborg, Denmark

Printed in Aalborg at Aalborg University

ISSN 1901-7294
DCE Thesis No. 37

Preface

This thesis is submitted as one of the requirements for obtaining the degree of Ph.D. according to the regulations put forward by The Doctoral School of Engineering and Science at Aalborg University, Denmark.

The thesis concerns the interaction between soil and pile for monopile foundations for offshore wind turbines. The thesis is divided into two volumes. The first volume presents the overall outcome of the Ph.D. fellowship. Further, the first volume is divided into four parts which cover research areas that have been investigated during the Ph.D. fellowship:

- **Part I – Review of laterally loaded piles in sand** – This part presents a review concerning the design of laterally loaded piles used as the foundation for offshore wind turbines. The Winkler approach and the p–y curve formulation for piles in sand, currently adopted by design regulations of the American Petroleum Institute, the International Organization for Standardization and Det Norske Veritas, are assessed thoroughly. The review highlights and assesses several limitations and uncertainties in the current design methodology.

- **Part II – Physical modelling of laterally loaded, non-slender piles in sand** – This part deals with physical modelling of laterally loaded non-slender piles. A new test set-up for small-scale tests on laterally loaded piles has been developed and validated. The test set-up facilitates the application of an overburden pressure to the soil such that the soil properties for the small-scale tests are similar to the soil properties for sand around full-scale foundations. Tests have been conducted on both statically loaded and cyclically loaded piles. A scaling law is presented and validated against the small-scale tests.

- **Part III – Numerical assessment of the initial part of p–y curves for piles in sand** – This part presents a parametric study on the initial part of p–y curves for piles in sand. The parametric study is conducted through numerical modelling by means of the three-dimensional finite difference program $FLAC^{3D}$. A new expression for the initial slope of p–y curves is determined so

as to accurately capture the behaviour of piles exposed to serviceability limit state loads.

- **Part IV – Design of offshore monopiles unprotected against scour** – This part deals with the design of offshore monopiles that are unprotected against the development of local scour. The time scale of the backfilling process as well as the relative density of the backfilled soil material is assessed through large-scale physical modelling. The significance of the results from the physical modelling on the design of foundations for offshore wind turbines is elucidated through a desk study.

The second volume of the thesis presents the test results from the physical modelling of laterally loaded non-slender piles in sand (Part II).

The Ph.D. thesis is based on the following collection of scientific papers and reports written by the author of the present thesis and in cooperation with other authors:

* Sørensen, S.P.H., Augustesen, A.H. & Ibsen, L.B. (2012). Revised expression for the static initial part of *p–y* curves for piles in sand. *Submitted for publication.*

* Sørensen, S.P.H., Ibsen, L.B. & Foglia, A. (2012). Testing of Laterally Loaded Rigid Piles with Applied Overburden Pressure. *Submitted for publication.*

* Sørensen, S.P.H. & Ibsen, L.B. (2012). Assessment of Scour Design for Offshore Monopiles Unprotected Against Scour. *Submitted for publication.*

Sørensen, S.P.H., Ibsen, L.B. & Frigaard, P. (2012). Relative Density of Backfilled Soil Material around Monopiles for Offshore Wind Turbines. *Accepted at the 22nd International Ocean and Polar Engineering Conference, XXII ISOPE, Rhodes, Greece.*

* Sørensen, S.P.H. & Ibsen, L.B. (2012). Experimental Comparison of Non-Slender Piles under Static Loading and under Cyclic Loading in Sand. *Accepted at the 22nd International Ocean and Polar Engineering Conference, XXII ISOPE, Rhodes, Greece.*

Leth, C.T., Sørensen, S.P.H., Klinkvort, R.T., Augustesen, A.H., Ibsen, L.B. & Hededal, O. (2012). A snapshot of present research at AAU and DTU on large-diameter piles in coarse-grained materials. *Proceedings of the Nordic Geotechnical Meeting, XVI NGM, Copenhagen, Denmark.*

Sørensen, S.P.H. & Ibsen, L.B. (2012). Small-scale testing of laterally loaded non-slender piles in a pressure tank. *Proceedings of the Nordic Geotechnical Meeting, XVI NGM, Copenhagen, Denmark.*

Roesen, H.R., Thomassen, K., Sørensen, S.P.H. & Ibsen, L.B. (2011). Evaluation of Small-Scale Laterally Loaded Monopiles in Sand. *Symposium Proceedings: 64th Canadian Geotechnical Conference and 14th Pan-American Conference on Soil Mechanics and Engineering, 5th Pan-American Conference on Teaching and Learning of Geotechnical Engineering, Toronto, Ontario, Canada: Pan-AM CGS Geotechnical Conference.*

Thomassen, K., Roesen, H.R., Sørensen, S.P.H. & Ibsen, L.B. (2011). Small-scale testing of laterally loaded monopiles in sand. *Symposium Proceedings: 64th Canadian Geotechnical Conference and 14th Pan-American Conference on Soil Mechanics and Engineering, 5th Pan-American Conference on Teaching and Learning of Geotechnical Engineering, Toronto, Ontario, Canada: Pan-AM CGS Geotechnical Conference.*

Brødbæk, K.T., Augustesen, A.H., Møller, M. & Sørensen, S.P.H. (2011). Physical modelling of large diameter piles in coarse-grained soil. *Proceedings of the 21st European Young Geotechnical Engineers' Conference, XXI EYGEC, 4-7. September, Rotterdam, The Netherlands.*

* Sørensen, S.P.H., Ibsen, L.B. & Frigaard, P. (2010). Experimental Evaluation of Backfill in Scour Holes around Offshore Monopiles. *Proceedings of the 2nd International Symposium on Frontiers in Offshore Geotechnics, II ISFOG, Perth, Australia, 8-10 November 2010. Balkema Publishers, A.A. / Taylor & Francis, The Netherlands, 2010, pp. 617-622.*

Frigaard, P. Lykke, T. Rodriguez, J.R.R., Sørensen, S.P.H., Martinelli, L., Lamberti, A., Troch, P., de Vos, L., Kisacik, D., Stratigaki, V., Zou, Q., Monk, K., Vandamme, J., Damsgaard, M.L. & Graversen, H. (2010). Loads on Entrance Platforms for Offshore Wind Turbines. *Proceedings of the HYDRALAB III Joiint Transnational Access User Meeting, Hannover, February 2010. Red. /Joachim Grüne, Mark Klein Breteier. Hannover: Forschungszentrum Küste FZK (Coastal Research Center), 2010, pp. 25-28.*

Augustesen, A.H., Sørensen, S.P.H., Ibsen, L.B., Andersen, L., Møller, M. & Brødbæk K.T. (2010). Comparison of calculation approaches for monopiles for offshore wind turbines. *In Proceedings of the 7th European Conference on Numerical Methods in Geotechnical Engineering, VII NUMGE, (eds. Benz and Nordal), 2.-4. June, Trondheim, Norway, CRC Press, Taylor & Francis Group, 901-906.*

Sørensen, S.P.H., Ibsen, L.B. & Augustesen, A.H. (2010). Effects of diameter on initial stiffness of p-y curves for large-diameter piles in sand. *In Proceedings of the 7th European Conference on Numerical Methods in Geotechnical Engineering, VII NUMGE, (eds. Benz and Nordal), 2.-4. June, Trondheim, Norway, CRC Press, Taylor & Francis Group, 907-912.*

Augustesen, A.H., Brødbæk, K.T., Møller, M., Sørensen, S.P.H., Ibsen, L.B., Pedersen, T.S. & Andersen, L. (2009). Numerical Modelling of Large-Diameter Steel Piles at Horns Rev. *In Proceedings of the 12th International Conference on Civil, Structural and Environmental Engineering Computing (eds. Topping, Costa Neves and Barros), 1.-4. September, Madeira, Portugal, Civil-Comp Press, Dun Eaglais, Kippen, UK, Paper 239.*

Sørensen, S.P.H., Brødbæk, K.T., Møller, M., Augustesen, A.H. & Ibsen, L.B. (2009). Evaluation of the Load-Displacement Relationships for Large-Diameter Piles in Sand. *In Proceedings of the 12th International Conference on Civil, Structural and Environmental Engineering Computing, (eds. Topping, Costa Neves and Barros), 1.-4. September, Madeira, Portugal, Civil-Comp Press, Dun Eaglais, Kippen, UK, Paper 244.*

* Sørensen, S.P.H., Brødbæk, K.T., Møller, M. & Augustesen, A.H. (2012). Review of laterally loaded monopiles employed as the foundation for offshore wind turbines. *DCE Technical Reports, No. 137, Department of Civil Engineering, Aalborg University, Aalborg, Denmark.*

\+ Sørensen, S.P.H. & Ibsen, L.B. (2011). Small-scale cyclic tests on non-slender piles situated in sand - Test results. *DCE Technical Reports, No. 118, Department of Civil Engineering, Aalborg University, Aalborg, Denmark.*

\+ Sørensen, S.P.H. & Ibsen, L.B. (2011). Small-scale quasi-static tests on non-slender piles situated in sand - Test results. *DCE Technical Reports, No. 112, Department of Civil Engineering, Aalborg University, Aalborg, Denmark.*

Copies of the publications marked with "*" are enclosed in the back of Vol. 1 of the thesis, while publications marked with "+" are enclosed in Vol. 2 of the thesis.

The Ph.D. fellowship has been funded through the research project "Seabed Wind Farm Interaction". The research project is funded by "The Danish Agency for Technology and Innovation" under the Program Committee for Energy and Environment, case no. 2104-07-0010. The funding is sincerely appreciated.

During the Ph.D. fellowship, supervision has been given by Professor Lars Bo Ibsen, Aalborg University, Denmark. I wish to thank Professor Lars Bo Ibsen for his guidance and support during the course of my studies. His guidance is greatly appreciated.

During the Ph.D. fellowship, I spent four months at the Centre for Offshore Foundation Systems (COFS), University of Western Australia, Perth, Western Australia, Australia, under the supervision of Professor Mark Randolph. At COFS, my work was concentrated on numerical modelling of the behaviour of non-slender laterally loaded piles. Further, Mark Randolph also provided me with great insight within the scope of physical modelling including practical use of dimensional analysis with

respect to laterally loaded piles. I would like to express gratitude to Professor Mark Randolph for his assistance and supervision during the time I spent at the University of Western Australia.

I would like to express gratitude to Kristian T. Brødbæk, Martin Møller and Anders H. Augustesen, COWI A/S, for their cooperation in connection with Part I of the thesis. Further, I wish to express my gratitude to Anders H. Augustesen for his cooperation in connection with Part III of the thesis.

Kristian T. Brødbæk, Martin Møller, Kristina Thomassen, Hanne R. Roesen, Linas Mikalauskas, Alejandro B. Moreno and Jose L. T. Diaz have assisted with the physical modelling related to Part II of the project. Their assistance is sincerely acknowledged. I also wish to acknowledge the technical staff at the Geotechnical Engineering Laboratory, Aalborg University for their assistance with the test set-up for the experimental work.

I wish to acknowledge the technical staff at the Large Wave Channel (GWK) of the Coastal Research Centre (FZK) in Hannover, Germany. The large-scale testing on the backfilling process presented in Part IV would not have been possible without their assistance and support.

I wish to thank my colleague Aligi Foglia for many fruitful discussions regarding physical modelling and for his cooperation in connection with Part III of the thesis.

Finally, I thank my colleagues, friends and family for moral support and helpfulness during the course of my studies.

Aalborg, May 2012

Søren Peder Hyldal Sørensen

Summary in English

Strong political and industrial forces, especially in Northern Europe, support the development of new technologies as well as improvements of existing technologies within the field of renewable energy. Offshore wind power is a domestic, sustainable and largely untapped energy resource. Today, the modern offshore wind turbine offers competitive production prices compared to other sources of renewable energy. Therefore, it is a key technology in breaking the dependence on fossil fuels and in achieving the energy and climate goals of the future.

For offshore wind turbines, the costs of foundation typically constitutes 20-30 % of the total costs. Hence, improved methods for the design of foundations for offshore wind turbines can increase the competitiveness of offshore wind energy significantly. The monopile foundation concept has been employed as the foundation for the majority of the currently installed offshore wind turbines.

The overall aim of the present thesis is to enable low-cost and low-risk foundations to be designed for future offshore wind farms. Therefore, the soil-pile interaction for non-slender, large-diameter offshore piles has been investigated.

A review of current design methods for laterally loaded piles is presented. The review focuses on the Winkler approach in which the pile is considered as a beam on an elastic foundation. The elastic foundation consists of a series of uncoupled springs with stiffnesses governed by means of p–y curves. The p–y curve formulation for piles in sand, which is currently adopted in design regulations of organisations such as the American Petroleum Institute, the International Organization for Standardization and Det Norske Veritas, is presented in detail. Limitations to the Winkler approach as well as limitations to the p–y curve formulation currently adopted by design regulations have been presented. The following uncertainties/limitations have been adressed in detail: shearing force between soil layers; ultimate soil resistance; influence of vertical loading on the lateral soil response; effect of pile flexibility; initial stiffness of p–y curves; choice of horizontal earth pressure coefficient; shearing force at the pile toe; shape of p–y curves; effect of soil layering; long-term cyclic loading; effect of scour/backfilling on the soil-pile interaction. Through the litterature study several limitations have been identified for the p–y curve formulation

currently recommended in the design regulation. These limitations need to be addressed in order to enable design of low-cost and low-risk monopile foundations for offshore wind turbines.

The behaviour of laterally loaded piles can be investigated by means of small-scale testing, large-scale testing, numerical modelling and by means of analytical methods. A new test set-up for the small-scale testing of laterally loaded piles has been developed. The test set-up enables the application of an overburden pressure to the soil. Hereby, traditional uncertainties for the soil parameters for small-scale tests have been avoided. These traditional uncertainties include very high friction angles and very low Young's modulus of elasticity in comparison with soil properties for full-scale foundations. Both a series of static tests and a series of cyclic tests have been conducted. A scaling law that includes an applied overburden pressure has been proposed. The scaling law has been validated against the small-scale tests. The pile rotation at failure depends on the applied overburden pressure such that the rotation at failure increases with increasing overburden pressure. This finding is similar to the increase of the strain at failure for increasing confining pressure which can be found for conventional drained triaxial tests on cohesionless materials. Cyclic tests have illustrated another significant difference between tests with and without overburden pressure applied: for the tests without overburden pressure, the cyclic loading caused a part of the soil volume to cave-in and a part of the soil volume to gap; for the tests with overburden pressure applied, no soil cave-in was observed.

A parametric study on the initial part of p–y curves has been conducted. In the parametric study, the influence of a broad spectre of parameters have been adressed. These parameters include: the pile diameter, the Young's modulus of elasticity for the soil, the friction angle, the pile flexibility, the loading eccentricity, and the depth below seabed. The parametric study has been conducted by means of $FLAC^{3D}$ which is a commercial, three-dimensional finite difference program. It has been concluded that the initial part of the p–y curves depends on the pile diameter, the Young's modulus of elasticity for the soil and the depth below seabed, while the friction angle, the loading eccentricity and the pile flexibility do not have any significant effect on the initial part of the p–y curves. Based on the findings from the numerical study, a modified expression for the initial stiffness of p–y curves has been proposed so the behaviour of piles exposed to serviceability limit state loads can be captured accurately.

A large-scale test on backfill around piles in waves has been conducted at the large wave flume (GWK) at the Coastal Research Centre (FZK) in Hannover. The time scale of the backfilling process has been found to be significantly smaller than what can be expected on the basis of previously published small-scale tests on the backfilling process. This illustrates that more research is needed regarding the time scale of backfilling in waves and that the scaling laws for the time scale of backfilling need further investigation. The relative density of the backfilled soil material has been measured to vary from 65 % to 80 %. Hereby, the backfilled soil material can be

categorised as medium dense to very dense and therefore the backfilled soil material can be expected to be rather stiff and to have a significant strength. Through a desk study, the significance of acounting for the time variation of scour/backfilling in the fatigue and ultimate limit state design has been elucidated.

The Ph.D. research project has lead to an improved understanding of the interaction between soil and pile for offshore pile foundations. Hereby, the research contributes to the design of low-cost and low-risk foundations for offshore wind turbines.

Resumé (Summary in Danish)

Udviklingen af nye teknologier samt forbedringer af eksisterende teknologier indenfor vedvarende energi bliver støttet af indflydelsesrige politikere, økonomisk stærke virksomheder og fonde. Denne politiske og industrielle støtte er især udbredt i Nordeuropa. Offshore vindenergi er en bæredygtig energiform og en i høj grad uudnyttet energiressource. Produktionspriserne for nye havvindmøller har efterhånden nået et niveau, hvor offshore vindenergi er konkurrencedygtig i forhold til andre former for vedvarende energi. Optimering af teknologien inden for offshore vindenergi er derfor særdeles vigtig, for at bryde afhængigheden af fossile brændstoffer samt for at møde fremtidens energi- og klimamål.

Omkostningerne forbundet med funderingen af havvindmøller udgør typisk 20-30 % af de samlede omkostninger for havvindmøller. Dermed kan forbedringer af de nuværende designmetoder for funderingen af havvindmøller være med til at øge konkurrenceevnen for offshore vindenergi væsentligt. Den mest anvendte funderingstype for offshore vindmøller er monopæle.

Det overordnede mål med denne afhandling er at optimere de nuværende designmetoder for monopæle fundamenter, således at konkurenceevnen for offshore vindmøller kan forbedres. Derfor er interaktionen mellem jord og pæl blevet undersøgt for stive offshore pæle.

Et litteraturstudie af de nuværende designmetoder for horisontalt belastede pæle præsenteres. Litteraturstudiet fokuserer på Winkler metoden, hvori pælen modelleres som en bjælke på et elastisk fundament. Det elastiske fundament består af en række ukoblede elastiske fjedre, hvoraf fjederstivhederne bestemmes ved brug af p–y kurver. p–y kurve formuleringen for sand, der i dag er inkorporeret i standarder fra the American Petroleum Institute, the International Organization for Standardization og Det Norske Veritas, præsenteres og analyseres. Begrænsninger både i forbindelse med Winkler metoden og i forbindelse med den nuværende p–y kurve formulering præsenteres. De følgende usikkerheder/begrænsninger analyseres og vurderes: forskydning mellem jordlag; ultimativ jordtryk; indflydelse af vertikal belastning på det horisontale jordtryk; betydningen af en pæls fleksibilitet; initialstivheden af p–y kurver; valg af horisontal jordtrykskoefficient; forskydning ved pælespidsen;

p–y kurvernes form; betydningen af lagdelt jord; betydningen af cyklisk belastning; betydningen af scour/backfill på interaktionen mellem jord og pæl. For at optimere designet af offshore pæle og hermed øge konkurrenceevnen for offshore vindenergi er det nødvendigt at undersøge de ovennævnte usikkerheder/begrænsninger.

Interaktionen mellem jord og pæl for horisontalt belastede pæle kan undersøges ved småskala forsøg, storskala forsøg, numerisk modellering og ved analytiske beregninger. En ny forsøgsopstilling for småskala forsøg af horisontalt belastede pæle er blevet udviklet. Forsøgsopstillingen muliggør påførslen af et overlejringstryk. Idet et overlejringstryk påføres, kan de traditionelle usikkerheder i forbindelse med bestemmelsen af jordens egenskaber ved småskala forsøg undgås/formindskes. For traditionelle småskala forsøg udført ved normalt spændingsniveau vil jorden have en meget stor friktionsvinkel samt en meget lille stivhed sammenlignet med egenskaberne for jorden omkring fuldskala pæle. Der er både udført en forsøgsserie med statisk og cyklisk belastning. En skaleringslov, der inkluderer det påførte overlejringstryk, er blevet udledt. Skaleringsloven er blevet valideret i forhold til forsøgsserien på stive pæle udsat for statisk belastning. Ud fra forsøgsserien hvor en statisk belastning er påsat er det erfaret, at pælens rotation ved brud stiger ved stigende overlejringstryk. Denne sammenhæng mellem pælens rotation og overlejringstrykket tilsvarer sammenhængen mellem brudtøjning og den mindste hovedspænding ved drænede triaksialforsøg. Ved de cykliske forsøg kunne det observeres, at der dannes et 'hul' (gap) bag pælen idet denne belastes. Udviklingen af dette 'hul' afhænger dog af om der er påført et overlejringstryk eller ej: for forsøgene uden overlejringstryk blev 'hullet' delvist tilbagefyldt (cave-in); for forsøgene med overlejringstryk blev tilbagefyldning af sandmateriale (cave-in) ikke observeret.

Et parametrisk studie vedrørende den initiale del af p–y kurver er udført. Betydningen af følgende parametre er undersøgt i det parametriske studie: pælens diameter; jordens elasticitetsmodul; jordens friktionsvinkel; pælens fleksibilitet; lastens excentricitet; samt dybden under havbunden. Det parametriske studie er udført ved brug af det kommercielle finite difference program $FLAC^{3D}$. Gennem det parametriske studie erfares det, at den initiale del af p–y kurverne afhænger af pælens diameter, jordens elasticitetsmodul samt dybden under havbunden, hvorimod friktionsvinklen, lastens excentricitet samt pælens fleksibilitet ikke har nogen signifikant betydning for den initiale del af p–y kurverne. Et modificeret udtryk for initialstivheden af p–y kurver for pæle i sand er blevet præsenteret baseret på det numeriske studie. Det modificerede udtryk er fremkommet således, at den initiale del af p–y kurverne for pæle i sand tilnærmes med god nøjagtighed.

I den store bølgerende (GWK) ved Coastal Research Centre (FZK) i Hannover er der udført et storskala forsøg på backfill omkring pæle i bølger. Tidsskalaen for backfill-processen var betydeligt mindre end hvad der kan forventes baseret på publicerede småskala forsøg omhandlende backfill. Dette tydeliggør nødvendigheden af udvidet forskning indenfor backfilling i bølger samt at de nuværende skaleringslove for tidsskalaen af backfill kræver yderligere validering. I storskala forsøget blev den

relative lejringstæthed fundet til 65-80 %, hvormed det kan konkluderes, at det tilbagefyldte sand-materiale har en høj stivhed og styrke. Betydningen af at tage højde for den tidslige variation i scour-dybde ved undersøgelse af udmattelses- og brudgrænsetilstanden er blevet belyst.

Ph.D.-projektet har ført til en øget forståelse af interaktionen mellem jord og pæl for offshore pælefundamenter. Ph.D.-projektet bidrager dermed til en øget konkurrenceevne for offshore vindenergi.

Contents

CHAPTER 1

Foundations for offshore wind turbines

Wind energy is a competitive and promising source of renewable energy, and hereby wind energy plays an important role when trying to break the dependence on fossil fuels and when trying to reduce carbon emissions. Wind energy is a sustainable source of energy. Today, the majority of the installed wind turbines are positioned onshore. However, in countries with dense populations and vast coastlines, offshore wind energy is an alternative to onshore wind energy. Placing wind turbines offshore offers advantages such as: higher wind speeds; less turbulent wind; less or no visual impact; and no human neighbours. However, both construction costs and maintenance costs are significantly higher for offshore wind turbines than for onshore wind turbines. To minimise the construction and maintainance costs, offshore wind turbines should preferably be placed near shore and at low water depths.

The first offshore wind farm was erected in Vindeby, Denmark, and consisted of 11 wind turbines with capacities of 450 kW. The first large-scale offshore wind farm was erected in 2003 at Horns Rev, Denmark. Horns Rev Offshore Wind Farm consists of 80 wind turbines, and it has a total capacity of 160 MW. In 2009, the capacity of offshore wind energy in Europe was approximately 2 GW. The European Wind Energy Association (EWEA) has set targets for the offshore wind energy capacities in Europe. By 2020 and 2030, the European offshore wind energy capacity should reach 40 GW and 150 GW, respectively. The installation of offshore wind energy is expected primarily to take place in Northern Europe. (www.ewea.org)

For offshore wind turbines, the costs of foundation typically constitutes of 20-30 % of the total costs. Therefore, it is of high interest to optimise the foundation design. This can be accomplished either by improving existing technologies or by developing new technologies.

Today, the majority of the installed offshore wind turbines have capacities up to

3.6 MW, are positioned within a distance of 10 km from shore and are located at positions with water depths less than 20 m. However, the installation of several offshore wind turbines with capacities of up to 7 MW, distances to shore of up to 100 km and water depths of up to 60 m have been consented/planned.

1.1 Loads acting on foundations for offshore wind turbines

Offshore wind turbines are exposed to environmental loads from waves, wind and currents. The foundations for offshore wind turbines are therefore exposed to large lateral loads as well as large overturning moments. The vertical loading originates from the selfweight of the wind turbine and of the foundation. Therefore, the vertical loading is rather small. The loading from wind and waves are cyclic. So, resonance between the loading frequency and the natural frequencies of the offshore wind turbine structure should be avoided. Further, the deformation/rotation of the foundation, due to long-term cyclic loading as well as the fatigue-life of the steel material of both the foundation and the wind turbine, should be investigated.

The frequency range of extreme waves is typically in the range of 0.07-0.14 Hz while the energy rich wind turbulency typically is below 0.1 Hz. The rotor of modern offshore wind turbines typically undergoes 10-20 revolutions per minute corresponding to a frequency of 0.17-0.33 Hz. This frequency is denoted the rotor frequency, 1P. Due to aerodynamic imbalances or imbalances in the mass distribution, minor excitations can take place with a frequency of 1P. The rotor blades pass the tower with a frequency of 3P, 0.5-1 Hz. Large excitations take place with this frequency due to the impulse-like excitation from blades passing the tower. Today, most foundations for offshore wind turbines are designed such that the first natural frequency of the wind turbine including foundation lies within 1P and 3P. The natural frequencies of offshore wind turbines depends on both the stiffness of the foundation and tower structure as well as on the stiffness of the interaction between soil and foundation. The stiffness of the material used for the tower and foundation can be predicted with high accuracy. However, determination of the stiffness of the interaction between the soil and the foundation is complicated. Furthermore, the cyclic loading might change this stiffness since cyclic loading can lead to possible softening/hardening of the soil. Furthermore, erosion of seabed material causes the stiffness og the interaction between soil and foundation to vary with time and sea conditions.

For offshore wind turbines, the permanent rotation of the foundation arising from installation as well as from long-term loading is typically required to be less than 0.5°. Therefore, an accurate prediction of the long-term variation of the stiffness of the interaction between soil and foundation is needed. An accurate prediction of this stiffness is also important when designing the steel material in the foundation

and tower against fatigue damage.

Besides loading from wind and waves, offshore wind turbine foundations are also loaded from currents. In comparison with wave loading, the loading from currents is rather small. Both currents and waves induce shear stresses on the seabed, and therefore they can cause erosion of seabed material near to the foundations. To avoid erosion of the seabed around offshore foundations, scour protection consisting of rock infill can be positioned.

For offshore wind turbines located in cold waters, drifting ice can induce major loads on the foundation. In order to minimise the loading arising from drifting ice, foundations for offshore wind turbines located in cold waters are typically designed with either an upward breaking cone or a downward breaking cone in the height of the mean water level.

1.2 Types of foundation for offshore wind turbines

Several types of foundation concepts can be employed as the foundation for offshore wind turbines, for instance the monopile foundation concept, the gravity based foundation concept, the bucket foundation concept, the jacket foundation concept and the tripod foundation concept. The majority of these concepts have originally been developed for the foundation of offshore structures for the oil and gas sector. Offshore structures used for the oil and gas sector, typically, have significant masses. Therefore, both the vertical and the lateral loading on the foundation are significant for foundations used in the offshore oil and gas sector. In contrast, the lateral loads and overturning moments are dominant for foundations used for offshore wind turbines. The choice of foundation depends on several factors: the water depth, the sea conditions, the soil conditions, the wind turbine size, etc.

1.2.1 The monopile foundation concept

The monopile foundation concept is presently the most used type of foundation for offshore wind turbines. Monopiles are typically hollow steel piles driven or drilled into the seabed. The pile diameter is typically 4-6 m, and the embedded pile length ranges from approximately 15 to 35 m. Until today, monopiles have been used for water depths up to approximately 25 m.

For monopiles, the loading is primarily transferred to the ground by means of lateral bedding as the vertical loading is small in comparison with the lateral loads and overturning moments. The upper soil layers of the bedding are therefore important for the load transfer.

To connect the monopile with the wind turbine tower, so-called transition pieces are used. The space between the transition pieces and the monopiles is typically grouted. In fig. 1, a monopile as well as a transition piece are shown.

Figure 1: Monopile foundation being loaded on board a vessel. The yellow pillar at the rear is a transition piece. www.dongenergy.com

After the lifetime of an offshore wind turbine, the monopile foundation is typically cut-off several meters below the seabed. This is a costly process and one of the downsides of the monopile foundation concept. Another disadvantage is the environmental concerns regarding the installation when pile driving is employed.

1.2.2 The gravity based foundation concept

Gravity based foundations employed in the offshore sector typically consist of caissons made of reinforced concrete, steel or composite material (see fig. 2). Caissons with a cellular design, so they can be floated to the site, are often used. As ballasting, sand, gravel, concrete, etc. can be employed. For gravity based foundations, the loads are transferred to the seabed by means of normal shear stresses at the base of the foundation. Hence, a large base as well as a large ballast are necessary to withstand the overturning moments. The hydrodynamic loads are generally large on gravity based foundations. For gravity based foundations, the subsoil close to the seabed surface needs to have a sufficient bearing capacity. Any soft top layers need to be removed prior to installation. Further, the seabed needs to be levelled and a course base layer should be placed prior to installation. The gravity based

foundations erected up till now are primarily erected at locations with water depths of up to 10 m. For larger water depths, the hydrodynamic loads will be very large, and subsequently the costs of foundation would be very large.

Figure 2: Gravity based foundation to be used as foundation at the Nysted Offshore Wind Farm. The gravity based foundation has been designed with a downward breaking ice cone. www.no-tiree-array.org.uk.

1.2.3 The bucket foundation concept

The bucket foundation concept is a rather new foundation concept for offshore wind turbines. The foundation type originates from the oil and gas sector in which suction anchors have been used for the anchoring of floating structures. A bucket foundation comprises of a steel cylinder closed at the top. The bearing behaviour of bucket foundations are similar to the classical foundation concept. Bucket foundations are installed into the seabed by creating a vacuum inside the pile. Initially, when a bucket foundation is to be installed, the selfweight of the structure will cause the bucket to sink a certain depth into the soil. Afterwards, the installation is continued by pumping out water from inside the bucket. This creates suction inside the bucket. Further, for cohesionless soils, the applied suction causes a flow of water from outside the bucket. This loosens the soil and therefore reduces the shaft resistance inside the

bucket and the base resistance. After the lifetime of the offshore wind turbine, the bucket foundation can be uninstalled by means of pumping water into the bucket. Hereby, a pressure will build up inside the bucket causing uplift.

In 2002, a bucket foundation was installed as foundation for a 3 MW wind turbine in an embanked area at Frederikshavn harbour, Frederikshavn, Denmark (see fig. 3). The bucket foundation concept has, furthermore, been employed for a met mast at Horns Rev 2. The bucket foundation concept is a promising foundation concept. However, it still needs to be proven that the concept can be used for a range of soil conditions and that the foundation can be handled during transport and installation in rough sea conditions.

Figure 3: Bucket foundation for a 3 MW wind turbine in Frederikshavn, Denmark. www.hornsrev.dk.

1.2.4 The tripod and jacket foundation concept

For water depths larger than approximately 30 m, the costs of foundation for the monopile foundation concept and the gravity based foundation concept are very large. For such water depths, use of the tripod or the jacket foundation concepts will typically be optimal. These two concepts can both be considered as steel frame structures. They are typically prefabricated and piles are typically used for the anchoring of the steel frames. Moreover, suction buckets can also be employed for the anchoring. The tripod foundation concept consists of a main pipe with three legs, while jacket foundations typically consists of a steel frame with four legs. For

the Alpha Ventus offshore wind farm, both the tripod and the jacket foundation concept have been used. The wind farm is located in the North Sea, approximately 45 km north of the German coastline. Both types of foundation support six 5 MW wind turbines. The tripod and the jacket foundations installed at Alpha Ventus are illustrated in fig. 4 and fig. 5, respectively.

Figure 4: Tripod foundation for a 5 MW wind turbine at the Alpha Ventus offshore wind farm, Germany. www.owt.de.

For steel frame structures such as the tripod or the jacket foundation concepts, the vertical loading as well as the overturning moments give rise to alternating tensile and compressive forces in the piles or suction buckets used to anchor the steel frame into the seabed. In order to minimise the tensile loading, which often is critical, additional balasting can be employed. The lateral loading is carried by either lateral bedding or by the use of piles that are inclined.

If piles are used for the anchoring of the steel frames, these should be cut-off several meters below the seabed at removal.

Figure 5: Jacket foundations for the 5 MW wind turbines at the Alpha Ventus offshore wind farm, Germany. www.panoramio.com.

1.2.5 Floating foundations

For very large water depths, floating foundation concepts might be optimal. Floating type foundations have been used succesfully in the offshore oil and gas industry. Untill today, floating foundations have, however, only been employed for one full-scale offshore wind turbine, the so-called Hywind, which has been installed approximately 10 km southwest of Karmøy, Norway. This floating foundation supports a 2.3 MW turbine and the water depth at the location is approximately 220 m. A ballast stabilised floating foundation has been employed at Hywind. A ballast stabilised floating foundation consists of a hollow steel cylinder filled with ballast consisting of water and rocks. The foundation is attached to the seabed by means of mooring lines.

CHAPTER 2

Aims of thesis and specific objectives

Offshore wind energy is a sustainable and largely untapped energy resource. For offshore wind turbines, the costs related to the foundation typically comprises of 20-30 % of the total costs. Hence, reduction in the costs of the foundation for offshore wind turbines can increase the competitiveness of offshore wind energy significantly. Reductions can be obtained by for instance:

- optimisation of existing types of foundations for offshore wind turbines.
- improvement of the design guidelines for existing types of foundations for offshore wind turbines such that the foundation behaviour can be predicted more accurately.
- development of new foundation concepts for offshore wind turbines.

The overall aims and specific objectives of the present Ph.D. research programme concern the monopile foundation concept, and they are within the field of geotechnical engineering. One of the specific objectives concerns coastal engineering as well as geotechnical engineering.

2.1 Overall aim

The overall aim was to improve the knowledge regarding the behaviour for laterally loaded, non-slender piles situated in the offshore environment and hereby to enable the construction of low-risk and low-cost monopile foundations for offshore wind turbines.

2.2 Specific objectives

The specific objectives were:

- to review the current knowledge regarding the behaviour of laterally loaded, non-slender piles in sand and further to identify, analyse and assess limitations in the current design guidelines for laterally loaded offshore piles.
- to develop a new test set-up for the small-scale testing of laterally loaded, non-slender piles. The new test set-up should enable the application of an overburden pressure to the soil such that the traditional uncertainties for small-scale testing related to small effective stresses in the soil can be avoided. The new test set-up should be proven through a test series on statically loaded and cyclically loaded piles.
- to investigate the stiffness of the interaction between pile and soil through numerical modelling and to establish a new formulation for the initial slope of p–y curves for piles in sand such that the pile behaviour for piles exposed to serviceability limit state loads can be captured accurately.
- to investigate the time scale of backfill in waves and further to investigate the relative density of backfilled soil material. Further, the effect of scour/backfilling on the design of offshore monopile foundations should be assessed.

CHAPTER 3

The research project

The research conducted in connection with the Ph.D. fellowship has, as previously mentioned, been divided into four parts. Part I presents a review of the current design methodology for offshore monopile foundations. Further, in Part I, uncertainties and limitations related to the current design methodology is presented and assessed. Two of these uncertainties and limitations have been investigated further in Part III and Part IV. In Part II, a new and innovative test set-up for laterally loaded piles is presented and validated against a large test series on laterally loaded piles.

In this chapter, the contents of the four research parts are presented. Further, an overview of the contents of the six publications, attached at the back of the present Ph.D. thesis, is presented. The overview includes background information, rationale, objectives and methods.

3.1 Part I – Review of laterally loaded piles in sand

Various design approaches exist for laterally loaded offshore monopiles. Organisations such as the American Petroleum Institute, the International Organization for Standardization and Det Norske Veritas (API, 2000; ISO, 2007; and DNV, 2010) recommend the use of the Winkler approach (Winkler, 1867) for the design of offshore monopiles exposed to lateral loading. This part of the research project consists of the scientific publication "Review of laterally loaded monopiles employed as the foundation for offshore wind turbines". The paper presents a review of the design approaches for offshore monopiles. The review focuses on the Winkler approach in which the interaction between soil and pile is addressed by means of p–y curves.

The p–y curve formulation for piles in sand currently adopted in API (2000), ISO (2007) and DNV (2010) is primarily based on the research presented in Cox et al. (1974), Reese et al. (1974), O'Neill and Murchison (1983), and Murchison and O'Neill (1984). The outline of the paper is as follows:

- **Introduction** – The monopile foundation concept for offshore wind turbines is presented. Furthermore, various design approaches for offshore monopiles are briefly described.
- ***p*–*y* curves and Winkler approach** – The Winkler approach is presented in detail. The presentation includes a historic timeline of the development of the Winkler approach as well as the development of p–y curve formulations for piles in sand.
- **Formulations of *p*–*y* curves for piles in sand** – The p–y curve formulation originally suggested by O'Neill and Murchison (1983) and currently adopted in design regulations such as API (2000), ISO (2007) and DNV (2010) is presented in detail. Both the analytical derivations/assumptions and the field tests that form the basis of the p–y curve formulation are presented.
- **Limitations of *p*–*y* curves** – Based on a review of published litterature concerning the behaviour of laterally loaded offshore monopiles, the uncertainties and limitations of the currently adopted p–y curve formulation for piles in sand is addressed in detail. Alternative p–y curve formulations as well as alternative design approaches for the design of offshore monopiles are assessed. The following uncertainties/limitations have been addressed: the shearing force between soil layers; the ultimate soil resistance; the influence of vertical pile load on the lateral soil response; the effect of soil-pile interaction; the effect of diameter on the initial stiffness of p–y curves; the choice of horizontal earth pressure coefficient; the shearing force at the pile-toe; the shape of p–y curves; the effect of layered soil; the effect of long-term cyclic loading; and the effect of scour on the soil-pile interaction.

This part of the thesis highlights uncertainties and limitations in the Winkler approach as well as in the currently used p–y curve formulation for piles in sand. Hereby, Part I of the thesis constitutes a basis for Parts II-IV.

3.2 Part II – Physical modelling of laterally loaded, non-slender piles

The behaviour of laterally loaded piles can be examined by means of, for instance, small-scale testing, large-scale testing, numerical modelling and analytical methods.

Since large-scale testing is expensive and time-consuming, small-scale testing is a useful tool for analysis of the behaviour of laterally loaded piles. Further, small-scale tests can be used for validation of numerical models. When conducting traditional small-scale tests on laterally loaded piles, the low effective stresses in the soil cause significant uncertainties regarding the soil properties. This part of the Ph.D. research project has concerned the development of a new and innovative test set-up for the small-scale testing of laterally loaded piles. The new test set-up has been developed and validated at the Geotechnical Laboratory at Aalborg University, Denmark.

Many researchers have published results from physical modelling on the behaviour of laterally loaded piles. For example, Mansur et al. (1964), Cox et al. (1974) and Bhushan et al. (1981) have investigated the behaviour of flexible piles in sand through physical modelling. The behaviour of non-slender piles has been investigated by, for instance, LeBlanc et al. (2010a) and Peralta and Achmus (2010). Their investigations were based on small-scale tests conducted at 1-g.

The new test set-up enables the application of an overburden pressure to the soil. By application of an overburden pressure to the soil, the traditional uncertainties related to the determination of the friction angle and the Young's modulus of elasticity for the soil can be overcome. Further, these parameters will be almost constant with depth when an overburden pressure is applied to the soil. However, the application of overburden pressure also causes the effective stresses to vary trapezoidally along the pile length instead of triangularly. For laterally loaded piles several researchers have proposed scaling laws, for instance, Gudehus and Hettler (1983), Peralta and Achmus (2010), and LeBlanc et al. (2010a). However, these scaling laws do not account for the overburden pressure applied to the soil. A new scaling law has therefore been developed so that small-scale tests on laterally loaded, non-slender piles with overburden pressure applied to the soil can be compared to small- and full-scale tests on laterally loaded, non-slender piles with no overburden pressure applied. This scaling law is presented in the paper "Testing of laterally loaded rigid piles with applied overburden pressure". The scaling law is validated against a series of static tests on laterally loaded, non-slender piles with and without overburden pressure applied to the soil. The outline of the paper is as follows:

- **Introduction** – The background for the test series on laterally loaded non-slender piles is presented. Further, the purpose of applying an overburden pressure to the soil during tests on laterally loaded piles is detailed.
- **Test set-up** – The test set-up is presented in detail. The description of the test set-up includes a description of the soil preparation, the soil properties, the pile properties, the measuring system and the method in which an overburden pressure has been applied to the soil.
- **Dimensional analysis** – A scaling law that enables the scaling of tests on laterally loaded piles with applied overburden pressure is presented.

- **Load-displacement relationships** – The test results are presented and the proposed scaling law is validated against the small-scale tests. Furthermore, a discussion on the advantages/disadvantages of applying an overburden pressure to the soil, when conducting small-scale tests on laterally loaded piles, is presented.
- **Potential implication for design** – The scaling law is used for the scaling of the small-scale tests to full-scale foundations.

In "Experimental Comparison of Non-Slender Piles under Static Loading and under Cyclic Loading in Sand", the pile behaviour of laterally loaded, non-slender piles exposed to static and cyclic loading are evaluated. The evaluation is based on a test series on small-scale piles in which an overburden pressure has been applied to the soil. In the paper, the advantages/disadvantages of applying an overburden pressure to the soil when conducting small-scale tests on laterally loaded piles exposed to static loading and cyclic loading are discussed. The paper outline is as follows:

- **Introduction** – The background for the test series on laterally loaded piles is presented.
- ***p–y* curve formulation** – The *p–y* curve formulation suggested by O'Neill and Murchison (1983) is briefly presented.
- **Delimitations concerning the current *p–y* curve formulation** – Delimitations concerning the *p–y* curve formulation proposed by O'Neill and Murchison (1983) is addressed. Especially the effect of flexible/rigid pile behaviour on the soil-pile interaction is discussed.
- **Test set-up** – The test set-up and the test programme is presented.
- **Results** – The test results are presented. The effect of overburden pressure on the static and cyclic pile behaviour is addressed in detail. The advantages/disadvangages of applying an overburden pressure to the soil when conducting small-scale tests on laterally loaded piles are evaluated based on the test results.

3.3 Part III – Numerical assessment of the initial part of *p–y* curves for piles in sand

For offshore monopiles employed as the foundation for offshore wind turbines, the sum of the rotation due to installation and of the rotation due to long-term loading is typically required to be less than 0.5°. Further, the first natural frequency of the wind turbine including foundation is designed to be within a narrow range so

fatigue damage to the steel material used for the foundation and for the wind turbine tower is minimised. Therefore, accurate prediction of the foundation stiffness and hereby also of the inital slope of the p–y curves is of high importance. In the p–y curve formulation suggested by O'Neill and Murchison (1983), the inital slope of the p–y curves depends only on the depth below seabed and the friction angle. Various researchers have investigated the initial slope of p–y curves for piles in sand, however, with contradictory conclusions: Terzaghi (1955), Vesic (1961), Ashford and Juirnarongrit (2005), and Fan and Long (2005) indicated that the initial slope of p–y curves for piles in sand should be independent of the pile diameter; Carter (1984) and Ling (1988) proposed a p–y curve formulation in which the initial slope of the p–y curves is linearly proportional with the pile diameter; Lesny and Wiemann (2006) suggested that the initial slope of p–y curves for piles in sand increases non-linearly with the depth below seabed. In this part of the thesis, the initial slope of p–y curves for piles in sand has been investigated by means of numerical modelling. A parametric study has been conducted with use of the commercial finite difference program $FLAC^{3D}$. The numerical study is presented in the scientific paper "Revised expression for the static initial part of p–y curves for piles in sand". The outline of the paper is as follows:

- ***p*–*y* curve formulation** – Briefly, the p-y curve formulation proposed by O'Neill and Murchison (1983) is presented. The validity of the formulation with respect to non-slender, large-diameter piles is discussed. Especially, the validity/accurateness of the initial slope of the p–y curves for non-slender large-diameter piles is addressed.

- **Numerical modelling** – A numerical model established in the commercial finite difference program $FLAC^{3D}$ is presented in detail. The numerical model is validated against the small-scale tests on laterally loaded, non-slender piles presented in Part II of the thesis.

- **Results** – A parametric study on the initial slope of p–y curves for piles in sand is presented. The parametric study is conducted by means of the numerical model. Based on the parametric study, a modified expression for the initial slope of p–y curves for piles in sand is presented. The modified expression aims at improving the prediction of the behaviour of monopiles exposed to serviceability limit state (SLS) loads. Although the modified expression has been determined so the pile behaviour can be predicted accurately for SLS-loads, the procedure used for the determination of the modified expression can with minor changes be used for the determination of a modified expression suitable for other limit states.

- **Example – Horns Rev 1** – The predicted pile behaviour when employing the modified expression for the initial slope of p–y curves and the initial slope of p–y curves as suggested by O'Neill and Murchison (1983), respectively, are

compared. Further, these predictions are compared with the results from three-dimensional analysis in $FLAC^{3D}$. The comparison is made for a monopile employed as the foundation for an offshore wind turbine at the Horns Rev 1 Offshore Wind Farm.

3.4 Part IV – Design of offshore monopiles unprotected against scour

Local erosion can take place around monopile foundations in the offshore environment. Hence, local scour holes can be formed causing decreased stiffness and capacity of the foundation. Scouring is especially an issue when the upper layers of the seabed consists of sandy or silty soils. The scour phenomena has been investigated by several researchers, for instance, Breuser et al. (1977), Sumer et al. (1992a), Sumer et al. (1992b) and Sumer et al. (1993). Local scouring can lead to scour depths of up to approximately $2.0D$. Hence, local scouring significantly decreases the stiffness and capacity of the foundation. Offshore monopiles can therefore be designed either with or without scour protection. If an offshore monopile is designed without scour protection, the monopile needs extra embedded length to account for the decrease in stiffness and capacity caused by the local scouring.

The local scour depth around monopiles unprotected against the development of scour depends on factors such as the pile diameter, the water depth, the sea conditions and the soil properties. Further, the scour depth does not change momentarily. Therefore, the scour depth depends on the variation with time of the current velocity, the water depth and the wave height. An equilibrium scour depth exists for a given sea condition. Generally, the equilibrium scour depth is large when currents are dominating and small when waves are dominating. The process in which the scour hole decreases is denoted backfilling. The knowledge regarding the backfilling process is currently rather limited. Hartvig et al. (2010) studied the time scale of backfilling and the shape of the scour hole during the backfilling process through small-scale testing. This part of the Ph.D. thesis consists of two scientific publications: the paper "Experimental Evaluation of Backfill in Scour Holes around Offshore Monopiles" and the paper "Assessment of scour design for offshore monopiles unprotected against scour". The paper, "Experimental Evaluation of Backfill in Scour Holes around Offshore Monopiles", presents a large-scale tests on the backfilling process around a vertical pile in waves. Both the time scale of backfilling as well as the properties of the backfilled soil material is evaluated through the large-scale test. An overview of the paper is given below:

- **Introduction** – The background for the paper is briefly stated.
- **Scour phenomenon** – A short review of the present knowledge regarding scour/backfilling around vertical offshore piles is presented.

- **Test set-up** – The test set-up employed for the backfill test at the large wave flume (GWK) at the coastal research centre (FZK) in Hannover, Germany is presented. The presentation includes the preparation of the initial scour hole, the water led-in, the wave generation as well as information concerning the taken soil samples and the conducted cone penetration tests.
- **Results** – The test results regarding the time-scale of backfilling for piles in waves and the relative density of the backfilled soil material are presented. Further, the impact of the test results on the design of offshore monopiles unprotected against the development of scour is shortly discussed.

The paper, "Assessment of scour design for offshore monopiles unprotected against scour", presents an adaptive scour design approach in which the variation of scour depth with time and sea conditions is considered. It should be emphasised that further research concerning the backfill process is needed before the adaptive scour design approach can be put into practice. The purpose of the adaptive scour design approach is merely to illustrate the potential savings that can be obtained by accounting for the variation in scour depth with time when designing monopile foundations that are unprotected against scour development. The outline of the paper is as follows:

- **Introduction** – The design of monopiles for offshore wind turbines and the scour/backfilling phenomena around vertical piles in waves is described.
- **Review of the scour/bacfkilling phenomena** – A review of the scour and backfilling phenomena for vertical piles in the offshore environment is presented. The review considers the equilibrium scour depth, the prediction of the variation of scour depth with time, and the properties of the backfilled soil material.
- **Adaptive scour design** – An adaptive scour design approach is presented. The design approach takes the variation of scour depth with time and the properties of the backfilled soil material into account.
- **Example – Design of monopile foundations for offshore wind turbines based on revised scour adaptive approach** – The fatigue limit state design and the ultimate limit state design of a monopile foundation for an offshore wind turbine is assessed for varying assumptions regarding the scour/backfilling conditions. The Horns Rev 1 Offshore Wind Farm has been employed as example.

CHAPTER 4

Conclusions

Offshore wind energy is a competitive and a largely untapped source of renewable energy. Hence, offshore wind energy plays a major role in the attempt to break the dependence on fossil fuels and in trying to reduce the human-induced carbon emission. The present Ph.D. thesis aims at improving the knowledge regarding the behaviour of laterally loaded, non-slender piles situated in the offshore environment. This can enable the construction of low-risk and low-cost monopile foundations for offshore wind turbines and hereby contribute to improved competitiveness for offshore wind energy. The Ph.D. thesis has been divided into four parts. Three of these parts deal with topics within the field of geotechnical engineering. The fourth research topic concerns both geotechnical engineering and coastal engineering.

In this chapter, the major contributions and main conclusions from the Ph.D. research project are summarised.

4.1 Part I – Review of laterally loaded piles in sand

In this part of the Ph.D. thesis, a litterature review of the present knowledge regarding the behaviour of laterally loaded piles has been presented. In the review, the Winkler approach and the p–y curve formulation originally proposed by O'Neill and Murchison (1983) have been used as reference points. The p–y curve formulation proposed by O'Neill and Murchison (1983) are based primarily on physical modelling on flexible piles. The monopiles used for the foundation of todays offshore wind turbines are non-slender, and therefore the applicability of the p–y curve formulation by O'Neill and Murchison (1983) can be questioned. Several limitations/uncertainties concerning the p–y curve formulation proposed by O'Neill and Murchison (1983)

were found and addressed: the shearing force between soil layers; the ultimate soil resistance; the influence of vertical pile load on the lateral soil response; the effect of soil-pile interaction; the effect of diameter on the initial stiffness of p–y curves; the choice of horizontal earth pressure coefficient; the shearing force at the pile-toe; the shape of p–y curves; the effect of layered soil; the effect of long-term cyclic loading; and the effect of scour on the soil-pile interaction. Of these uncertainties and limitations, especially the effect of diameter on the initial stiffness of p–y curves, the effect of long-term cyclic loading on the accumulated pile rotation and on the foundation stiffness, and the effect of scour on the soil-pile interaction are important for the design of monopile foundations for offshore wind turbines.

For offshore wind turbines, it is of great interest to enable accurate predictions of the foundation stiffness, so the rotation of the foundation and the natural frequencies of the wind turbine can be predicted accurately. Therefore, it is also important to be able to determine the initial stiffness of p–y curves for laterally loaded piles in sand with high accuracy. The initial stiffness of p–y curves for laterally loaded piles in sand has been investigated by several researchers. Terzaghi (1955), Vesic (1961), Reese et al. (1974), Ashford and Juirnarongrit (2005) concluded that the initial stiffness is independent of the pile diameter. In contrast, Carter (1984) and Ling (1988) found that the the initial stiffness is linearly proportional to the pile diameter. Further, both a linear and a non-linear effect of the depth below seabed on the initial stiffness has been suggested. Hence, more research is needed to enable accurate predictions of the stiffness of monopile foundations in sand.

Offshore wind turbines are exposed to long-term cyclic loading due to primarily wind and waves. It is therefore important to include the effect of long-term cyclic loading on the soil-pile interaction. This has been investigated by several researchers by means of either small-scale testing or by implementing results from cyclic triaxial tests in three-dimensional numerical models.

For monopile foundations for offshore wind turbines, the pile behaviour for long-term cyclic loading is of great interest when determining the accumulated tilt of the foundation and when predicting the time variation of the first natural frequency of the structure. Cyclic loading is only in a very simplified manner incorporated in the p–y curve formulations proposed by O'Neill and Murchison (1983). The accumulation of pile deflection due to long-term cyclic loading have been investigated by means of both numerical modelling and small-scale tests. Most researchers conclude that the pile deflection accumulates exponentially with the number of cycles. Further, factors such as the relative density, the ratio between the cyclic load amplitude and the static capacity as well as the ratio between the maximum and minimum load during a load cycle affect the accumulated rotation.

For random cyclic loading, contradicting conclusions have been presented. For instance, LeBlanc et al. (2010b) found that the accumulated pile rotation is independent of the loading sequency, while Peralta and Achmus (2010) concluded that the

loading sequence influences the accumulated pile rotation.

Only a limited number of researchers have investigated the variation of the stiffness of the soil-pile interaction with cyclic loading. LeBlanc et al. (2010a) suggested that the stiffness increases logarithmically with the number of cycles independently of the relative density of the soil. However, they only considered piles in loose to medium dense sand. Hence, further research is needed to enable a better prediction of the pile behaviour for long-term cyclic loading. Especially full-scale tests could lead to a better understanding of this topic.

Both global and local scour will take place for offshore piles installed without scour protection. The scour depth will depend on the sea conditions and therefore the scour depth will vary with time. The presence of global and local scouring around offshore monopiles lead to decreased stiffnesses and capacities of monopile foundations. Design regulations such as ISO (2007) and API (2010) suggest a simplified method for modification of p–y curves due to scouring. However, the method relies on empirical consideration and needs to be validated. Lin et al. (2010) pointed out that the soil becomes overconsolidated when scouring takes place. Hence, the coefficient of horizontal earth pressure and the friction angle of the soil increases. Lin et al. (2010) present a method in which the p–y curves can be modified so that the overconsolidation of the soil is taken into account.

Due to changing sea conditions, the depth of the scour holes around unprotected offshore piles will vary with time. Knowledge is needed regarding the properties of backfilled soil material. Such knowledge can be essential for optimising the fatigue design of monopiles that are designed unprotected against scour development.

4.2 Part II – Physical modelling of laterally loaded, non-slender piles

A new and innovative test set-up for the small-scale testing of laterally loaded piles has been developed. The new test set-up for laterally loaded piles enables the application of an overburden pressure to the soil. Traditionally, when conducting small-scale tests at normal stress level, the friction angle will be high and the Young's modulus of elasticity for the soil will be low due to low effective stresses. Furthermore, accurate determination of these parameters is very difficult for small-scale tests, since triaxial tests at confining pressures less than 5-10 kPa are subject to large uncertainties. When an overburden pressure is applied to the soil, the uncertainties mentioned above can be avoided. The new test set-up has been validated based on a large test series on laterally loaded piles. Small-scale tests with and without overburden pressure applied to the soil have been conducted for both statically loaded and cyclically loaded, non-slender piles. The main findings of the physical modelling were as follows:

- The test set-up worked as planned. Generally, the uncertainties related to the test set-up was found to decrease when overburden pressure was applied to the soil.

- Rather similar load-displacement relationships was found for tests on open-ended and closed-ended piles, respectively. Therefore, the shear and normal stresses acting on the pile toe only slighly affected the behaviour of the test piles.

- The pile stiffness and the pile capacity increases significantly when applying an overburden pressure to the soil.

- A scaling law has been proposed for the behaviour of non-slender, laterally loaded piles. The scaling law captures the behaviour of piles with overburden pressure applied to the soil. The scaling law was validated against the small-scale tests for loading eccentricities of 0.74 L_p to 1.54 L_p and slenderness ratios of 3 to 6.

- In a normalised plot of the moment-rotation relationship, the tests with overburden pressure generally has a lower stiffness than the tests without overburden pressure applied to the soil. Further, the pile rotation at failure was found to increase for increasing value of the overburden pressure. These findings is analogue to the relationship between the strain at failure and the confining stress in triaxial tests.

- For the tests on cyclically loaded piles, the formation of a gap behind the pile was found to depend on whether overburden pressure has been applied to the soil. The gap was significantly more pronounced for the tests with overburden pressure applied to the soil than for the tests without overburden pressure applied to the soil. The reason for this observation needs further examination. Further, the presence of a gap behind large-scale piles installed in cohesionless soils needs to be investigated.

- During unloading for the cyclic tests, friction along the sides of the pile was observed. The friction, however, only had a moderate value. This indicates that the pile capacity is governed primarily by frontal resistance.

- Comparison of the load-displacement relationships for static and cyclic loading indicated that the accumulated pile displacement is primarily governed by the largest applied loading. Similarly, LeBlanc et al. (2010b) also concluded that the accumulated pile displacement depends primarily on the largest applied loading.

4.3 Part III – Numerical assessment of the initial part of p–y curves for piles in sand

In the litterature review presented in Part I of the thesis, it was pointed out that several researchers have investigated the initial stiffness of p–y curves for piles in sand, however, with contradictory conclusions. For offshore wind turbines, it is a major concern to enable accurate estimations of the foundation stiffness. Therefore, accurate predictions of the initial stiffness of p–y curves for piles in sand is similarly a major concern. In the present part of the thesis, a numerical study on the initial slope of p–y curves for piles in sand has been presented. The aim of the numerical study has been to investigate which paramers affect the initial slope of the p–y curves for piles in sand. The commercial three-dimensional finite difference program $FLAC^{3D}$ was employed for the numerical study. The numerical model was succesfully calibrated/validated against the experimental tests on laterally loaded piles presented in Part II of the thesis.

The initial slope of p–y curves for piles in sand was found to depend on the depth below seabed, the pile diameter and the Young's modulus of elasticity for the soil. The friction angle, the loading eccentricity and the pile flexibility were found not to affect the initial slope of the p–y curves. A modified expression for the initial slope of p–y curves for piles in sand was fitted to the numerical simulations so that accurate predictions of the pile behaviour for piles exposed to serviceability limit state loads has been enabled. The modified expression is not expected to be well-suited when investigating the first natural frequency of an offshore wind turbine. However, by implementation of an associative model capturing the small strain behaviour of soil, a similar method can be used to determine values for the initial slope of p–y curves which should be employed for accurate determination of the first natural frequency.

4.4 Part IV – Design of offshore monopiles unprotected against scour

Around offshore piles situated in cohesionless soils, currents and waves can lead to the development of scour holes. The size of these scour holes will vary with time given that the sea conditions affect the equilibrium scour depth. Much research has been conducted so far on the equilibrium scour depth for varying sea conditions. Furthermore, the time scale of the process in which the scour depth increases has similarly been studied intensively. However, little knowledge exists regarding the time scale of the process in which the scour depth decreases (backfilling). Furthermore, no knowledge exists regarding the relative density of backfilled soil material. The variation of scour depth with time as well as the relative density of the backfilled soil material have a significant influence on the stiffness and capacity of offshore

pile foundations. A large-scale test on backfilling around piles in waves has been conducted at the large wave flume (GWK) at the coastal research centre (FZK) in Hannover, Germany. Both the time scale and the relative density of the backfilled soil material has been investigated. Due to limited time available at the large wave flume, it has only been possible to conduct one test on the backfill around piles in waves. Therefore, the conclusions of the study on the backfilling process for piles in waves are only indicative and further research is needed to validate the findings. The following results were observed:

- The normalised time scale of backfilling determined in the large-scale test was significantly smaller than the normalised time scale of backfilling for the small-scale tests reported by Hartvig et al. (2010). The Shields parameter and the Keulegan-Carpenter number for the small- and large-scale tests were of similar values. Therefore, the dependency of the time scale on these parameters cannot explain the significant difference in the normalised time scale. The large-scale test hereby demonstrates that more research is needed regarding the time-scale of backfilling around piles in waves. Further, the scaling of the time scale of backfilling needs further investigation.

- The relative density of the backfilled soil material was found to be approximately 80 % at the new soil surface and decreasing with depth to 65 % at the bottom of the original scour hole. The relative density was determined after the waves were stopped. Therefore, the variation of the relative density with time has not been investigated. Further, it is not known whether the backfilled soil material underwent liquefaction during the backfilling process. Further research is needed regarding the influence of the Shields parameter, the Keulegan-Carpenter number and time on the backfilling process.

- The backfilling process around piles in combined waves and current needs to be investigated.

- Since, the findings of Hartvig et al. (2010) contradicts the results of the large-scale test, the backfilling process around piles needs to be investigated through a combination of small- and large-scale tests.

A desk study has been conducted concerning the influence of the time variation of scour depth and the relative density of backfilled soil material on the design of monopiles for offshore wind turbines. The soil profile, foundation geometry and wind turbine geometry of the Horns Rev 1 Offshore Wind Farm has been employed in the desk study. From the desk study, the variation of the scour depth with time as well as the properties of the backfilled soil material were shown to have a major impact on especially the fatigue life of an offshore wind turbine. Several assmuptions have been employed in the desk study. Therefore, the desk study should only be seen as indicative. However, based on the desk study, it can be concluded that accounting

for the time variation of scour depth in the design can reduce the foundation costs significantly. It is emphasised that further research is needed regarding the time scale of backfill around piles and regarding the properties of backfilled soil in order to enable a more optimised foundation design.

4.5 Concluding remarks

The research project in the present Ph.D. thesis was aimed at improving the design of offshore monopiles used as the foundation for offshore wind turbines. The behaviour of offshore non-slender, large-diameter offshore piles were studied through a combination of physical and numerical modelling. The outcome of the research has lead to an improved understanding of the behaviour of offshore piles and hence the research contributes to an improved economic feasibility of offshore wind energy.

CHAPTER 5

References

API, 2000. *Recommended practice for planning, designing, and constructing fixed offshore platforms - Working stress design, API RP2A-WSD*, American Petrolium Institute, Washington, D.C., 21. edition.

Ashford S. A., and Juirnarongrit T., March 2003. Evaluation of Pile Diameter Effect on Initial Modulus of Subgrade Reaction. *Journal of Geotechnical and Geoenvironmental Engineering*, **129**(3), pp. 234-242.

Bhushan, K., Lee, L.J., and Grime, D. B., 1981. Lateral Load Tests on Drilled Piers in Sand. *Drilled Piers and Caissons*, ASCE, pp. 114.131.

Breuser, H., Nicolett, G., and Shen, H., 1977. Local scour at cylindrical piers. *Journal of Hydraulic Research*, **15**, pp. 211-252.

Carter D. P., 1984. A Non-Linear Soil Model for Predicting Lateral Pile Response. *Rep. No. 359, Civil Engineering Dept,. Univ. of Auckland, New Zealand.*

Cox W. R., Reese L. C., and Grubbs B. R., 1974. Field Testing of Laterally Loaded Piles in Sand. *Proceedings of the Sixth Annual Offshore Technology Conference*, Houston, Texas, paper no. OTC 2079.

DNV, 2010. *Design of Offshore Wind Turbine Structures, DNV-OS-J101.* Det Norske Veritas, Det Norske Veritas Classification A/S.

Fan C. C., and Long J. H., 2005. Assessment of existing methods for predicting soil response of laterally loaded piles in sand. *Computers and Geotechnics* **32**, pp. 274-289.

Gudehus G., and Hettler A., 1983. Model Studies of Foundations in Granular Soil, *In Development in Soil Mehcanics and Foundation Engineering 1*, pp. 29-63.

Hartvig P. A., Thomsen J. M., and Andersen T. L., 2010. Experimental study of the development of scour & backfilling. *Coastal Engineering Journal*, **52**, pp. 157-194.

ISO, 2007. Petroleum and natural gas industries - Fixed steel offshore structures. *International Organization for Standardization*, ISO 19902:2007 (E).

LeBlanc C., Houlsby G. T., and Byrne B. W., 2010a. Response of Stiff Piles to Long-term Cyclic Loading, *Geotechnique*, **60**(2), pp. 79-90.

LeBlanc C., Houlsby G. T., and Byrne B. W., 2010b. Response of stiff piles to random two-way lateral loading. *Geotechnique*, **60**(9), pp. 715-721.

Lesny K., and Wiemann J., 2006. Finite-Element-Modelling of Large Diameter Monopiles for Offshore Wind Energy Converters. *Geo Congress 2006, February 26 to March 1*, Atlanta, GA, USA.

Lin C., Bennett C., Han J., and Parsons R. L., 2010. Scour effects on the response of laterally loaded piles considering stress history of sand. *Computers and Geotechnics*, **37**, pp. 1008-1014.

Ling L. F., 1988. Back Analysis of Lateral Load Test on Piles. *Rep. No. 460, Civil Engineering Dept., Univ. of Auckland, New Zealand.*

Mansur, C. I., Hunter, A. H., and Davisson, M. T., 1964. Pile Driving and Loading Tests - Lock and Dam No 4, *Arkansas River and Tributaries, Fruco and Associates*, St. Louis, Missouri.

Murchison J. M., and O'Neill M. W, 1984. Evaluation of *p–y* relationships in cohesionless soils. *Analysis and Design of Pile Foundations. Proceedings of a Symposium in conjunction with the ASCE National Convention*, pp. 174-191.

O'Neill M. W., Murchison J. M., 1983. An Evaluation of p-y Relationships in Sands. *Research Report No. GT-DF02-83*, Department of Civil Engineering, University of Houston, Houston, Texas, USA.

Peralta P., and Achmus M., 2010. An experimental investigation of piles in sand subjected to lateral cyclic loads, *Physical Modelling in Geotechnics*, Taylor & Francis Group, London.

Reese L. C., Cox W. R., and Koop, F. D., 1974. Analysis of Laterally Loaded Piles in Sand. *Proceedings of the Sixth Annual Offshore Technology Conference*, Houston, Texas, **2**, paper no. OTC 2080.

Sumer, B. M., Christiansen, N., and Fredsøe, J., 1992a. Time scale of scour around a vertical pile. *Third International Offshore and Polar Engineering Conference*,

ISOPE, San Francisco, USA, pp. 308-315.

Sumer, B. N., Fredsøe, J., and Christiansen, N., 1992b. Scour around Vertical Pile in Waves. *Journal of Waterway, ort, Coastal and Ocean Engineering*, **118**(1), pp. 15-31.

Sumer, B. M., Christiansen, N., Fredsøe, J., 1993. Influence of cross section on wave scour around piles. *Journal of Waterway, Port, Coastal and Ocean Engineering*, **119**(5), pp. 477-495.

Terzaghi K., 1955. Evaluation of coefficients of subgrade reaction. *Geotechnique*, **5**(4), pp. 297-326.

Vesic A. S., 1961. Beam on Elastic Subgrade and the Winkler's Hypothesis. *Proceedings of the 5th International Conference on Soil Mechanics and Foundation Engineering*, Paris, **1**, pp. 845-850.

Winkler E., 1867. Die lehre von elasticzitat and festigkeit (on elasticity and fixity), Prague, 182 p.

CHAPTER 6

Enclosed scientific papers

Sørensen, S.P.H., Brødbæk, K.T., Møller, M. & Augustesen, A.H. (2012). Review of laterally loaded monopiles employed as the foundation for offshore wind turbines. *DCE Technical Reports, No. 137, Department of Civil Engineering, Aalborg University, Aalborg, Denmark.*

Sørensen, S.P.H., Ibsen, L.B. & Foglia, A. (2012). Testing of Laterally Loaded Rigid Piles with Applied Overburden Pressure. *Submitted for publication.*

Sørensen, S.P.H. & Ibsen, L.B. (2012). Experimental Comparison of Non-Slender Piles under Static Loading and under Cyclic Loading in Sand. *Proceedings of the 22nd International Ocean and Polar Engineering Conference, XXII ISOPE, Rhodes, Greece.*

Sørensen, S.P.H., Augustesen, A.H. & Ibsen, L.B. (2012). Revised expression for the static initial part of p–y curves for piles in sand. *Submitted for publication.*

Sørensen, S.P.H., Ibsen, L.B. & Frigaard, P. (2010). Experimental Evaluation of Backfill in Scour Holes around Offshore Monopiles. *Proceedings of the 2nd International Symposium on Frontiers in Offshore Geotechnics, II ISFOG, Perth, Australia, 8-10 November 2010. Balkema Publishers, A.A. / Taylor & Francis, The Netherlands, 2010, pp. 617-622.*

Sørensen, S.P.H. & Ibsen, L.B. (2012). Assessment of Scour Design for Offshore Monopiles Unprotected Against Scour. *Submitted for publication.*

Title:

Review of laterally loaded monopiles employed as the foundation for offshore wind turbines.

Authors:

Sørensen, S. P. H., Brødbæk, K. T., Møller, M., and Augustesen, A. H.

Year of publication:

2012

Published in:

DCE Technical Reports, Department of Civil Engineering, Aalborg University, Aalborg, Denmark, No. 137.

Number of pages:

48

Review of laterally loaded monopiles employed as the foundation for offshore wind turbines

S. P. H. Sørensen[1];K. T. Brødbæk[2]; M. Møller[2]; and A. H. Augustesen[3]

Aalborg University, February 2012

Abstract

The monopiles foundation concept is often employed as the foundation for offshore wind turbine converters. These piles are highly subjected to lateral loads and overturning moments due to wind and wave forces. Typically monopiles with diameters of 4 to 6 m and embedded pile lengths of 15 to 30 m are necessary. In current practice these piles are normally designed by use of the p–y curve method although the method is developed and verified for small-diameter, slender piles. In the present paper a review of the existing p–y curve formulations for piles in sand is presented. Based on numerical and experimental studies presented in the literature, advances and limitations of the current p–y curve formulations are outlined. The review focuses on the design of monopile foundations for offshore wind turbine converters.

1 Introduction

It is a predominating opinion that the global warming is caused by the emission of greenhouse gasses. Therefore, it is of high political interest to reduce the emission of greenhouse gasses. This can be accomblished by investments in renewable energy. Wind power is a very competitive source of renewable energy, and therefore the market for both onshore and offshore wind farms is expected to expand. In 2008, the wind energy capacity in the world was approximately 120 GW of which Europe accounted for 65 GW. In 2030, the wind energy capacity in Europe is expected to reach 400 GW corresponding to an increase of 515 % compared to the capacity in 2008. Currently, the majority of wind turbines are placed onshore due to lower construction costs onshore than offshore. However, dense populations and built-up areas limit the number of suitable locations on land. Therefore, the development of offshore wind farms are enforced. In 2011, the offshore wind energy capacity in Europe was approximately 4 GW, while the capacity in 2030 is expected to increase to approximately 150 GW. (see www.ewea.org)

Several concepts for offshore wind turbine foundations exist, for instance, monopile foundations, gravitational foundations, bucket foundations, tripods, jacket foundations, and floating foundation concepts. The choice of foundation concept primarily depends on site conditions and the dominant type of loading. At moderate water depths the most common foundation principle is monopiles, which are single steel pipe piles driven open-ended into the soil. According to LeBlanc et al. (2009) monopiles installed recently have

[1]M. Sc., Ph.D. Student in Civil Engineering, Dept. of Civil Engineering, Aalborg University, Sohngaardsholmsvej 57, 9000 Aalborg, Denmark.

[2]M. Sc. in Civil Engineering, COWI A/S

[3]M. Sc., Ph.D. in Civil Engineering, COWI A/S

diameters around 4 to 6 m and a pile slenderness ratio, L/D, around 5 where L is the embedded pile length and D is the outer pile diameter.

For offshore wind turbine foundations the serviceability and fatigue limit states are often governing for the design. The foundations should be designed such that the accumulated rotation is less than the requirements of the wind turbine producer. Often the rotation due to installation is not allowed to exceed 0.25° and the accumulated rotation due to loads is restricted to 0.25°. Furthermore, the foundation should be designed such that resonance with the rotor frequency, the blade passing frequency, and the energy rich frequency of the environmental loads is avoided. Hence, the stiffness of the foundation for offshore wind turbines is of great importance. The blade passing frequency and the rotor frequency of the wind turbine are typically in the range of 0.5-1.0 and 0.17-0.33 Hz, respectively. Monopile foundations for offshore wind turbines are typically designed such that the first natural frequency of the structure is between the blade passing frequency and the rotor frequency.

In current design of laterally loaded offshore monopiles, the winkler model approach is normally used. Further, p–y curves are typically used to describe the interaction between pile and soil. A p–y curve describes the non-linear relationship between the soil resistance acting against the pile wall, p, and the lateral deflection of the pile, y. Note that there in the present paper is distinguished between soil resistance, p, and ultimate soil resistance, p_u. The soil resistance is given as the reaction force per unit length acting on the pile. The ultimate soil resistance is given as the maximum value of soil resistance.

Several formulations of p–y curves exist depending on the type of soil. These formulations are originally formulated to be employed in the offshore oil and gas sector. However, they are also used for offshore wind turbine foundations, although piles with significantly larger diameter and significantly smaller slenderness ratio are employed for the foundation of these.

In the present paper the formulation and implementation of p–y curves for piles in sands proposed by Reese et al. (1974), O'Neill and Murchison (1983), and design regulations of organs such as the American Petroleum Institute and Det Norske Veritas API (API, 2000; and DNV, 2010) will be presented and analysed. However, alternative methods for designing laterally loaded piles have been proposed in the literature. Alternative approaches can generally be classified as follows:

- The limit state method.
- The subgrade reaction method.
- The elasticity method.
- The strain-wedge method.
- The finite element/difference method.
- Model tests

Simplest of all the methods are the limit state methods considering only the ultimate soil resistance (e.g. Hansen, 1961; Broms, 1964; Petrasovits and Award, 1972; Meyerhof et al., 1981; Prasad and Chari, 1999; and Zhang et al., 2005).

The simplest method for predicting the pile deflection is the subgrade reaction method, e.g. Reese and Matlock (1956) and Matlock and Reese (1960). In this case the soil resistance is assumed linearly dependent on the pile deflection. Small- and full-scale tests though substantiate a non-linear relationship between soil resistance and pile deflection. The subgrade reaction method must therefore be considered too simple and highly inaccurate. In addition the subgrade reaction method is

not able to predict the ultimate lateral pile resistance.

The p–y curve method assumes a non-linear dependency between soil resistance and pile deflection and is therefore able to produce a more accurate solution. In both the p–y curve method and the subgrade reaction method the Winkler approach, cf. section 2, is employed to calculate the lateral deflection of the pile and the internal forces in the pile. When employing the Winkler approach the pile is considered as a beam on an elastic foundation. The beam is supported by a number of uncoupled springs with spring stiffness' given by p–y curves. When using the Winkler approach the soil continuity is not taken into account as the springs are considered uncoupled.

The elasticity method, e.g. Banerjee and Davis (1978), Poulos (1971), and Poulos and Davis (1980), includes the soil continuity. However, the response is assumed to be elastic. As soil is more likely to behave elasto-plastically, this elasticity method is not to be preferred unless only small strains are considered. Hence, the method is only valid for small strains and thereby not valid for calculating the ultimate lateral pile resistance.

The strain-wedge method was originally proposed by Norris (1986) and was originally able to predict the respons of flexible piles exhibited to lateral loading. Since then, the model has been developed further by, for instance, Ashour et al. (1998) and Ashour and Norris (2003) such that it can account for, among others, layered soils and soil liguefaction. The strain-wedge method links the traditional Winkler approach with the three-dimensional behaviour of soils determined from triaxial tests.

Another way to deal with the soil continuity and the non-linear behaviour is to apply a three-dimensional finite element/difference model (e.g. Abdel-Rahman and Achmus, 2005; Fan and Long, 2005; Lesny and Wiemann, 2006; Sørensen et al., 2009; Lin et al., 2010; and Sørensen et al., 2010). When applying a three-dimensional numerical model both deformations and the ultimate lateral resistance can be determined. Due to the complexity of a three-dimensional model, substantial computational power is needed and calculations are often very time consuming. Phenomena such as liquefaction and gaps between soil and pile are at present hard to handle in the models. Hence, anumerical modelling is a useful tool but the accuracy of the results is highly dependent on the applied constitutive soil models as well as the calibration of these models.

Model tests can be conducted to investigate the behaviour of laterally loaded piles. Model tests at large scale are very expensive. Hence, small-scale tests are often preferred. When conducting small-scale tests at normal stress level, the friction angle of the soil is high and Young's modulus of elasticity is low compared to the soil properties for full-scale tests. To overcome this issue, small-scale tests can be conducted in either a centrifuge or in a pressure tank in which an overburden pressure can be applied to the soil. Small-scale tests have been conducted by, for instance, Barton et al. (1983), Georgiadis et al. (1992), Verdue et al. (2003), Sørensen et al. (2009), LeBlanc et al. (2010a), LeBlanc et al. (2010b), Klinkvort and Hededal (2010), and Brødbæk et al. (2011). When conducting small-scale tests appropriate scaling laws are necessary for the scaling to full-scale. Scaling laws applicable for laterally loaded piles have been proposed by several authors (e.g. Gudehus and Hettler, 1983; Peralta and Achmus, 2010; Leblanc et al., 2010a; and Bhattacharya et al., 2011).

In this paper the Winkler model approach and the p–y curves proposed by Reese et al. (1974) and Murchison and O'Neill

(1984) are presented in detail. These p–y curves are valid for piles situated in cohesionless soil materials. The limitations of the Winkler model approach and the p–y curves are discussed. Further, research within the field of laterally loaded piles situated in sand is presented. The paper adresses monopile foundations for offshore wind turbines.

2 p–y curves and Winkler approach

As a consequence of the oil and gas industry's expansion in offshore platforms in the 1950s, models for designing laterally loaded piles were required. The key problem is the soil-structure interaction as the stiffness parameters of the pile, E_p, and the soil, E_s, may be well known but at the soil-pile interface the combined parameter E_{py} is governing and unknown. In order to investigate the soil-pile interaction, a number of field tests on fully instrumented flexible piles have been conducted and various expressions for various soil conditions have been derived to predict the soil pressure acting on a pile subjected to lateral loading.

Historically, the derivation of the p–y curve method for piles in sand is as follows:

- Analysing the response of beams on an elastic foundation, the soil is characterised by a series of linear-elastic uncoupled springs, introduced by Winkler (1867).
- Hetenyi (1946) presents a solution to the beam on elastic foundation problem.
- McClelland and Focht (1958) as well as Reese and Matlock (1956) suggest the basic principles in the p–y curve method.
- Investigations by Matlock (1970) indicates that the soil resistance in one point is independent of the pile deformation above and below that exact point.
- Tests on fully instrumented test piles in sand installed at Mustang Island are carried out in 1966 and reported by Cox et al. (1974).
- A semi-empirical p–y curve expression is derived based on the Mustang Island tests, cf. Reese et al. (1974). The expression becomes the state-of-the-art in the following years.
- O'Neill and Murchison proposes a new p–y curve formulation with a tangent hyperbolic shape.
- Murchison and O'Neill (1984) compare the p–y curve formulations proposed by Reese et al. (1974), with the expression by O'Neill and Murchison (1983) and two simplified expressions (also based on the Mustang Island tests) by testing the formulations against a database of relatively well-documented lateral pile load tests. The formulation of O'Neill and Murchison (1983) was found to provide better results compared to the original expressions formulated by Reese et al. (1974). The expression of O'Neill and Murchison (1983) was later adopted by design regulations of organs such as the American Petroleum Institute (API) and Det Norske Veritas (DNV).

Research has been concentrated on deriving empirical (e.g. Reese et al. 1974) and "analytical" (e.g. Ashour et al. 1998) p–y curve formulations for different types of soil giving the soil resistance, p, as a function of pile displacement, y, at a given point along the pile. The soil pressure at a given depth, x_t, before and during an

excitation is sketched in fig. 1b. The passive pressure on the front of the pile is increased as the pile is deflected the distance y_t while the active pressure at the back is decreased.

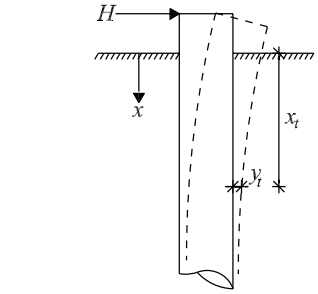

(a) Pile bending due to lateral loading.

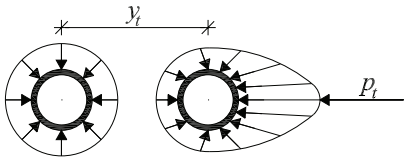

(b) Stresses on a pile before and during lateral excitation.

Figure 1: Distribution of stresses before and during lateral excitation of a circular pile. p_t denotes the net force acting on the pile at the depth x_t, after Reese and Van Impe (2001).

An example of a typical p–y curve is shown in fig. 2a. The curve has an upper horizontal limit denoted by the ultimate soil resistance, p_u. The horizontal line implies that the soil has an ideal plastic behaviour meaning that no loss of shear strength occurs with increasing strain. The subgrade reaction modulus, E_{py}, at a given depth, x, is defined as the secant modulus p/y. E_{py} is thereby a function of both lateral pile deflection, y, depth, x, as well as the physical properties and load conditions. E_{py} does not uniquely represent a soil property, but is simply a convenient parameter that describes the soil-pile interaction. E_{py} decreases with increased deflection, cf. fig. 2b. A further examination of the shape of p–y curves is to be found in section 3.

Since the soil-pile interaction is three-dimensional and highly nonlinear a simplified and convenient way to obtain the

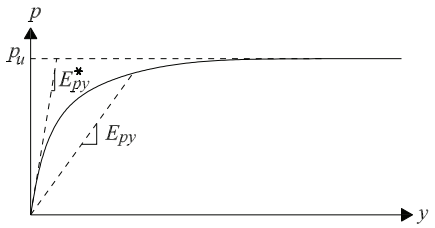

(a) p–y curve.

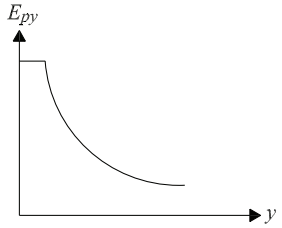

(b) Variation of subgrade reaction modulus.

Figure 2: Typical p–y curve and variation of the modulus of subgrade reaction at a given point along the pile, after Reese and Van Impe (2001).

soil resistance along the pile is to apply the Winkler approach in which the soil resistance is modelled as uncoupled nonlinear springs with stiffness E_{py} acting on an elastic beam as shown in fig. 3. By employing uncoupled springs layered soils can conveniently be modelled.

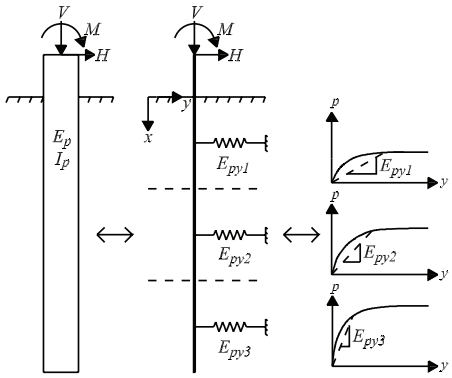

Figure 3: The Winkler approach with the pile modelled as an elastic beam supported by nonlinear uncoupled springs.

The governing equation for beam deflection was stated by Timoshenko (1941). The equation for an infinitesimal small element, dx, located at depth x, subjected to lateral loading, can be derived from static equilibrium. The sign convention in fig. 4 is employed. N, V, and M defines the axial force, shear force and bending moment

in the pile, respectively. The axial force, N, is assumed to act in the cross-section's centre of gravity.

Equilibrium of moments and differentiating with respect to x leads to the following equation where second order terms have been neglected:

$$\frac{d^2M}{dx^2} + \frac{dV}{dx} - N\frac{d^2y}{dx^2} = 0 \qquad (1)$$

Following relations are used:

$$M = E_pI_p\kappa \qquad (2)$$

$$\frac{dV}{dx} = -p \qquad (3)$$

$$p(y) = -E_{py}y \qquad (4)$$

E_p and I_p are the Young's modulus of elasticity of the pile and the second moment of inertia of the pile, respectively. κ is the curvature strain of the beam element.

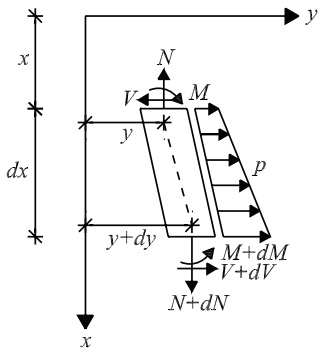

Figure 4: Sign convention for infinitesimal beam element.

With use of (2)–(4) and the kinematic assumption $\kappa = \frac{d^2y}{dx^2}$ which is assumed in Bernoulli-Euler beam theory the governing fourth-order differential equation for determination of deflection is obtained:

$$E_pI_p\frac{d^4y}{dx^4} - N\frac{d^2y}{dx^2} + E_{py}y = 0 \qquad (5)$$

In (5) the shear strain, γ, in the beam is neglected. This assumption is only valid for relatively slender beams. For short and rigid beams the Timoshenko beam theory, that takes the shear strain into account, is preferable. The following relations are used:

$$V = G_pA_v\gamma \qquad (6)$$

$$\gamma = \frac{dy}{dx} - \omega \qquad (7)$$

$$\kappa = \frac{d\omega}{dx} \qquad (8)$$

G_p and A_v are the shear modulus and the effective shear area of the beam, respectively. ω is the cross-sectional rotation as defined in fig. 5. In Timoshenko beam theory the shear strain and hereby the shear stress is assumed to be constant over the cross section. However, in reality the shear stress varies parabolic over the cross section. The effective shear area is defined so the two stress variations give the same shear force. For a pipe the effective shear area can be calculated as:

$$A_v = 2(D - t)t \qquad (9)$$

where t is the wall thickness of the pipe.

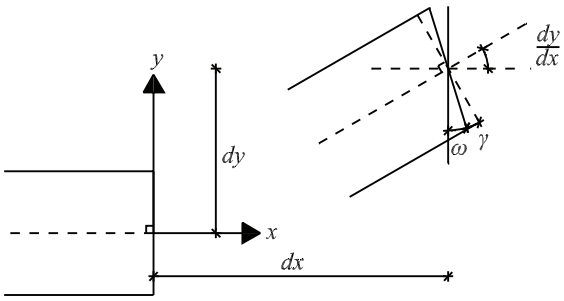

Figure 5: Shear and curvature deformation of a beam element.

By combining (1)–(4) and (6)–(8) two coupled differential equations can be formulated to describe the deflection of the Timoshenko beam:

$$GA_v\frac{d}{dx}\left(\frac{dy}{dx} - \omega\right) - E_{py}y = 0 \qquad (10)$$

$$E_pI_p\frac{d^3\omega}{dx^3} - N\frac{d^2y}{dx^2} + E_{py}y = 0 \qquad (11)$$

In the derivation of the differential equations the following assumptions have been used:

- The beam is straight and has a uniform cross section.
- The beam has a longitudinal plane of symmetry, in which loads and reactions lie.
- The beam material is homogeneous, isotopic, and elastic. Furthermore, plastic hinges do not occur in the beam.
- Young's modulus of elasticity of the beam material is similar in tension and compression.
- Beam deflections are small.
- The beam is not subjected to dynamic loading.

3 Formulations of p–y curves for piles in sand

p–y curves describing the static and cyclic behaviour of piles in cohesionless soils are presented followed by a discussion of their validity and limitations, cf. section 4. Only the formulation made by Reese et al. (1974), hereafter denoted Method A, and the formulation proposed by O'Neill and Murchison (1983) and implemented in design regulations such as API (2000) and DNV (2010), Method B, will be described. Both p–y curve formulations are empirically derived based on full-scale tests on free-ended piles at Mustang Island.

3.1 Full-scale tests at Mustang Island

Tests on two fully instrumented, identical piles located at Mustang Island, Texas as described by Cox et al. (1974), are the starting point for the formulation of p–y curves for piles in sand. The test setup is shown in fig. 6 and 7.

To install the test- and reaction piles a Delmag-12 diesel hammer was used. The test piles were steel pipe piles with diameters of $D = 0.61$ m (24 in) and wall thicknesses of $wt = 9.5$ mm (3/8 in). The embedded length of the piles were 21.0 m (69 ft) which corresponds to a slenderness ratio of $L/D = 34.4$. The piles were instrumented with a total of 34 active strain gauges mounted from 0.3 m above the mudline to 9.5 m (32 ft) below the mudline. The strain gauges were bonded directly to the inside of the pile in 17 levels with highest concentration of gauges near the mudline. The horizontal distance between the centre of the two test piles was 7.5 m (24 ft and 8 in), cf. fig. 7. Between the piles the load cell was installed on four reaction piles. The minimum horizontal distance from the centre of a reaction pile to the centre of a test pile was 2.8 m (9 ft and 4 in). Hence, from each test pile, two reaction piles were placed each with an angle of approximately 28° from the direction of loading. Hence, the total center to center distance from each test pile to the nearest reaction piles were 3.2 m corresponding to $5.2D$. According to Remaud et al. (1998), a trailing pile positioned respectively $4D$ and $6D$ away from the leading pile has in general a reduction in stiffness and capacity of 18 and 7 %, respectively. Therefore, a minor effect from the reaction piles must be expected. Neither Cox et al. (1974) nor Reese et al. (1974) mentions whether they account for group effects in the analysis of the pile tests.

Prior to pile installation, two soil borings were made, each in a range of 3.0 m (10 ft) from a test pile. The soil samples showed a slight difference between the two areas where the piles were installed, as one boring contained fine sand in the top 12 m (40 ft) and the other contained silty fine sand. The strength parameters were derived from standard penetration tests according to Peck et al. (1953). The standard penetration tests showed large variations in the number of blows per ft. Espe-

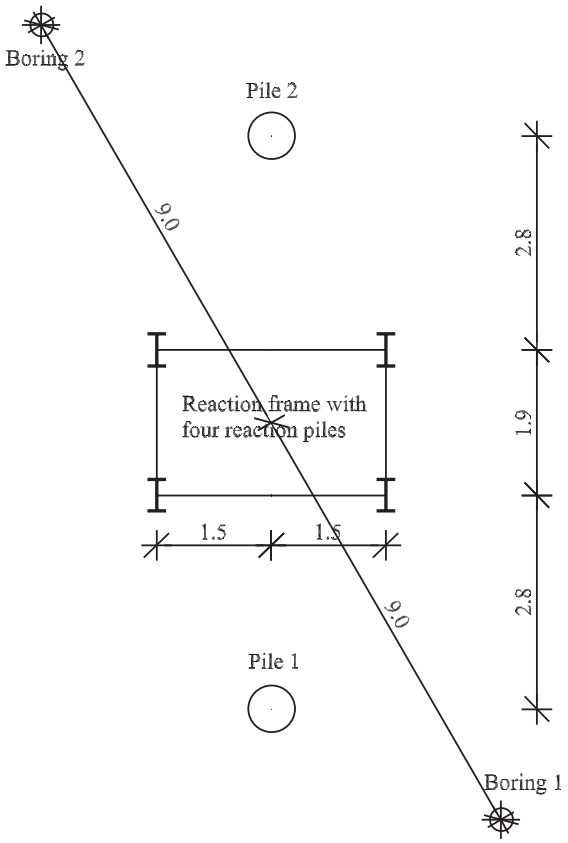

Figure 6: Plan drawing of the test setup for the Mustang Island tests, after Cox et al. (1974). Measures in meter.

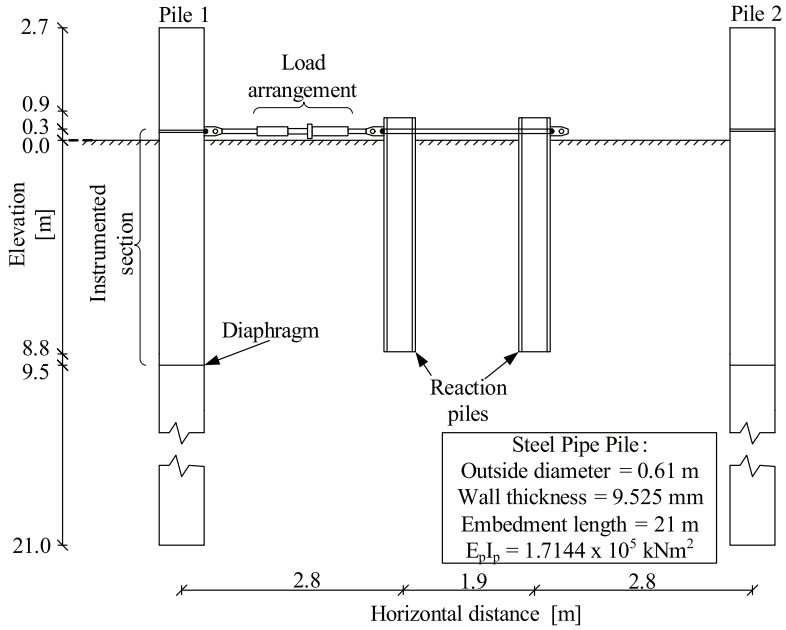

Figure 7: Cross-sectional view of the test setup for the Mustang Island tests, after Cox et al. (1974).

cially in the top 12 m (40 ft) of both borings the number of blows per 30 cm varied from 10 to 80. From 12 to 15 m (40 to 50 ft) beneath the mudline clay was encountered. Beneath the clay layer the strength increased from 40 to 110 blows per 30 cm. From 18 m (60 ft) beneath the mudline to the total depth the number of blows per 30 cm decreased from 110 to 15. The water table was located at the soil surface, implying fully saturated soil.

The piles were in total subjected to seven horizontal load cases consisting of two static and five cyclic. Pile 1 was at first subjected to a static load test 16 days after installation. The load was applied in increments until a maximum load of 267 kN (60000 lb) was reached. The maximum load was determined as no failure occurred in the pile. After the static load test on pile 1 two cyclic load tests were conducted with varying load amplitude. A maximum of 25 load cycles were applied. 52 days after installation a pull-out test was conducted on pile 2. A maximum of 1780 kN (400000 lb) was applied causing the pile to move 25 mm (1 inch). After another week pile 2 was subjected to three cases of cyclic loading and finally a static load test. For the cyclic loading a maximum of 100 load cycles were applied. The static load case on pile 2 was performed immediately after the third cyclic load case which might affect the results. Reese et al. (1974) do not clarify whether this effect is considered in the analyses.

3.2 Method A

Method A is the original method based on the Mustang Island tests, cf. Reese et al. (1974). The p–y curve formulation consists of three curves: an initial straight line, p_1, a parabola, p_2, and a straight line, p_3, all assembled to one continuous piecewise differentiable curve, cf. fig. 8. The last straight line from (y_m,p_m) to (y_u,p_u) is bounded by an upper limit characterised by the ultimate soil resistance, p_u.

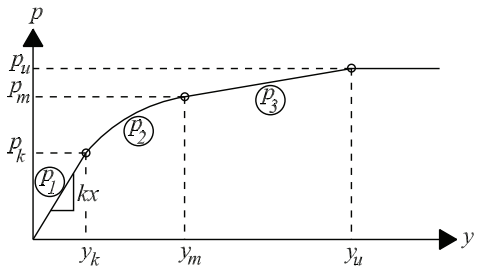

Figure 8: p–y curve for static loading using method A, after Reese et al. (1974).

Ultimate soil resistance

The total ultimate lateral resistance, F_{pt}, is equal to the passive force, F_p, minus the active force, F_a, acting on the pile. The ultimate resistance can be estimated analytically by means of either statically or kinematically admissible failure modes. At shallow depths a wedge will form in front of the pile assuming that the Mohr-Coulomb failure criterion is valid. Reese et al. (1974) uses the wedge shown in fig. 9 to analytically calculate the passive ultimate resistance at shallow depths, p_{cs}. By using this failure mode a smooth pile is assumed, and therefore no tangential forces occur at the pile surface. The active force is also computed from Rankine's failure mode, using the minimum coefficient of active earth pressure.

At deep depths the sand will, in contrast to shallow depths, flow around the pile and a statical failure mode as sketched in fig. 10 is used to calculate the ultimate resistance. The transition depth between these failure modes occurs, at the depth where the ultimate resistances calculated based on the two failure modes are identical.

The ultimate resistance per unit length of the pile can for the two failure modes be

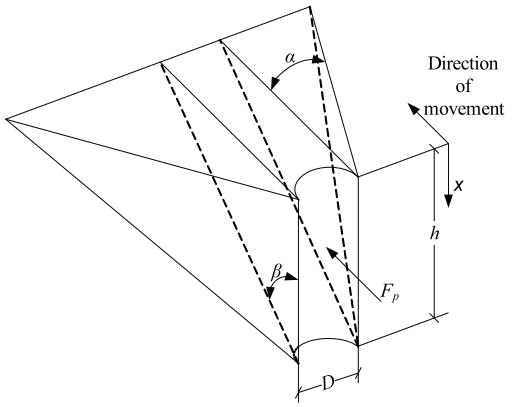

Figure 9: Failure mode at shallow depths, after Reese et al. (1974).

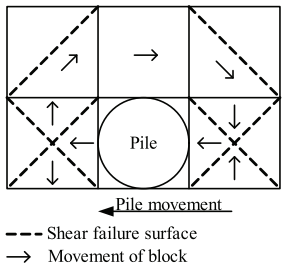

Figure 10: Failure mode at deep depths, after Reese et al. (1974).

calculated according to (12) and (13):

$$p_{cs} = \gamma' x \frac{K_0 x \tan\varphi_{tr} \sin\beta}{\tan(\beta-\varphi_{tr})\cos\alpha} + \gamma' x \frac{\tan\beta}{\tan(\beta-\varphi_{tr})}(D - x\tan\beta\tan\alpha) + \gamma' x (K_0 x \tan\varphi_{tr}(\tan\varphi_{tr}\sin\beta - \tan\alpha) - K_a D) \quad (12)$$

$$p_{cd} = K_a D\gamma' x(\tan^8\beta - 1) + K_0 D\gamma' x \tan\varphi_{tr}\tan^4\beta \quad (13)$$

p_{cs} is valid at shallow depths and p_{cd} at deep depths, γ' is the effective unit weight, and φ_{tr} is the angle of internal friction based on triaxial tests. The factors α and β measured in degrees can be estimated by the following relations:

$$\alpha = \frac{\varphi_{tr}}{2} \quad (14)$$

$$\beta = 45^\circ + \frac{\varphi_{tr}}{2} \quad (15)$$

Hence, the angle β is estimated according to Rankine's theory which is valid if the pile surface is assumed smooth. The factor α depends on the friction angle and load type. However, the effect of load type is neglected in (14). K_a and K_0 are the coefficients of active horizontal earth pressure and horizontal earth pressure at rest, respectively:

$$K_a = \tan^2(45 - \frac{\varphi_{tr}}{2}) \quad (16)$$

$$K_0 = 0.4 \quad (17)$$

The value of K_0 depends on several factors, e.g. the friction angle, but (17) does not reflect that.

The theoretical ultimate resistance, p_c, as function of depth is shown in fig. 11. As shown, the transition depth increases with diameter and angle of internal friction. Hence, for piles with a low slenderness ratio the transition depth might appear far beneath the pile-toe.

By comparing the theoretical ultimate resistance, p_c, with the full-scale tests at Mustang Island, Cox et al. (1974) found a poor agreement. Therefore, a coefficient A is introduced when calculating the actual ultimate soil resistance, p_u, employed in the p–y curve formulations:

$$p_u = Ap_c \quad (18)$$

The variation of the coefficient A with non-dimensional depth, x/D, depends on whether static or cyclic loading is applied. The variation of A is shown in fig. 12a. The deformation causing the ultimate soil resistance, y_u, cf. fig. 8, is defined as $3D/80$.

p–y curve formulation

The soil resistance per unit length, p_m, at $y_m = D/60$, cf. fig. 8, can be calculated as:

$$p_m = Bp_c \quad (19)$$

B is a coefficient depending on the non-dimensional depth x/D, and whether static og cyclic loading is considered. The variation of B with non-dimensional depth is

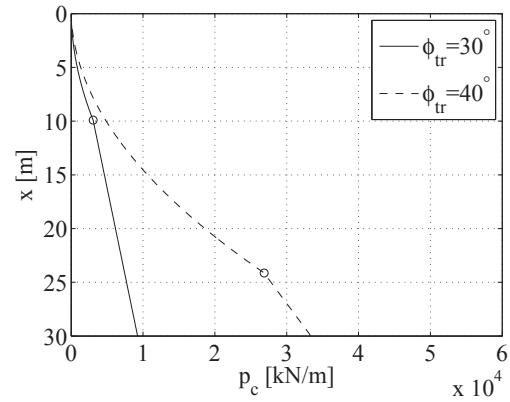

(a) $D = 1.0$ m

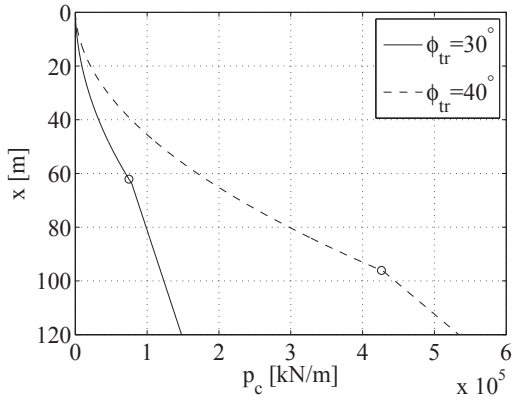

(b) $D = 4.0$ m

Figure 11: Theoretical ultimate resistance, p_c, as function of the depth. $\gamma' = 10$ kN/m^3 has been used to plot the figure. The transition depths are marked with circles.

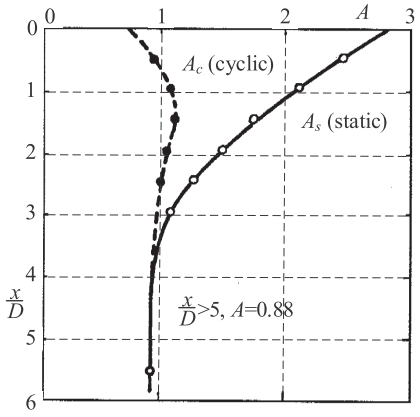

(a) Non-dimensional coefficient A for determining the ultimate soil resistance, p_u.

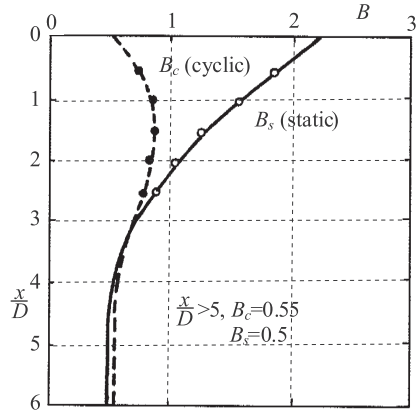

(b) Non-dimensional coefficient B for determining the soil resistance, p_m.

Figure 12: Non-dimensional variation of A and B, after Reese et al. (1974).

illustrated in fig. 12b. Hence, cyclic loading is taken into account by a reduction of the non-dimensional constants A and B. Cyclic loading only affects the p–y curves significantly at depths from the soil surface to $x/D = 3.5$.

The slope of the initial straight line, p_1 as shown in fig. 8, depends on the initial modulus of subgrade reaction, k, and the depth x. This is due to the fact that the in-situ Young's modulus of elasticity also increases with depth. Further, it is assumed that the slope of the initial straight line increases linearly with depth since laboratory test shows, that the initial slope of the stress-strain curve for sand is a linear function of the confining pressure, cf. Terzaghi (1955). The initial tangent stiffness of the p–y curves is in the following denoted E^*_{py}. The initial straight line is given by:

$$p_1(y) = E^*_{py} y = kxy \qquad (20)$$

Reese et al. (1974) suggest that the value of k only depends on the relative density/internal friction angle for the sand. On basis of full-scale experiments values of k for loose sands, for medium dense sands, and for dense sands are 5.4 MN/m^3 (20 lbs/in^3), 16.3 MN/m^3 (60 lbs/in^3), and 34 MN/m^3 (125 lbs/in^3), respectively. The values are valid for sands below the water table. Earlier estimations of k has also been made, for example by Terzaghi (1955), but according to Reese and Van Impe (2001) these methods have been

based on intuition and insight. Design regulations, e.g. API (2000) and DNV (2010), recommend the use of the curve shown in fig. 13. The curve only shows data for relative densities up to approximately 80 %, which causes large uncertainties in the estimation of k for very dense sands.

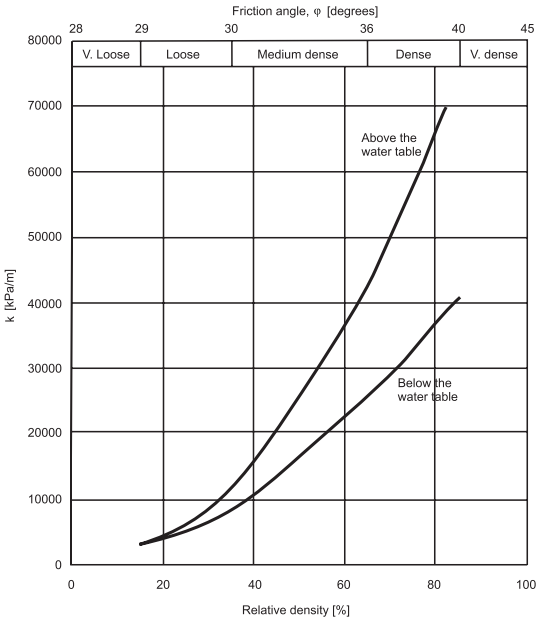

Figure 13: Variation of initial modulus of subgrade reaction k as function of relative density, after API (2000).

The equation for the parabola, p_2, cf. fig. 8, is described by:

$$p_2(y) = Cy^{1/n} \tag{21}$$

where C and n are constants. The constants and the parabola's start point (y_k,p_k) are determined by the following criteria:

$$p_1(y_k) = p_2(y_k) \tag{22}$$

$$p_2(y_m) = p_3(y_m) \tag{23}$$

$$\frac{\partial p_2(y_m)}{\partial y} = \frac{\partial p_3(y_m)}{\partial y} \tag{24}$$

The constants can then be calculated by:

$$n = \frac{p_m}{my_m} \tag{25}$$

$$C = \frac{p_m}{y_m^{1/n}} \tag{26}$$

$$y_k = (\frac{C}{kx})^{n/(n-1)} \tag{27}$$

where m is the slope of the line, p_3.

3.3 Method B

O'Neill and Murchison suggested a modified formulation of the p–y curves. The modified expression is currently recommended in the design regulations, e.g. API (2000) and DNV (2010). In their modified p–y curve formulation, the analytical expressions for the ultimate soil resistance, (12) and (13), are approximated using the dimensionless parameters C_1, C_2 and C_3:

$$p_u = \min \left(\begin{array}{l} p_{us} = (C_1 x + C_2 D)\sigma'_v \\ p_{ud} = C_3 D \sigma'_v \end{array} \right) \tag{28}$$

The constants C_1, C_2 and C_3 can be determined from fig. 14.

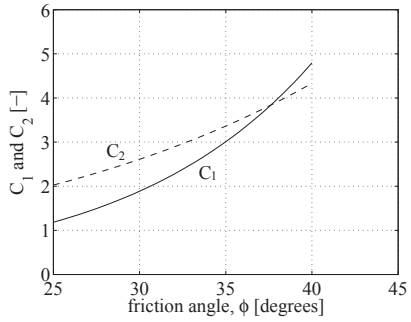

(a) C_1 and C_2.

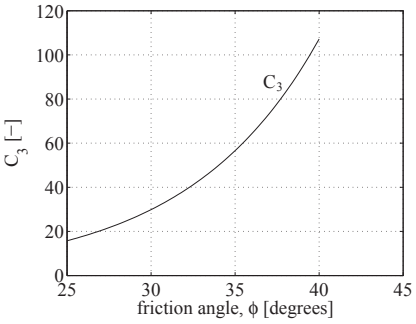

(b) C_3.

Figure 14: Variation of the parameters C_1, C_2 and C_3 as function of angle of internal friction, after API (2000).

A hyperbolic formula is used to describe the relationship between soil resistance and pile deflection instead of a piecewise formulation as proposed by method A:

$$p(y) = Ap_u \tanh\left(\frac{kx}{Ap_u} y\right) \tag{29}$$

The coefficient A could either be determined from fig. 12a or by:

$$A = \begin{pmatrix} 3.0 - 0.8\frac{H}{D} \geq 0.9 & \text{, static loading} \\ 0.9 & \text{, cyclic loading} \end{pmatrix} \quad (30)$$

Since:

$$\frac{dp}{dy}\,|_{y=0} = Ap_u \frac{\frac{kx}{Ap_u}}{\cosh^2(\frac{kxy}{Ap_u})}\,|_{y=0} = kx \quad (31)$$

the p–y curve's initial slope is then similar using the two methods, cf. (20). Also the upper bound of soil resistance will approximately be the same. However, there is a considerable difference in soil resistance predicted by the two methods when considering the pile deflection between y_k and y_u as shown in fig. 15. The soil parameters from tab. 1 has been used to construct the p–y curves shown in fig. 15.

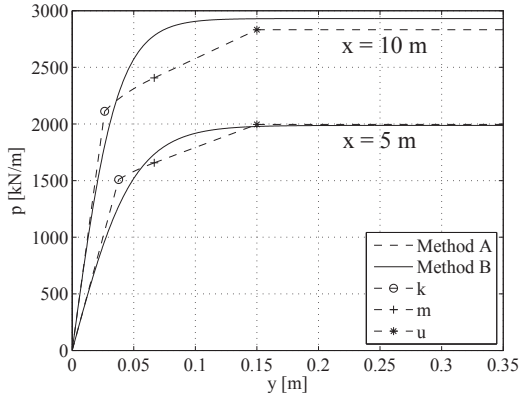

Figure 15: Example of p–y curves based on method A and B. The points k, m, and u refers to the points (y_k,p_k), (y_m,p_m), and (y_u,p_u), respectively, cf. fig. 8.

Table 1: Soil parameters used for plotting the p–y curves in fig. 15.

γ' [kN/m^3]	ϕ_{tr} [°]	D [m]	k [kN/m^3]
10	30	4.2	8000

3.4 Comparison of methods

A comparison of both static and cyclic p–y curves has been made by Murchison and O'Neill (1984) based on a database of 14 full-scale tests on 10 different sites. The pile diameters varied from 51 mm (2 in.) to 1.22 m (48 in.). Both timber, concrete and steel piles were considered. The soil friction angles ranged from 23° to 42°. The test piles' slenderness ratio's are not provided.

Murchison and O'Neill (1984) compared the p–y curve formulations formulated by Reese et al. (1974), Bogard and Matlock (1980), Scott (1980), and O'Neill and Murchison (1983) with the full-scale tests using the Winkler approach. The predicted pile-head deflection, maximum moment, M_{max}, and the depth of maximum moment were compared according to the error, E:

$$E = \frac{|\text{predicted value - measured value}|}{\text{measured value}} \quad (32)$$

In the analysis it was desired to assess the formulations ability to predict the behaviour of steel pipe monopiles. Multiplication factors were therefore employed. The error, E, was multiplied by a factor of two for pipe piles, 1.5 for non-pipe driven piles and a factor of one for drilled piers. When predicted values were lower than the measured values the error was multiplied by a factor of two. By using these factors unconservative results are penalised and pipe piles are valued higher in the comparison. In tab. 2 the average value of E for static p–y curves are shown for the four methods, and in tab. 3 the average value of E is shown for the cyclic p–y curves. As shown, the formulation proposed by O'Neill and Murchison (1983), cf. method B, results in a lower average value of E. The standard deviation of E was not provided in the comparison.

In their comparison of the four p-y curve formulations with the database of tests, Murchison and O'Neill (1984) observed that method A often predicted larger displacement than what was measured. Hence, method A seems to be conserva-

Table 2: Average values of the error, E, for the static pile tests. The methods are compared for pile-head deflection, maximum moment and depth to maximum moment.

	Pile-head deflection	$M_{\max}$	Depth to $M_{\max}$
Reese et al. (1974)	2.08	0.75	0.58
Bogard and Matlock (1980)	1.95	0.73	0.52
Scott (1980)	2.31	0.58	0.37
O'Neill and Murchison (1983)	1.44	0.44	0.40

Table 3: Average values of the error, E, for the cyclic pile tests. The methods are compared for pile-head deflection, maximum moment and depth to maximum moment.

	Pile-head deflection	$M_{\max}$	Depth to $M_{\max}$
Reese et al. (1974)	1.15	0.61	0.16
Bogard and Matlock (1980)	1.22	0.55	0.12
O'Neill and Murchison (1983)	0.55	0.5	0.16

tive. In contrast method B were neither found to be conservative nor unconservative.

Murchison and O'Neill (1984) analysed the sensitivity to parameter variation for method B. The initial modulus of subgrade reaction, k, the internal friction angle, φ, and the effective unit weight, γ', were varied. They found that a 10 % increase in either φ or γ' resulted in an increase in pile-head deflection of up to 15 and 10 %, respectively. For an increase of 25 % in k an increase of up to 10 % of the pile-head deflection was found. The sensitivity analysis also shows that k has the greatest influence on pile-head deflection at small deflections and that φ has a great influence at large deflections. Murchison and O'Neill (1984) state that the sizes of the errors in tab. 2 cannot be explained by parameter uncertainties. The amount of data included in the database was very small due to the unavailability of appropriately documented full-scale tests and Murchison and O'Neill (1984) therefore concluded that a further study of the soil-pile interaction was needed.

4 Limitations of p–y curves

The p–y curve formulations for piles in cohesionless soils are developed for piles with diameters much less than 4 to 6 m which is often necessary for nowadays monopiles. Today, there is no approved method for dealing with these large-diameter, non-slender offshore piles, which is why the design regulations are still adopting the original p–y curve formulations (Reese et al., 1974; O'Neill and Murchison, 1983; API, 2000; and DNV, 2010).

The p–y curve formulations are derived on the basis of the Mustang Island tests which included only two identical piles and a total of seven load cases. Furthermore, the tests were conducted for only one pile diameter, one type of sand, only circular pipe piles, etc. Taking into account the number of factors that might affect the behaviour of a laterally loaded pile and the very limited number of full-scale tests performed to validate the method, the influence of a broad spectra of parameters in the p–y curves are still to be clarified. When considering offshore wind turbine foundations a validation of stiff piles with a slenderness ratio of $L/D < 10$ is needed. It is desirable to investigate this as it might have a significant effect on the initial stiffness which is not accounted for in the p–y curve method. Briaud et al. (1984) postulate that the soil response depends on the flexibility of the pile. Criteria for stiff versus flexible behaviour of piles have been

proposed by various authors, for example, Dobry et al. (1982), Budhu and Davies (1987), and Poulus and Hull (1989). The difference in deformation behaviour of a stiff and a flexible pile is shown in fig. 16. A pile behaves rigidly when the following criterion is fullfilled (Poulus and Hull, 1989):

$$L < 1.48 \left(\frac{E_p I_p}{E_s} \right)^{0.25} \tag{33}$$

E_s is Young's modulus of elasticity of the soil. The criterion for flexible pile behaviour is (Poulus and Hull, 1989):

$$L > 4.44 \left(\frac{E_p I_p}{E_s} \right)^{0.25} \tag{34}$$

According to (33) a monopile with an outer diameter of 4 m, an embedded length of 20 m and a wall thickness of 0.05 m behaves rigidly if $E_s < 7.6$ MPa. In contrast, the pile exhibits a flexible behaviour if $E_s > 617$ MPa. Even dense sands have $E_s < 100$ MPa, so the recently installed monopiles for offshore wind turbines behave, more like rigid than flexible piles.

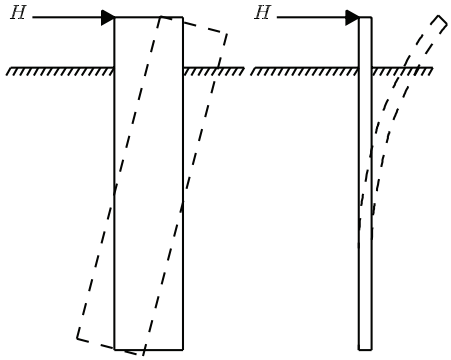

Figure 16: Rigid versus flexible pile behaviour.

The current expression for the ultimate soil resistance is an analytical expression derived for a lateral pile translation. A correction factor for the ultimate soil resistance based on full-scale tests on flexible piles is emloyed. However, as monopiles for offshore wind turbines behave more rigidly than flexibly the combination of the analytical expression and the correction factor might be a poor approximation of the ultimate soil resistance for rigid piles. Hence, the ultimate soil resistance needs validation for large-diameter, non-slender piles.

Only small pile-head rotations are acceptable for modern wind turbine foundations. The allowable pile rotation is provided by the wind turbine supplier. Typically 0.5° of accumulated plastic pile rotation is acceptable. Furthermore, it is of high importance to avoid resonance of the wind turbine with the blade frequency, the rotor frequency and the energy rich frequency of the loading. Hence, it is important to model the foundation stiffness correctly. Appropriate values for the initial stiffness of the p–y curves are therefore necessary.

When using the p–y curve method, the pile bending stiffness is employed when solving the beam on an elastic foundation problem. However, no importance is given to the pile bending stiffness in the formulation of the p–y curves. Hence, E_{py} is independent of the pile properties. The validity of this assumption can be questioned as E_{py} is a parameter describing the soil-pile interaction.

When decoupling the non-linear springs associated with the Winkler model approach another error is introduced, since the soil in reality acts as a continuum.

The design regulations suggests the use of a tangent hyperbolic p–y curve, cf. (29). The reason for this is based on the comparison reported by Murchison and O'Neill (1984) of four different p–y curve formulations. When using this approach, the initial slope of the p–y curves and the ultimate soil resistance governs the shape of the curve. However, the validity of the tangent hyperbolic formulation can be questioned.

The p–y curve formulation is based on full-scale tests on piles installed in rather homogeneous soil. However, often piles are to be installed in a strongly layered strat-

ification. The effect of layered soil on the soil-pile interaction therefore needs to be investigated.

Offshore wind turbines are exposed to cyclic loading from wind and waves. During the lifetime of an offshore wind turbine (typically 20 years) the foundation will be exposed to few load cycles of high load amplitude and $10^6 - 10^8$ load cycles of low to intermediate load amplitude. The p–y curve formulations proposed by Reese et al. (1974) and O'Neill and Murchison (1983) are based on full-scale tests on piles for the oil and gas sector. In these full-scale tests, the pile behaviour for cyclic loading with up to 100 load cycles was investigated. Hence, the behaviour of the piles with respect to long-term cyclic loading were not investigated. The accumulated pile deflection and the change in pile stiffness due to long-term cyclic loading therefore needs to be adressed.

Around pile foundations in the offshore environment, erosion of soil material can occur due to turbulence. Scour holes will therefore form around the pile foundations. Scour is especially an issue for cohesionless soil materials. Scour holes can when they are fully developed be up to $1.3D$ (DNV, 2010). When a scour hole has been formed, soil support is lost. Hence, the p–y curves needs modification to account for scour.

In the following a number of assumptions and not clarified parameters related to the p–y curve method are treated separately. The treated assumptions and parameters are:

- Shearing force between soil layers.
- The ultimate soil resistance.
- The influence of vertical pile load on lateral soil response.
- Effect of soil-pile interaction.
- Effect of diameter on initial stiffness of p–y curves.
- Choice of horizontal earth pressure coefficient.
- Shearing force at the pile-toe.
- Shape of p–y curves.
- Layered soil.
- Long-term cyclic loading.
- Scour effect on the soil-pile interaction.

4.1 Shearing force between soil layers

Employing the Winkler model approach, the soil response is divided into layers each represented by non-linear springs. As the springs are uncoupled, the layers are considered to be independent of the lateral pile deflection above and below that specific layer, giving that the soil layers are considered as smooth layers able to move relatively to each other without loss of energy to friction. Pasternak (1954) modified the Winkler approach by taking the shear stress between soil layers into account. The soil resistance per length of the pile is given by:

$$p(y) = -E_{py}^{p} y - G_s \frac{dy}{dx} \qquad (35)$$

where G_s is the soil shear modulus. The traditional subgrade reaction modulus, $E_{py} = p/y$, may indirectly contain the soil shear stiffness as the p–y curve formulation has been fitted to full-scale tests. E_{py}^{p}, cf. (35), is a modulus of subgrade reaction without contribution from the soil shear stiffness.

Belkhir et al. (1999) examines the significance of shear between soil layers by comparing the CAPELA design code, which can take the shear between soil layers into account, with the French PILATE design

code, which employes smooth boundaries. The two design codes are compared with the results of 59 centrifuge tests conducted on long and flexible piles. Analyses show concordance between the two design codes when shear between soil layers is not taken into account. Furthermore, the analyses shows a reduction varying from 5 % to 14 % in the difference between the maximum moments determined from the centrifuge tests and the numerical simulations when taking the shear between the soil layers into account. However, it is not clear from the paper whether or not the shear between soil layers is dependent on pile properties such as pile diameter, slenderness ratio, etc. Furthermore, it is not clarified whether the authors distinguish between E_{py} and E_{py}^{p}.

4.2 The ultimate soil resistance

The p–y curve formulations according to Method A and Method B are both dependent on the ultimate soil resistance. The method for estimation of p_u is therefore evaluated in the following.

Failure modes

When designing large-diameter monopiles in sand, the transition between the presumed failure modes will most often occur beneath the pile-toe, cf. fig. 11b. Therefore, the ultimate soil resistance at shallow depths is governing for monopile foundations for offshore wind turbines. However, several uncertainties concerning the expression for the ultimate soil resistance at shallow depths exist.

The prescribed method for calculating the ultimate soil resistance at shallow depths assumes that the pile is smooth, which means that no skin friction appears between the pile wall and the soil, and further the formation of a Rankine failure is assumed. However, in reality a pile is neither perfectly rough nor perfectly smooth, and the assumed failure mechanism is therefore not correct. According to Harremoës et al. (1984) a Rankine failure takes place for a perfectly smooth wall and a Prandtl failure for a perfectly rough wall. Sketches of the two types of failure are shown in fig. 17a and fig. 17b, respectively. Due to the fact that the pile is neither smooth nor rough a combination of a Rankine and Prandtl failure will occur.

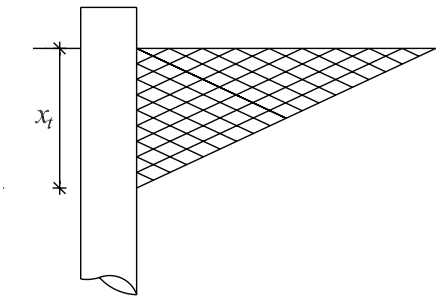

(a) Failure mode proposed by Rankine for a smooth interface at shallow depth.

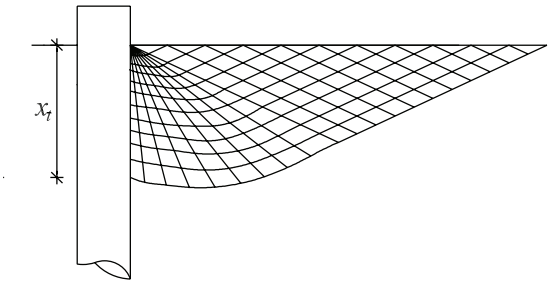

(b) Failure mode proposed by Prandtl for a rough interface at shallow depth.

Figure 17: Rankine and Prandtl failure modes.

In (12) the angle α, which determines the horizontal spread of the wedge, appears. Through experiments Reese et al. (1974) postulate that α depends on both the void ratio, the friction angle, and the type of loading. However, the influence of void ratio and type of loading is neglected in the expression of α, cf. (14).

Monopiles for offshore wind turbines are non-slender piles with high bending stiffness. The piles therefore deflect as almost rigid piles. As the piles are exposed to eccentric loading, the pile deformation pattern primarily consists of rotation around

a point of zero deflection. Hence, the pile deflection at the pile toe is negative. However, when calculating the ultimate soil resistance according to method A and B the rotational pile behaviour and hereby negative pile deflections beneath the point of zero deflection is disregarded. For non-slender piles, a failure mode as shown in fig. 18 could potentially form. This failure mode is derived for a two-dimensional case assuming a smooth pile surface. The failure mode consists of stiff elastic zones and Rankine failures.

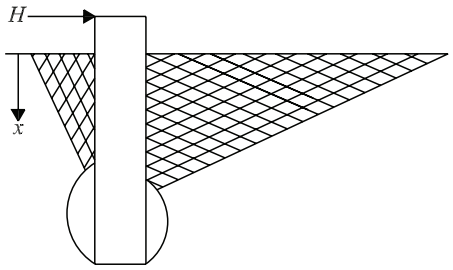

Figure 18: Possible failure mode for a non-slender pile at shallow depth, after Harremoës et al. (1984).

Soil dilatancy

The effect of soil dilatancy is not included in method A and B, and thereby the effects of volume changes during pile deflection are ignored.

Fan and Long (2005) investigated the influence of soil dilatancy on the ultimate soil resistance by use of a three-dimensional, non-linear finite element model. The constitutive model proposed by Desai et al. (1991) incorporating a non-associative flow rule was employed in the analyses. The finite element model was calibrated based on the full-scale tests at Mustang Island. The magnitudes of ultimate soil resistance were calculated for two compactions of one sandtype with similar friction angles ($\varphi_{tr} = 45°$) but different angles of dilatancy. The dilatancy angles are not directly specified by Fan and Long (2005). Estimates have therefore been made by interpretation of the relation between volumetric strains and axial strains. Dilatancy angles of approximately 22° and 29° were found. An increase in ultimate soil resistance of approximately 50 % were found with the increase in dilatancy angle. In agreement with laboratory tests, where the dilatancy in dense sands contributes to strength, this makes good sense. It should be noted that the dilatancy angle and the soil friction angle are related such that soil materials with a high value for the friction angle typically also has a high value for the dilatancy angle. Hence, the effect of soil dilatance might be implicitly incorporated in the expression for the ultimate resistance and the correction factor A. Further, it should be noted that accurate determination of the dilatancy angles requires expensive soil tests, for example, triaxial tests.

Alternative methods

Besides the prescribed method for calculating the ultimate soil resistance several other formulations exist (e.g. Hansen, 1961; Broms, 1964; Petrasovits and Award, 1972; Meyerhof et al., 1981; and Prasad and Chari, 1999). Fan and Long (2005) compared the methods of Hansen (1961) and Broms (1964) with method B and a finite element solution. In the comparison, the pile diameter, the friction angle, and the coefficient of horizontal earth pressure were varied. Hansen's method showed the best correlation with the finite element model, whereas Broms' method resulted in conservative values of the ultimate soil resistance. Further, a significant difference between the finite element solution and method B was found. Method B was found to produce conservative results at shallow depths and non-conservative results at deep depths. The results of the comparison are shown in fig. 19.

The expression of the ultimate soil resistance formulated by Hansen (1961),

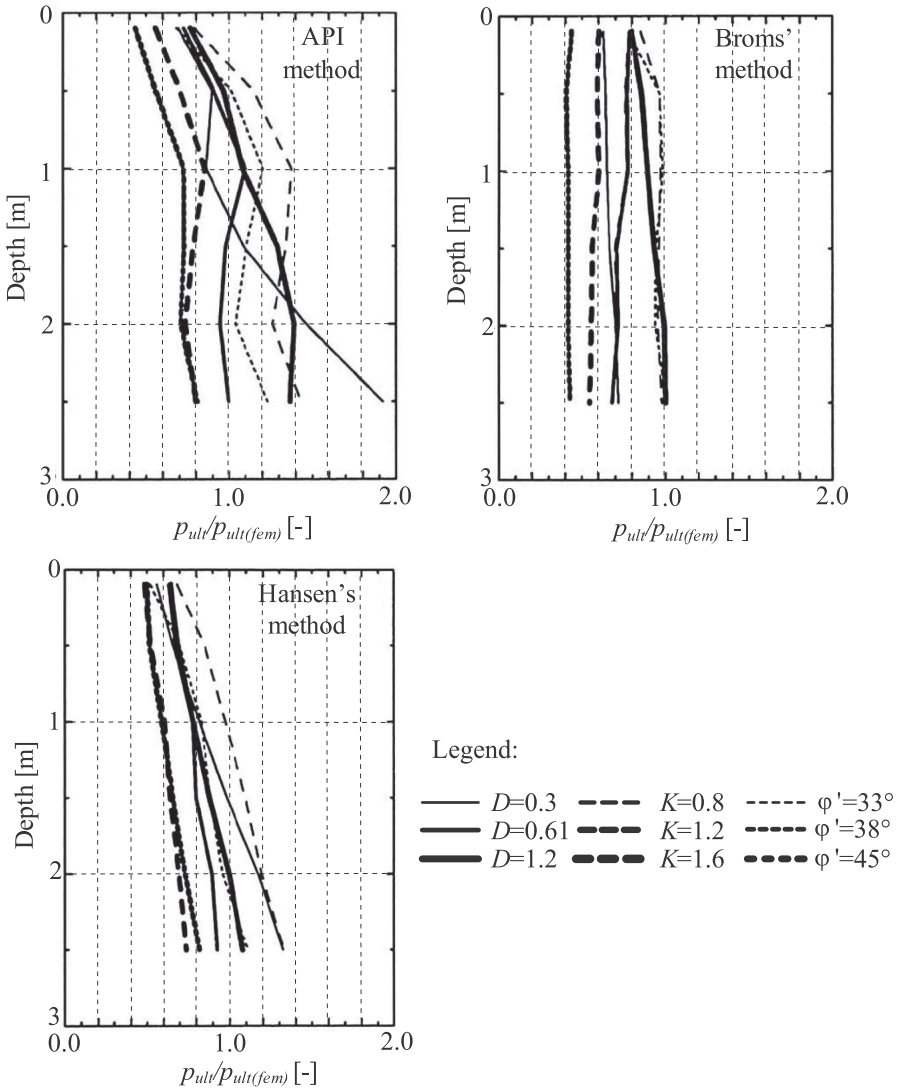

Figure 19: Comparison of the ultimate soil resistance estimated by Broms' method, Hansen's method, and method B with a finite element model, after Fan and Long (2005). $p_{ult}/p_{ult(fem)}$ defines the ratio of the ultimate soil resistance calculated by the analytical methods and the ultimate soil resistance calculated by the finite element model.

Broms (1964), Petrasovits and Award (1972), Meyerhof et al. (1981), and Reese et al. (1974) all assumes the soil pressure to vary uniformly with the pile width. Prasad and Chari (1999) formulated an expression based on small-scale tests on rigid piles instrumented with pressure transducers. They measured the variation of soil pressure with depth and horizontal position on the pile. The test piles had diameters of 0.102 m and slenderness ratios of 3-6. They determined failure as the point in which the load-displacement curves started to be linear. Hence, a horizontal asymptote was not reached and it can be argued whether or not their definition of failure is reasonable. Various researchers have expressed criteria for pile failure, for instance, LeBlanc et al. (2010). They considered a horizontally loaded pile to be in failure when the normalised pile rotation, $\overline{\Theta}$, exceeds 4 °. They defined the normalised pile rotation as:

$$\overline{\Theta} = \Theta \sqrt{\frac{p_a}{\gamma' L}} \tag{36}$$

Failure was by Prasad and Chari (1999) found at pile displacements of 0.2-0.4D.

Based on the load tests on rigid piles, they formulated a new expression for the ultimate soil resistance for laterally loaded rigid piles in which the ultimate soil resistance depends on parameters such as the friction angle, the pile diameter, the pile length and the depth of the point of zero pile deflection. Their expression consists of three linear curves describing the variation of the ultimate soil resistance with depth. The expressions of Hansen (1961), Broms (1964), Petrasovits and Award (1972), Meyerhof et al. (1981) and Prasad and Chari (1999) are sketched in fig. 20. All except Prasad and Chari (1999) postulate that the ultimate resistance at the depth of zero pile deflection is non-zero.

When calculating the ultimate soil resistance according to method A and B, the side friction as illustrated in fig. 21 is neglected. To take this into account Briaud and Smith (1984) has proposed a model where the ultimate soil resistance, p_u, is calculated as the sum of the net ultimate frontal resistance, Q, and the net ultimate side friction, F:

$$p_u = Q + F = (\eta P_{max} + \xi \tau_{max})\, D \quad (37)$$

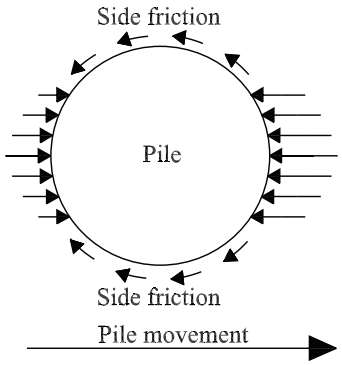

Figure 21: Side friction and soil pressure on the front and the back of the pile due to lateral deflection.

where P_{max} denotes the maximum frontal soil pressure acting on the pile, τ_{max} denotes the maximum shear stress acting on the pile, and η and ξ are dimensionless constants. For circular piles Zhang et al. (2005) recommends the use of (38)-(41) for P_{max}, τ_{max}, η and ξ.

$$P_{max} = K_p^2 \gamma x \quad (38)$$

$$\tau_{max} = K \gamma x \tan(\delta) \quad (39)$$

$$\eta = 0.8 \quad (40)$$

$$\xi = 1.0 \quad (41)$$

Zhang et al. (2005) propose the side friction and frontal resistance to vary with depth similar to the variation proposed by Prasad and Chari (1999). They compared their method with small- and large-scale tests and found their method to be slightly conservative as the pile capacities calculated by their proposed method in average was 8 % smaller than the meassured pile capacities. Further, parameters such as the embedded pile length, the slenderness ratio, the eccentricity ratio, e/L, and the friction angle did not affect the accuracy of their method, cf. fig. 22.

The importance of including side friction in the formulation of p–y curves is for the model proposed by Zhang et al. (2005) unaffected by the diameter since both the ultimate frontal resistance and the net ultimate side friction vary linearly with diameter. However, the ultimate frontal resistance varies non-linearly with diameter in the model proposed by Reese et al. (1974). The importance of side friction might therefore be more significant for large-diameter monopiles than for small-diameter piles.

Summary

Several assumptions are employed when calculating the ultimate soil resistance according to Reese et al. (1974) and the design regulations, e.g. API (2000) and DNV (2010). These methods do not account for friction between pile and soil as the pile surface is assumed smooth. Furthermore, the failure modes are determined

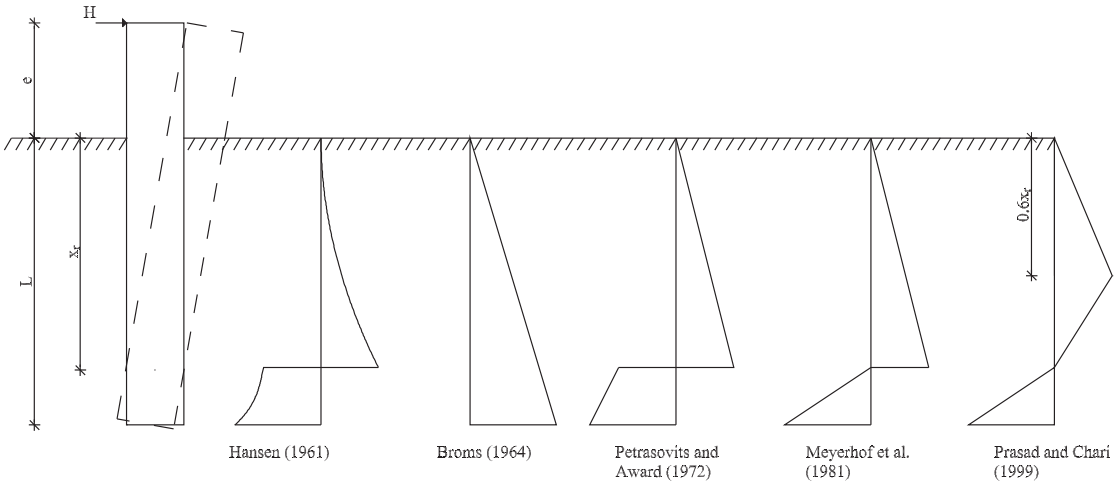

Figure 20: Sketch of the expressions of ultimate resistance proposed by Hansen et al. (1961), Broms (1964), Petrasovits and Award (1972), Meyerhof et al. (1981) and Prasad and Chari (1999), Zhang et al. (2005).

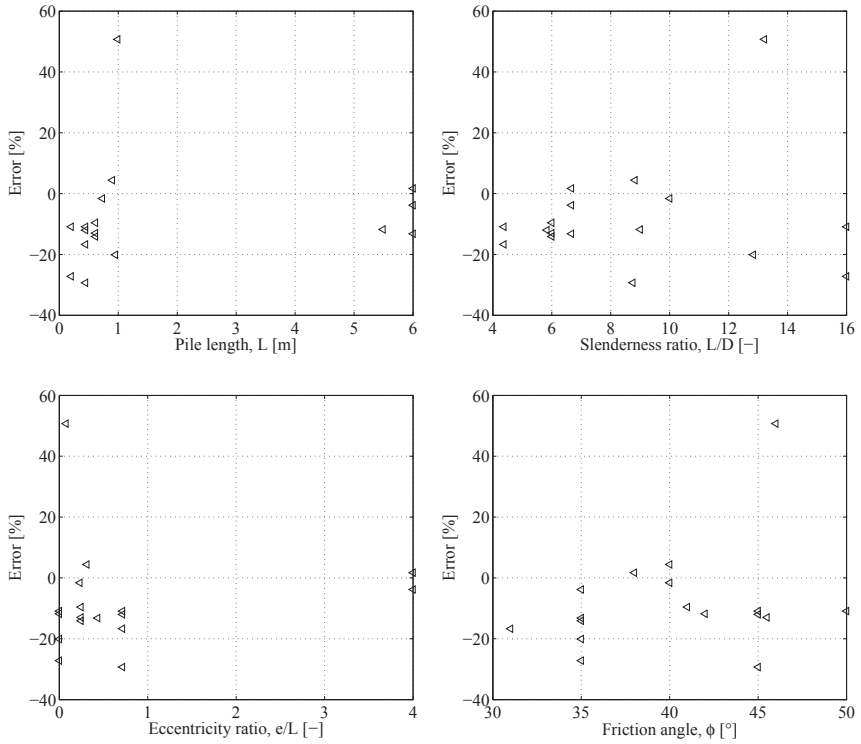

Figure 22: Error in percent between between the predicted pile capacity estimated by means of the method by Zhang et al. (2005) and experimental tests, after Zhang et al. (2005)

for lateral pile translation. Hence, deflections beneath the point of zero pile deflection are accounted for in a very simplified maner. Thus, the assumed failure modes are inaccurate especially for non-slender piles.

The dilatancy of the soil affects the soil strenght, but it is neglected in the expressions for the ultimate soil resistance.

Several methods for determining the ultimate soil resistance exist. The method proposed by Hansen (1961) were found to

correlate better with a finite element model than the methods proposed by Reese et al. (1974) and Broms (1964). In order to take the effect of side friction into account a model was proposed by Zhang et al. (2005) based on the findings of Briaud and Smith (1984) and Prasad and Chari (1999). Predictions regarding the ultimate soil resistance correlate well with laboratory and full-scale tests when using this model.

4.3 The influence of vertical load on lateral soil response

In current practice, piles are analysed separately for vertical and horizontal behaviour. Karthigeyan et al. (2006), Abdel-Rahman and Achmus (2006), Achmus et al. (2009a), and Achmus and Thieken (2010) investigated the effect of combined static vertical and lateral loading on the lateral and vertical pile response in sand through three-dimensional numerical modelling. Karthigeyan et al. (2006) adopted a Drucker-Prager constitutive model with a non-associated flow rule in their numerical modelling. Abdel-Rahman and Achmus (2006), Achmus et al. (2009a) and Achmus and Thieken (2010) all adopted the Mohr-Coulomb constitutive model with a non-associated flow rule. Further, they modelled the soil stiffness as stress-dependent.

Karthigeyan et al. (2006) calibrated the numerical model against two different kinds of field data carried out by Karasev et al. (1977) and Comodromos (2003). A concrete pile with a diameter of 0.6 m and a slenderness ratio of 5 were tested, cf. Karasev et al. (1977). The soil strata consisted of stiff sandy loam in the top 6 m underlain by sandy clay. Comodromos (2003) performed the tests in Greece. The soil profile consisted of silty clay near the surface with thin sublayers of loose sand. Beneath a medium stiff clay layer a very dense sandy gravel layer was encountered. A pile with a diameter of 1 m and a slenderness ratio of 52 were tested. A reasonable agreement between the field tests and the numerical model was found. Achmus and Thieken (2010) validated their numerical model against the model tests of Das et al. (1976) and Meyerhof and Sastry (1985). A good agreement were found. Abdel-Rahman and Achmus (2006) did not report whether their numerical model was validated against experimental tests. However, Abdel-Rahman and Achmus (2006) and Achmus and Thieken (2010) both used the commercial three-dimensional finite element programme ABAQUS and further they employed similar constitutive models. Therefore, the numerical model employed by Abdel-Rahman and Achmus (2006) is assumed also to fit the static model tests well.

To investigate the influence of vertical load on the lateral response in sand, Karthigeyan et al. (2006) modelled a squared concrete pile (1200 $\times$ 1200 mm) with a length of 10 m. Two types of sand were tested, a loose and a dense sand with friction angles of 30° and 36°, respectively. The vertical load was applied in two different ways, simultaneously with the lateral load (SAVL) and prior to the lateral load (VPL). Compressional vertical loading with values of 0.2, 0.4, 0.6, and 0.8 times the vertical pile capacity were applied. The conclusion of the analyses was that the lateral capacity of piles in sand increases under vertical loading. The increase in lateral capacity depended on how the vertical load was applied and on the relative density of the soil. The highest increase was in the case of VPL with a dense sand. For the dense sand with a lateral deflection of 5 % of the side length the increase in lateral capacity was, in the case of SAVL, of up to 6.8 %. The same situation in the case of VPL resulted in an increase of up to 39.3 %. Due to vertical loads higher vertical soil stresses and thereby higher horizontal stresses occur,

which also mobilise larger friction forces along the length of the pile. Therefore, the lateral capacity increases under the influence of vertical loading.

Abdel-Rahman and Achmus (2006), Achmus et al. (2009a) and Achmus and Thieken (2010) analysed the effect of combined vertical and lateral loading on both the vertical and lateral pile stiffness and capacity. Furthermore, they both considered compressive as well as tensile vertical loading. Abdel-Rahman and Achmus (2006) modelled the behaviour of hollow steel piles with pile diameters of 2.0 and 3.0 m and embedded pile lengths of 20 m, Achmus et al. (2009a) modelled concrete piles with diameters of 2.0 m and pile lengths of 10 and 30 m, while Achmus and Thieken (2010) modelled the behaviour of reinforced concrete piles with diameters of 0.5-3.0 m and embedded pile lengths of 15 m. They all considered piles installed in medium dense sand with a friction angle of 35°. The vertical and lateral loading was applied simultaneously. Abdel-Rahman and Achmus (2006) found that for axial compression the effect of combined loading increases both the pile lateral stiffness and pile lateral capacity, allthough the increase was very moderate. The vertical stiffness and capacity were found to increase significantly. The effect of combined loading was found to be more significant for rigid than flexible piles. This confirms the results reported by Karthigeyan et al. (2006). For axial tension no change were found in the lateral pile stiffness. However, the lateral pile capacity was found to decrease for combined loading. The vertical pile stiffness was found to decrease, while the vertical capacity was found to increase for combined lateral and vertical loading. The numerical modelling of Achmus et al. (2009a), and Achmus and Thieken (2010) confirmed the observations of Abdel-Rahman and Achmus (2006). Furthermore they presented interaction diagrams to be used for combined loading.

The above mentioned analysis of the effect of combined lateral and vertical loading on the lateral pile behaviour emphasize that both the vertical stiffness and capacity as well as the lateral stiffness and capacity are positively affected when the vertical loading is compressive. However, the effect is small when the vertical and lateral loads are applied simultaneously. Foundations for offshore wind turbines are exhibited to a constant vertical compressive load originating from the selfweight of the turbine and the foundation itself. In contrast, the horizontal loading is cyclic. Hence, the vertical loading is applied prior to the lateral loading, and combined loading might therefore significantly increase the pile stiffness and capacity of monopiles for offshore wind turbines. However, it should be emphasized that combined loading needs to be examined for cyclic loading and that the above mentioned findings needs to be examined further through experimental testing.

4.4 Effect of soil-pile interaction

No importance is attached to the pile bending stiffness, E_pI_p, in the formulation of the p–y curves. Hereby, E_{py} is independent of the pile properties, which seems questionable as E_{py} is a soil-pile interaction parameter. Another approach to predict the response of a flexible pile under lateral loading is the strain wedge (SW) model developed by Norris (1986). The method incorporates the pile properties. The concept of the SW model is that the traditional parameters in the one-dimensional Winkler approach can be characterised in terms of three-dimensional soil-pile interaction. The SW model was initially established to analyse free-headed piles embedded in uniform soils. Since then it has been improved such that it, for instance, can account for fixed pile head conditions, layered soils, soil liquefaction, pile group ef-

fects, and cyclic loading (Ashour et al., 1998; Ashour and Norris, 2000; Ashour et al., 2002; Ashour and Norris, 2003; and Lesny and Hinz, 2009).

The SW model parameters are related to a three-dimensional passive wedge developing in front of the pile subjected to lateral loading. The wedge has a form similar to the wedge associated with method A, as shown in fig. 9. However the angles α and β are given by:

$$\alpha = \varphi_m \tag{42}$$

$$\beta = 45° + \frac{\varphi_m}{2} \tag{43}$$

where φ_m is the angle of mobilised internal friction.

The purpose of the method is to relate the stresses and strains of the soil in the wedge to the subgrade reaction modulus, E_{py}. The SW model described by Ashour et al. (1998) assumes a linear deflection pattern of the pile over the passive wedge depth, h, as shown in fig. 23. The dimension of the passive wedge depends on two types of stability: local and global stability. To obtain local stability the SW model should satisfy equilibrium and compatibility between the pile deflection, the strains in the soil and the soil resistance acting on the pile wall. This is obtained by an iterative procedure where an initial horizontal strain in the wedge is assumed.

After assuming a passive wedge depth the subgrade reaction modulus can be calculated along the pile. Based on the calculated subgrade reaction modulus the pile-head deflection can be calculated from the one-dimensional Winkler approach. Global stability is obtained when concordance between the pile-head deflection calculated by the Winkler approach and the SW-model is achieved. The passive wedge depth is varied until global stability is obtained.

The pile bending stiffness influence the pile deflection pattern calculated by the one-dimensional Winkler approach and hereby also the wedge depth. Hence, the pile bending stiffness influences the p–y curves calculated by the SW-model.

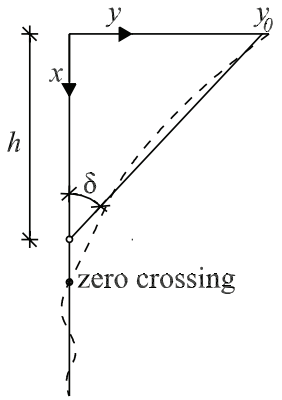

Figure 23: Linear deflection assumed in the SW-model, shown by the solid line. The dashed line shows the real deflection of a flexible pile. After Ashour et al. (1998).

The equations associated with the SW model are based on the results of isotropic drained triaxial tests. Hereby an isotropic soil behaviour is assumed at the site. The SW model takes the real stresses into account by dealing with a stress level, defined as:

$$SL = \frac{\Delta\sigma_h}{\Delta\sigma_{hf}} \tag{44}$$

where $\Delta\sigma_h$ and $\Delta\sigma_{hf}$ are the mobilised horizontal stress change and the horizontal stress change at failure, respectively. The spread of the wedge is defined by the mobilised friction angle, cf. (42) and (43). Hence the dimensions of the wedge depends on the mobilised friction.

Although the SW model is based on the three-dimensional soil-pile interaction, and although it is dependent on both soil and pile properties, there are still significant uncertainties related to the model. The model does not take the active soil pressure that occurs at the back of the pile into account, which is a non-conservative consideration. Furthermore, the wedge only accounts for the passive soil pressure at the top front of the pile and neglects the passive soil pressure beneath the zero

crossing point which will occur for a non-slender pile, cf. section 4.2. The assumption of an isotropic behaviour of the soil in the wedge seems unrealistic in most cases for sand. To obtain isotropic behaviour the coefficient of horizontal earth pressure, K, needs to be 1, which is not the case for most sands.

Ashour et al. (2002) criticise the p–y curve method as it is based and verified through a small number of tests. However, the SW model, has according to Lesny et al. (2007) been verified only for slender piles.

Ashour and Norris (2000) investigated by means of the SW model, the influence of pile stiffness on the lateral response for conditions similar to the Mustang Island tests. p–y curves at a depth of 1.83 m are shown in fig. 24 for different values of E_pI_p. The p–y curve proposed by Reese et al. (1974) is also presented in the figure. It is seen that there is a good concordance between the p–y curve formulation proposed by Reese et al. (1974) and the SW model for similar pile properties. It should be noted that in fig. 24, the p–y curve determined by means of the SW model depends on the pile bending stiffness such that an increase in the pile bending stiffness results in an increase in both the stiffness and the ultimate capacity of the p–y curves. For other pile and soil properties, Ashour and Norris (2000), found that an increase in the pile bending stiffness led to less stiff p–y curves. Hence, they conclude that the pile bending stiffness affects the p–y curves, but that the effect is dependent on the type of soil and the type of loading. Furthermore, they found that the effect of pile bending stiffness on the SW p–y curves is more significant for dense soils than for loose soils.

By means of the SW model Ashour and Norris (2000) found that the pile bending stiffness affects the shape of the p–y curves significantly. Fan and Long (2005) investigated the effect of pile bending stiffness

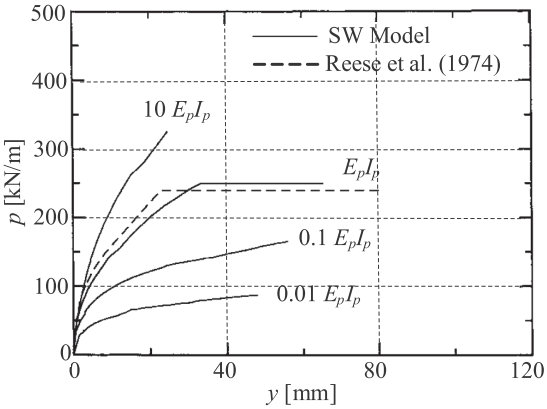

Figure 24: The influence of pile bending stiffness, after Ashour et al. (2000).

on the soil-pile interaction for piles situated in sand by means of numerical modelling. Fan and Long (2005) employed the constitutive model proposed by Desai et al. (1991). Both numerical models were validated against field tests. They calculated p–y curves by integration of the normal and shear stresses in soil surrounding the pile. Fan and Long (2005) did not find an effect of the pile bending stiffness on the shape of the p–y curves. In fig. 25 p–y curves calculated by means of the numerical model by Fan and Long can be observed for varying depht below soil surface and varying pile bending stiffness. For piles situated in clayey soil, Kim and Jeong (2011) found similar results. They also investigated the effect of bile bending stiffness by means of numerical modelling.

The conclusions of Fan and Long (2005) as well as Kim and Jeong (2011) contradicts the findings of Ashour and Norris (2000). More insight into the effect of the pile bending stiffness on the soil-pile interaction is therefore needed.

4.5 Effect of diameter on initial stiffness of p–y curves

The initial modulus of subgrade reaction, k, is according to API (2000), DNV (2010), and Reese et al. (1974) only dependent on the relative density of the

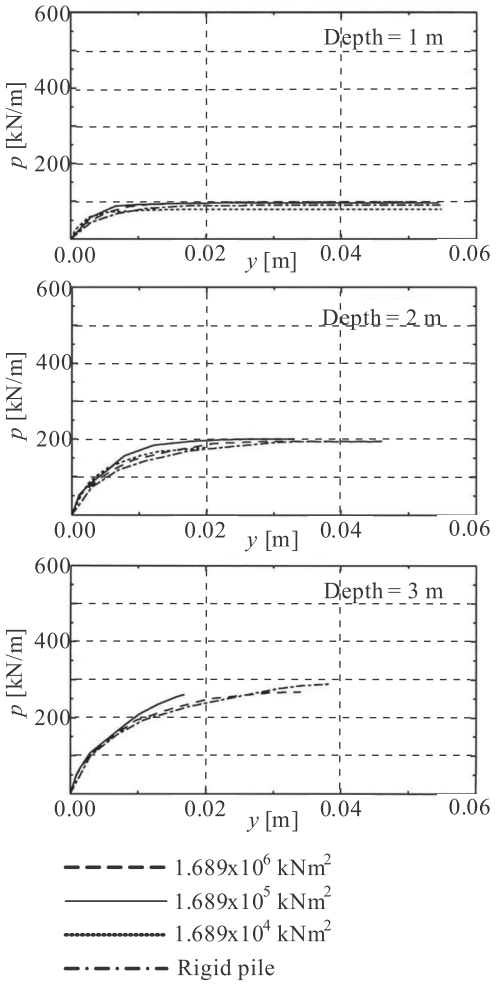

Figure 25: Effect of pile bending stiffness, after Fan and Long (2005).

soil. The dependency is shown in fig. 13. Hence, the methods A and B do not include E_pI_p and D in the determination of k. Different studies on the consequences of neglecting the pile parameters have been conducted over time with contradictory conclusions. Ashford and Juirnarongrit (2003) point out the following three conclusions in a summarization of previous research:

- Terzaghi (1955) analysed the effect of pile diameter on the modulus of subgrade reaction by consideration of stress bulbs forming in front of laterally loaded piles. Terzaghi concluded that by increasing the pile diameter the stress bulb formed in front of the pile is stretched deeper into the soil. This results in a greater deformation due to the same soil pressure at the pile. Terzaghi therefore postulated that the soil pressure acting on the pile wall is linearly proportional to the inverse of the pile diameter giving that the modulus of subgrade reaction, E_{py}, is independent on the diameter.

- Vesic (1961) proposed a relation between the modulus of subgrade reaction used in the Winkler approach and the soil and pile properties. This relation showed that E_{py} is independent of the diameter for circular and squared piles.

- Pender (1993) refers to two reports conducted by Carter (1984) and Ling (1988). Assuming a simple hyperbolic soil model for the relationship between soil resistance and pile deflection, they backcalculated values of E^*_{py} and p_u from field tests. In the backcalculation they assumed that Young's modulus of elasticity of the soil and therefore also the intial subgrade reaction modulus were constant with depth. Based on the backcalculations they proposed an expression of E^*_{py} which is linearly proportional to the pile diameter.

Pender et al. (2007) comments on the research of Carter (1984) and Ling (1988) and their conclusion of E^*_{py} varying linearly with pile diameter. Pender et al. (2007) questions the validity of a constant value of E_s with depth. Instead they propose E_s to be proportional to either the square root of the depth or to the depth. They suggests that the findings of Pender (1993) was due to a false assumption of the variation of Young's modulus of elasticity with depth. They, conclude that E^*_{py} is independent of the pile diameter.

The conclusions made by Terzaghi (1955) and Vesic (1961) concerns the subgrade re-

action modulus, E_{py}, while the conclusions made by Pender (1993) concerns the intial modulus of subgrade reaction, E^*_{py}. The conclusions of Terzaghi (1955) and Vesic (1961) might also be applicable for the initial modulus of subgrade reaction, k, and the initial stiffness, E^*_{py}.

Based on the investigations presented by Terzaghi (1955), Vesic (1961), Pender (1993), and Pender et al. (2007), it must be concluded that no clear correlation between the initial modulus of subgrade reaction and the pile diameter has been realised. Ashford and Juirnarongrit (2005) contributed to the discussion with their extensive study of the problem which was divided into three steps:

- Numerical modelling by means of a simple finite element model.
- Analyses of vibration tests on large-scale concrete piles.
- Back-calculation of p–y curves from static load tests on the concrete piles.

The finite element analysis was according to Ashford and Juirnarongrit (2005) very simple and did not account very well for the soil-pile interaction since friction along the pile, the effect of soil confinement, and gaps on the back of the pile were not included in the model. In order to isolate the effect of the diameter on the magnitude of E_{py}, the bending stiffness of the pile was kept constant when varying the diameter. The conclusion of the finite element analysis were that the diameter had some effect on the pile-head deflection as well as the moment distribution. An increase in diameter led to a decreasing pile-head deflection and a decreasing depth to the point of maximum moment. However, Ashford and Juirnarongrit (2005) concluded that the effect of increasing the diameter appeared to be relatively small compared to the effect of increasing the bending stiffness, E_pI_p.

The second part of the work by Ashford and Juirnarongrit (2005) dealt with vibration tests on large-scale monopiles. The tests included three instrumented piles with diameters of 0.6, 0.9, and 1.2 m (12 m in length) and one pile with a diameter of 0.4 m and a length of 4.5 m. All piles were cast-in-drilled-hole and made up of reinforced concrete. They were installed at the same site consisting of slightly homogenous medium to very dense weakly cemented clayey to silty sand. The piles were instrumented with several types of gauges, i.e. accelerometers, strain gauges, tiltmeters, load cells, and linear potentiometers. The concept of the tests were that by subjecting the piles to small lateral vibrations, the soil-pile interaction at small strains could be investigated.

Based on measured accelerations, the natural frequencies of the soil-pile system were determined. These frequencies were in the following compared to the natural frequencies of the system determined by means of a numerical model. Two different expressions for the modulus of subgrade reaction, E_{py}, were used: one that is linearly dependent; and one that is independent on the diameter. The strongest correlation was obtained between the measured frequencies and the frequencies computed by using the relation independent of the diameter. Hence, the vibration tests substantiate Terzaghi and Vesic's conclusions. It is noticed that the piles were only subjected to small deflections, hence $E_{py} \approx E^*_{py}$.

Finally, Ashford and Juirnarongrit (2005) performed a back-calculation of p–y curves from static load cases. From the back-calculation a soil resistance was found at the ground surface. This is in contrast to the p–y curves for sand given by Reese et al. (1974) and the recommendations in API (2000) and DNV (2010) in which the initial stiffness, E^*_{py}, at the ground surface is zero. The resistance at the ground surface might be a consequence of cohesion in

the slightly cemented sand or a result of magnification of measurement uncertainties when double-differentiating the strain-gauge measurements.

Furthermore, a comparison of the results from the back-calculations for the various pile diameters indicated that the effects of pile diameter on E^*_{py} were insignificant. The three types of analyses conducted by Ashford and Juirnarongrit (2005) therefore indicate the same: the effect of the diameter on E^*_{py} is insignificant.

Fan and Long (2005) investigated the influence of the pile diameter on the soil response by means of numerical modelling. They employed the constitutive model proposed by Desai et al. (1991) and a non-associative flow rule in their numerical model. By varying the diameter and keeping the bending stiffness, E_pI_p, constant in their finite element model they investigated the influence of the pile diameter on the initial subgrade reaction modulus. The results are given as curves normalised by the diameter and vertical effective stress as shown in fig. 26. No significant correlation between diameter and initial stiffness is observed. It must be emphasised that the investigation considered only slender piles.

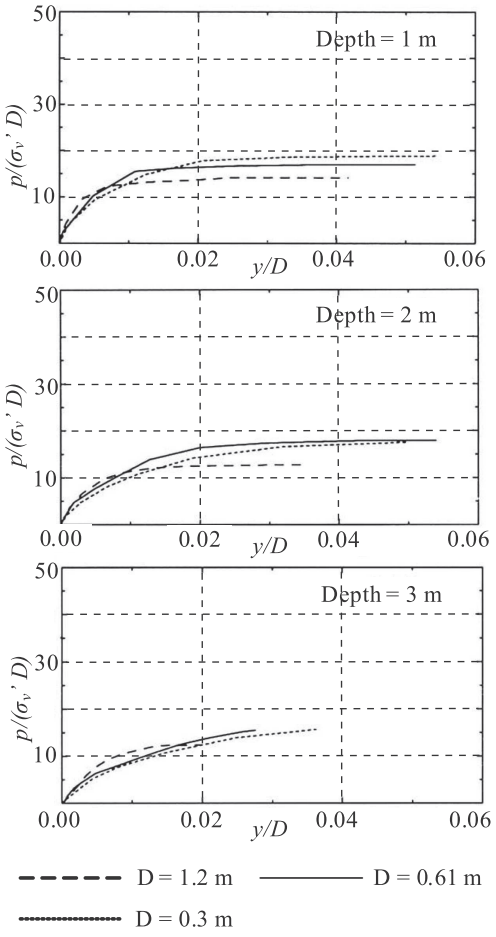

Figure 26: Effect of changing the diameter, after Fan and Long (2005).

For non-slender piles the bending stiffness might cause the pile to deflect almost as a rigid object. Therefore, the deflection at the pile-toe might cause a significant soil resistance near the pile toe. Thus a correct prediction of the variation of initial stiffness with depth is important in order to determine the correct pile deflection.

Based upon a design criterion demanding the pile to be fixed at the toe, Lesny and Wiemann (2006) investigated by back-calculation the validity of the assumption of a linearly increasing E^*_{py} with depth. The investigation indicated that E^*_{py} is overestimated for large-diameter piles at great depths. Therefore, they suggested a power function, to be used instead of a linear relation, cf. fig. 27. A finite element model was made in order to validate the power function. The investigations showed that employing the power function approach gave deflections more similar to the numerical modelling than by using the traditional linear approach in the p–y curve method. However, it was emphasised that the method should only be used for determination of pile length. The p–y curves still underestimates the pile-head deflections even though the parabolic approach is used.

The above mentioned investigations all made by means of cohesionless soils are summarised in tab. 4. From this tabular it is obvious that more research is needed.

Looking at cohesive materials the tests are also few. According to Ashford

Table 4: Chronological list of investigations concerning the effects of diameter on the initial stiffness of the p–y curve formulations.

Author	Method	Conclusion
Terzaghi (1955)	Analytical	Independent
Vesic (1961)	Analytical	Independent
Carter (1984)	Analytical expression calibrated against full-scale tests	Linearly dependent
Ling (1988)	Validation of the method proposed by Carter (1984)	Linearly dependent
Ashford and Juirnarongrit (2005)	Numerical and large-scale tests	Insignificant influence
Fan and Long (2005)	Numerical	Insignificant influence
Lesny and Wiemann (2006)	Numerical	Initial stiffness is non-linear for long and large-diameter piles
Pender et al. (2007)	Analytical expression calibrated against full-scale tests	Independent

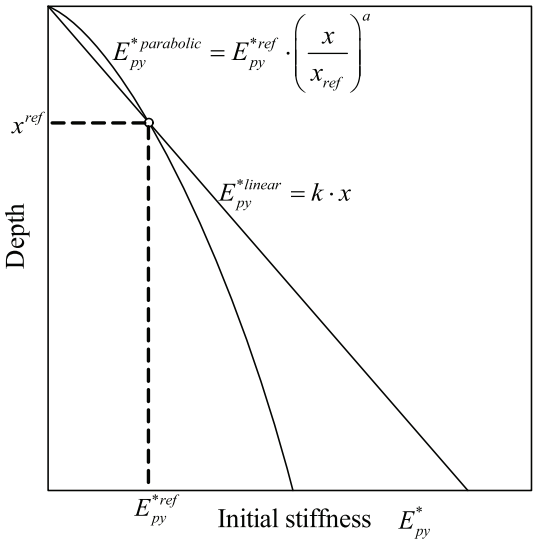

Figure 27: Variation of initial stiffness, E_{py}^{*}, as function of depth, after Lesny and Wiemann (2006). The linear approach is employed in Reese et al. (1974) and the design codes, e.g. API (2000) and DNV (2010). The exponent a can be set to 0.5 and 0.6 for dense and medium dense sands, respectively.

and Juirnarongrit (2005) the most significant findings are presented by Reese et al. (1975), Stevens and Audibert (1979), O'Neill and Dunnavant (1984), and Dunnavant and O'Neill (1985).

Reese et al. (1975) back-calculated p–y curves for a 0.65 m diameter pile in order to predict the response of a 0.15 m pile. The calculations showed a good approximation of the moment distribution, but the deflections however were considerably underestimated compared to the measured values associated with the 0.15 m test pile.

Based on published lateral pile load tests Stevens and Audibert (1979) found that deflections computed by the method proposed by Matlock (1970) and API (1987) were overestimated. The overestimation increases with increasing diameter leading to the conclusion that the modulus of subgrade reaction, E_{py}, increases for increasing diameter.

By testing laterally loaded piles with diameters of 0.27 m, 1.22 m, and 1.83 m in an overconsolidated clay, O'Neill and Dunnavant (1984) and Dunnavant and O'Neill (1985) found that there were a non-linear relation between deflection and diameter. They found that the deflection at 50 %

of the ultimate soil resistance generally decreased with an increase in diameter. Hence, E_{py} increases with increasing pile diameter.

Kim and Jeong (2011) and Jeong et al. (2011) investigated the effect of pile diameter on the initial stiffness through numerical modelling. They considered piles situated in clay. They found that the intial stiffness of the p–y curves increases linearly with the square root of the pile diameter.

4.6 Choice of horizontal earth pressure coefficient

When calculating the ultimate soil resistance by method A the coefficient of horizontal earth pressure at rest, K_0, equals 0.4 even though it is well-known that the relative density/the internal friction angle influences the value of K_0. In addition, pile driving may increase the coefficient of horizontal earth pressure K.

The influence of the coefficient of horizontal earth pressure, K, is evaluated by Fan and Long (2005) for three values of K and an increase in ultimate soil resistance were found for increasing values of K. The increase in ultimate soil resistance is due to the fact, that the ultimate soil resistance is primarily provided by shear resistance in the sand, which depends on the horizontal stress.

Reese et al. (1974), and O'Neill and Murchison (1983) and thereby also API (2000) and DNV (2010) consider the initial modulus of subgrade reaction k to be independent of K. Fan and Long (2005) investigated this assumption. An increase in K results in an increase in confining pressure implying a higher stiffness. Hence, k is highly affected by a change in K such that k increases with increasing values of K.

4.7 Shearing force at the pile-toe

Recently installed monopiles have diameters around 4 to 6 m and a pile slenderness ratio around 5. Therefore, the bending stiffness, E_pI_p, is quite large compared to the pile length. The pile curvature will therefore be small and the pile will almost behave as a rigid object as shown in fig. 28.

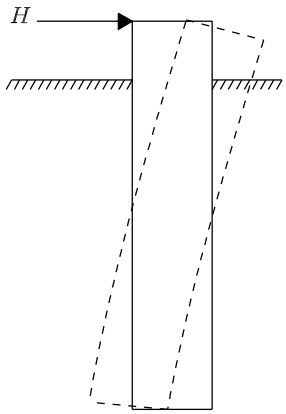

Figure 28: Deflection curve for non-slender pile.

As shown in fig. 28 there is a significant negative deflection at the pile-toe. This deflection causes shearing stresses at the pile-toe to occur, which increase the total lateral resistance. According to Reese and Van Impe (2001) a number of tests have been made in order to determine the shearing force at the pile-toe, but currently no results from these tests have been published and no methods for calculating the shearing force as a function of the pile toe deflection have been proposed.

Due to rigid pile behaviour normal stresses at the pile toe will inflict a bending moment on the pile toe resulting in a bigger pile stiffness and capacity. Research is needed to establish a relationship between the pile toe rotation and the applied moment at the pile toe.

4.8 Shape of p–y curves

Currently, a tangent hyperbolic function is employed to describe the shape of p–y curves for piles in sand, cf. (29) and O'Neill and Murchison (1983). Other shapes of p–y curves has also been proposed to describe the relationship between the soil resistance acting on the pile wall and the pile deflection, for instance, Reese et al. (1974), Scott (1980), PHRI (1980), and Carter (1984). Reese et al. (1974) suggested the use of a piecewise curve consisting of an initial straight line, a parabola, and a straight line. These three curves were assembled into one continuous piecewise differentiable curve, cf. Method A. Scott (1980) proposed a p–y curve for sand consisting of two straight lines. His recommendation was based on centrifuge tests of laterally loaded piles. The expression of Scott (1980) is not bounded by an upper limit. Hence, the ultimate soil resistance is not considered in that method. Murchison and O'Neill (1984) compared these three expressions with a series of field tests on flexible piles and found the tangent hyperbolic function to fit best with the tests. Carter (1984) proposed the use of a hyperbolic expression for p–y curves in sand:

$$p(y)^n = \frac{y}{1/E_{py}^* + y/p_u^n} \qquad (45)$$

where n is a dimensionless constant. Carter (1984) proposed to use $n = 1$ for sand and $n = 0.2$ for clay. Ling (1988) confirmed the hyperbolic expression by comparison with 28 full-scale tests on flexible piles.

PHRI (1980) proposes the use of a p–y curve formulation in which the soil resistance is proportional with the square of the pile deflection. Hence, this p–y curve formulation is not bounded by an upper limit. Terashi (1989) found a good agreement between this p–y curve expression and centrifuge tests on flexible piles situated in dense sand.

The accuracy of the p–y curves proposed by O'Neill and Murchison (1983), Carter (1984), and PHRI (1980) needs to be compared and validated for non-slender piles.

4.9 Layered soil

The p–y curve formulations of Reese et al. (1974), Murchison and O'Neill (1974), etc. considers piles situated in homogeneous soil. However, the soil stratification is rarely homogeneous. A few analytical studies on the effect of layered soils have been conducted, for instance, Davisson and Gill (1963), Khadilkar et al. (1973), Naik and Peyrot (1976), and Dordi (1977). However, these analyses do not consider the non-linearity of the soil.

Georgiadis (1983) proposed a new approach to develop p–y curves in a layered soil stratification. The approach involves the determination of an equivalent depth, h, for all soil layers existing below the upper soil layer. The equivalent depth of layer i is determined by solving h_i in the following equation:

$$F_1 + ... + F_{i-1} = F_i \Rightarrow \qquad (46)$$

$$\int_0^{H_1} p_u dx + ...+ \int_{h_{i-1}}^{h_{i-1}+H_{i-1}} p_u dx = \int_0^{h_i} p_u dx \qquad (47)$$

where F_1 is the sum of the ultimate soil resistance for layer 1, F_{i-1} is the sum of the ultimate soil resistance for the $(i-1)$'th, and F_i is the sum of the ultimate soil resistance for the i'th layer. H_1, H_{i-1}, and H_i are the layer thickness of soil layer 1, $i-1$, and i, respectively. h_{i-1} and h_i are the equivalent depth of the soil layers $i-1$ and i.

Georgiadis (1983) validated his method against a field test at Lake Austin on a pile with a diameter of 0.152 m and an embedded pile length of 4.9 m. Hence, the length to diameter ratio was 32.2 and the pile can be considered as flexible. The soil stratification at the site consisted of 0.38 m of stiff clay overlying a medium dense sand layer. The proposed method for layered soil fitted the field test very well.

It should be emphasized that the method of Georgiadis (1983) for deriving p–y curves for layered soils is developed and validated for flexible piles. The method still needs validation for piles behaving rigidly.

Based on numerical analyses Yang and Jeremic (2005) as well as McGann et al. (2012) investigated laterally loaded piles situated in a layered soil stratification. Yang and Jeremic (2005) modelled the behaviour of a flexible square pile situated in a stratification of sand and soft clay. They conducted numerical simulations with both a sand-clay-sand and a clay-sand-clay stratification. The analysis of McGann et al. (2012) is based on circular piles situated in seismic areas exposed to lateral spreading. They considered piles installed in sands with a loose liquified intermediate layer.

Yang and Jeremic (2005) used von Mises constitutive model to model the clay and the Drucker-Prager constitutive model for the sand. They modelled a pile with a width of 0.429 m and a length of 13.7 m. Hence, the slenderness ratio was 31.9. Similar to Georgiadis (1983) they found that the upper layers affected the p–y curves of the lower layers. Further, they found that the lower layers also affected the p–y curves of the upper layers in such a way that the p–y curves of a stiff upper layer are reduced near a soft intermediate layer. The size of the reduction was found to depend on the distance to the interlayer, such that the largest reduction took place at the interlayer. For the clay-sand-clay stratification they found that the stiff intermdiate layer resulted in increased soil resistance in the upper clay layer.

McGann et al. (2012) used the Drucker-Prager constitutive model in their numerical model. They modelled a circular pile with a diameter varying from 0.61 m to 2.5 m. Similar to Yang and Jeremic (2005) they found that the intermediate layer affects the soil resistance of the upper layer. According to McGann et al. (2012) the stiff soil near the interface of the weaker intermediate layer can be pushed into the weaker layer as the pile deflects laterally. This explains the reduction in the soil resistance of the stiff soil layers.

Based on their numerical simulations, McCann et al. (2012) presented an expression for the reduction of the soil resistance of the upper and lower layer. The reduction depends exponentially on the distance from the intermediate layer. Other parameters such as the pile diameter, the depth of the intermediate layer, the friction angle of the upper and lower layers, and the thickness of the intermediate layer were also included in the expression for the reduction. The analysis of McGann et al. (2012) considered the intermediate layer as liquefied. Their expression is therefore only validated for stratifications with an intermediate layer which is liquefied. The expression might however also be valid in stratifications where the intermediate layer is significantly softer than the upper and lower layers, for instance stratifications with an organic intermediate layer.

4.10 Long-term cyclic loading

Offshore wind turbines are exposed to cyclic loading from the wind and wave forces. During the lifetime of an offshore wind turbine the foundation will be exposed to a few number of load cycles with

large amplitudes due to storms and further to 10^6-10^8 load cycles with low or intermediate amplitudes. The ratio between the minimum and maximum load in each cycle, ζ_c, will vary with time. The ratio between the maximum load in each cycle and the static pile capacity is in the following denoted as ζ_b. When designing monopile foundations for offshore wind turbines it should be ensured that the accumulated pile rotation is less than the value specified by the wind turbine supplier. Similarly, it should also be ensured that the natural frequency of the combined structure is within the range specified by the wind turbine supplier. Typically, the foundation is designed such that the natural frequency of the combined structure is within the rotor frequency and the blade passing frequency. According to LeBlanc (2009), wind turbines are often designed such that the rotor frequency is in the range of 0.17-0.33 Hz, while the blade passing frequency typically is in the range of 0.5-1.0 Hz. The energy rich wind turbulence lies below a frequency of 0.1 Hz, and the frequency of extreme waves is typically in the range of 0.07-0.14 Hz. When a pile is exposed to cyclic loading, the stiffness of the soil might change due to a reconfiguration of the soil particles. Therefore, knowledge regarding the influence of cyclic loading on the stiffness of the soil-pile interaction is necessary for accurate determination of the accumulated pile rotation and of the variation of the natural frequency for the combined structure with time.

The p–y curve formulations proposed by Reese et al. (1974) and O'Neill and Murchison (1983) accounts for cyclic loading by means of reductions of the empirical factors A and B. Hence, the accumulated pile deflection is accounted for, however, in a very simplified manner. Changes in the initial stiffness of the p–y curves is not accounted for, since A only affect the upper limit of soil resistance (Method A and B), and B the soil resistance at a pile deflection of $y = D/60$ (Method A). The parameters A and B for cyclic loading are based on few tests on flexible piles with up to approximately 100 load cycles. Further, the influence of relative density, installation method, number of cycles, etc. are not included in the expression of A and B for cyclic loading. Hence, these p–y curve formulations are incomplete in describing the cyclic pile behaviour of monopile foundations for offshore wind turbines.

The behaviour of laterally loaded piles subjected to cyclic loading has been investigated by means of experimental testing and numerical modelling. The major findings are summarised in the following. The pile and soil properties as well as loading conditions for the experimental testing which is referred to regarding the behaviour of cyclically loaded piles are summarised in tab. 5.

Long and Vanneste (1994) summarises previous research regarding the behaviour of cyclically loaded piles:

- Prakash(1962), Davisson and Salley (1970), and Alizadeh and Davisson (1970) considered the cyclic pile response based on model and field tests. Prakash (1962) and Davisson and Salley (1970) conducted model tests on aluminium pipe piles with outer diameters of 12.7 mm (0.5 in) and embedded pile lengths of 0.533 m (21 in). Hence the slenderness ratio is 40 and the piles can be considered as flexible. The piles were situated in medium dense dry sand. Alizadeh and Davisson (1970) conducted field tests on a pile with an outer diameter of 0.4 m and a slenderness ratio of 40. The pile was situated in a layered soil consisting of silty sand to gravelly sand. Prakash (1962), Davisson and Salley (1970) as well as Alizadeh and Davisson (1970) concluded that for 50 or more load cycles the cyclic stiffness of the modulus of subgrade reaction is approximately 30 % of the

Table 5: Pile, soil and loading properties for the model and field tests used for investigation of the behaviour of cyclically loaded piles.

	Pile diameter D [m]	Embedded pile length L [m]	Slenderness ratio L/D [-]	Soil compaction	ζ_b [-]	ζ_c [-]	N [-]
Cox et al. (1974)/ Reese et al. (1974)	0.61	21.0	34	medium dense to very dense		(-1)-(-0.25)	0-100
Prakash (1962)	0.0127	0.533	40	Medium dense			100
Davisson and Salley (1970)	0.0127	0.533	40	Medium dense			4
Alizadeh and Davisson (1970)	0.400	16	40	Loose		0	100
Little and Briaud (1988b)	0.510-1.065	29.6-39.0	32-60	Medium dense		0-0.5	21
Long and Vanneste (1994)	0.145-1.430	3.8-39.0	3-84	Loose to dense		(-1.0)-0.5	5-500
Lin and Liao (1999)	0.145-1.430	5.0-21.0	4-84	Loose to dense		(-1.0)-0.1	4-100
Peng et al. (2006)	0.0445	0.400	9	Medium dense	0.2-0.6	(-1)-(-0.6)	10000
Peralta and Achmus (2010)	0.060-0.063	0.200-0.500	3-8	Medium dense		0	10000
LeBlanc et al. (2010a)	0.080	0.360	4.5	very loose to loose	0.20-0.53	(-1.0)-1.0	7000-65000
LeBlanc et al. (2010b)	0.080	0.360	4.5	very loose to loose	0.28-0.53	0	100-10000

static stiffness.

- Broms (1964) similarly considered the cyclic pile behaviour based on the subgrade reaction method. He found that the degradation of the static stiffness depends on the relative density of the soil, such that the stiffness is reduced to 25 % of the static stiffness for loose soils and to 50 % for dense soils. The mentioned reductions in subgrade reaction modulus was for 40 load cycles.

- Little and Briaud (1988b) proposed to degrade the soil resistance in the p–y curve formulation with the number of load cycles by means of an exponential expression: $p_c = p_s N^{-a}$. The cyclic soil resistance is denoted p_c, the static soil resistance is denoted p_s, the number of load cycles is denoted N and a is an empirical factor. The expression was validated against 12 pressuremeter tests on model piles with outer diameters of 34.5 mm (1.36 in) situated in dry sand. Further, the expression was validated against six field tests on pipe piles driven or drilled into the soil. The piles had outer diameters of 0.510 m to 1.065 m, embedded pile lengths of 29.6 to 39.0 m and slenderness ratios of 32 to 60. The piles therefore exhibited a slender pile behaviour. The pile slender-

ness ratio varied from 37 to 59. The piles were installed in medium dense sand.

Long and Vanneste (1994) analysed 34 field tests on piles exposed to cyclic lateral loading. The pile dimensions were $D = 0.145 - 1.43$ m, $L_p = 3.8 - 39.0$ m, $L_p/D = 3 - 84$. Various pile cross-sections and installation methods were used for the 34 field tests. The soil compaction varied from loose to dense and the number of load cycles varied from 5 to 500. Based on back-analyses of the field tests, they proposed to degrade the static p–y curve formulation proposed by Reese et al. (1974) in the following way to account for cyclic loading:

$$p_N = p_1 * N^{-0.4t} \tag{48}$$

$$y_N = y_1 * N^{0.6t} \tag{49}$$

where p_N is the soil resistance after N cycles, p_1 is the static soil resistance, y_N is the pile deflection after N cycles, y_1 is the static pile deflection, and t is a dimensionless parameter. The dimensionless parameter t was found to depend primarily on ζ_c, but also the installation method and the relative density were found to exhibit a minor influence on t. They found that t assumes the largest values for one-way cyclic loading with $\zeta_c = 0.0 - 0.5$.

Lin and Liao (1999) proposed a method for determination of the accumulated pile displacement caused by mixed lateral loading. Their method is based on the expression for the cumulative strains due to mixing of different amplitude loads proposed by Stewart (1986) and on Miner's rule (Miner, 1945). In their method, they assume that the representative lateral strain can be calculated from the pile deflection as $\epsilon = y/(2.5D)$. This relationship between the lateral strain and the pile deflection was originally suggested by Kagawa and Kraft (1980). Lin and Liao (1999) suggest that the relationship, R_s, between the lateral strain after N cycles, ϵ_N, and the lateral strain after one cycle, ϵ_1, is given as:

$$R_s = \frac{\epsilon_N}{\epsilon_1} = 1 + t\ln(N) \tag{50}$$

where t depends on the relative density, the installation method, ζ_c and the ratio between the pile length and the pile/soil relative stiffness, T. They calibrated the parameter t against 20 field tests on piles with outer pile diameters of 0.145-1.43 m, embedded pile lengths of 5.0-21.0 m and slenderness ratios of 4-84. The installation method varied and further the soil compaction varied from loose to dense. They validated their method against the field tests presented by Little and Briaud (1988b). A reasonable agreement were found with the tests. It should be noted that the number of load cycles in the field tests were limited to a maximum of 100 cycles.

Peng et al. (2006) invented a new testing device for cyclic loading of laterally loaded piles. By means of the new testing device they conducted two-way cyclic tests with 10000 cycles and both balanced and unbalanced cyclic loading. They concentrated on the development of the innovative testing device and only presented few results from cyclic load tests. The test results they presented were for a pile with an outer diameter of 44.5 mm, an embedded pile length of 400 mm and a slenderness ratio of 9. The pile was situated in a dry sand with $I_D = 71.7$ %. The loading frequency were varied from 0.45-0.94 Hz. The applied cyclic loading had $\zeta_b = 0.2 - 0.6$ and $\zeta_c = (-1) - (-0.6)$. They concluded that the pile displacement increases for increasing loading frequency. Whether this was due to resonance between the natural frequency of the pile and the loading was not discussed. They found that the accumulated pile displacement is significantly greater for unbalanced loading than balanced loading, which is similar to the findings of Long and Vanneste (1994) and Lin and Liao (1999). Further,

they found that within 10000 load cycles the accumulated pile deflection continued to increase.

Lesny and Hinz (2007) proposed to model the cyclic pile behaviour by means of a combination of finite element modelling and cyclic triaxial testing. They implemented the results from undrained, unconsolidated, stress-controlled cyclic triaxial tests in the constitutive model. The method for the finite element modelling of the cyclic pile behaviour includes the following steps:

- At first the variation of load versus number of load cycles is estimated. The loading is divided into a number of load levels each with a corresponding number of load cycles.
- For varying load levels the induced states of stresses in the soil is calculated by finite element analysis using soil parameters for static loading.
- Triaxial tests are conducted according to the determined stress conditions.
- The accumulated plastic strain per load level is calculated, and their sum is determined with use of Miner's rule (Miner, 1945).
- The soil properties are modified to account for the cyclic behaviour, and the pile behaviour is determined by means of finite element modelling employing the updated soil parameters.

The method proposed by Lesny and Hinz (2007) needs to be validated against cyclic tests on laterally loaded piles.

Achmus et al. (2009b) analysed the cyclic pile behaviour of non-slender large-diameter piles through numerical modelling employing the Mohr-Coulomb constitutive model. The cyclic behaviour ofthe soil was implemented through a degrading soil stiffness. The formulation proposed by Huurman (1996), which is based on triaxial testing of cohesionless soil, was applied to express the stiffness degradation. Achmus et al. (2009b) presented a parametrical study on the accumulation of pile deflection due to cyclic loading in which the pile diameter, the pile length, the loading eccentricity, the relative density and ζ_b was varied within $D = 2.5 - 7.5$ m, $L = 20 - 40$ m, $e = 0 - 40$ m, medium dense to dense sand and $\zeta_b = 0 - 0.6$. For all the simulations one-way loading with $\zeta_c = 0$ were applied. Based on the parametric study they presented design charts relating the ratio between the static and cyclic pile deflection (accumulation rate of deformation) with ζ_b for varying numbers of load cycles. They found that the pile diameter, the embedded pile length, and the relative soil density affect the accumulation rate of deformation through their effect on the static pile capacity and hence also their effect on the normalized load.

Peralta and Achmus (2010) conducted a series of 1-g tests on both flexible and rigid piles in order to investigate the behaviour of cyclic loaded piles. The pile dimensions was $D = 60 - 63mm$ and $L = 200 - 500mm$. The pile material employed for the tests varied from steel to high density poly-ethylene (HDPE). The piles made of HDPE behaved as slender piles due to the significantly lower Young's modulus of elasticity for HDPE. One-way cyclic loading with $\zeta_c = 0$ were considered. For each test, the 10000 load cycles were applied. They attempted to fit both an exponential and a logaritmic expression for the accumulation of displacement to the test results, as proposed by Long and Vanneste (1994) and Lin and Liao (1999), respectively. They concluded that the exponential function for the displacement accumulation fitted well with the experimental tests on rigid piles while the logarithmic expression fitted the flexible piles well. They presented a comparison of the evaluation of accumulated pile deflec-

tion for two equivalent irregular load patterns: one in which the cyclic load amplitude ascended; and one in which the cyclic load amplitude descended. From the comparison it could be observed that the accumulated load displacement was approximately 25 % higher for the irregular cyclic load pattern with ascending loads than the pattern with descending loads.

LeBlanc et al. (2010a) and LeBlanc et al. (2010b) investigated the cyclic behaviour of non-slender piles through small-scale testing at 1-g. They tested a pile with an outer diameter of 80 mm and an embedded pile length of 360 mm. The slenderness ratio was hereby 4.5 implying rigid pile behaviour. They conducted tests at relative soil densities of 4 and 38 %. The pile was exposed to a series of cyclic load tests with varying ζ_b and ζ_c. ζ_b was varied between 0.2 and 0.53, while ζ_c was varied from -1 to 1. The values of ζ_b corresponds to loads ranging from the fatigue limit state (FLS) to the serviceability limit state (SLS).

LeBlanc et al. (2010a) considered the accumulated pile rotation and the change in pile stiffness for continouos long-term cyclic loading. Regarding the accumulated pile rotation, they proposed the following expression:

$$\frac{\Delta\theta(N)}{\theta_s} = T_b(\zeta_b,I_D)T_c(\zeta_c)N^{0.31} \qquad (51)$$

where T_b and T_c are dimensionless functions. They found that T_b increases for increasing values of both ζ_b and I_D, while they proposed a nonlinear variation of T_c with ζ_c. For ζ_c equal to either -1 or 1, e.i. two-way cyclic loading with a mean value of 0 and static loading, respectively, they suggested that T_c is 0, while for $\zeta_c = 0$, the dimensional function T_c assumes a value of 1. The maximum value of T_c was proposed to 4 at $\zeta_c = -0.6$, which implies that two-way cyclic loading with $\zeta_c = -0.6$ give rise to significantly larger pile rotations than one-way cyclic loading.

In LeBlanc et al. (2010a) also the variation of pile stiffness, $k = M/\theta$, was investigated. They found that the pile stiffness increases with the number of load cycles, and further that the increase is independent of factors such as ζ_b, ζ_c, and I_D. It seems questionable that the relative density should have no influence on the increase in pile stiffness. Therefore cyclic tests at higher values of relative density are needed to further extrapolate the findings from LeBlanc et al. (2010a).

LeBlanc et al. (2010b) investigated the accumulated pile rotation for piles exposed to random cyclic loading. They found that the sequence of loading has no significant influence on the accumulated pile rotation. Further, they found that the number of cycles to neutralise N reversal load cycles is more than N. Based on that they concluded that conservatively it can be assumed that N load cycles are necessary to neutralise N reversal load cycles. Based on the experimental tests they proposed a method to account for random cyclic loading in the determination of the accumulated pile rotation. They suggested to divide a time-series of random cyclic loading into a number of load sequences by means of the extended rainflow method proposed by Rychlik (1987). The accumulated pile rotation of the the i'th load sequence, θ_i, can then be determined by means of the following equations:

$$\Delta\theta_i = ((\Delta\theta_{i-1})^{1/0.31} + (\theta_s T_b T_c)_i^{1/0.31} N_i)^{0.31} \qquad (52)$$

$$\theta_i = \Delta\theta_i + \max(\theta_{s,1},...,\theta_{s,i}) \qquad (53)$$

where the subscript i denotes the i'th load sequence. The equations are based on the findings in LeBlanc et al. (2010a) and Miner's rule (Miner, 1945).

Achmus et al. (2010a) validated the numerical model proposed by Achmus et al. (2009b) against the small-scale tests reported by LeBlanc et al. (2010a). A reasonable agreement between the numerical model and the experimental findings

were found. However, further validation of the numerical model is needed. It should be noted that the cyclic soil behaviour which they assumed in their numerical model was not based on the sand material employed in the tests by LeBlanc et al. (2010a).

Summary

The effect of continouos long-term cyclic loading on the accumulated pile rotation/deflection has been investigated experimentally for both slender and non-slender piles. For slender piles several model and field tests have been reported in the litterature. The number of load cycles have however for the majority of these tests been less than 100. For non-slender piles the experimental research on the cyclic pile behaviour relies on model tests. The majority of the researchers propose an exponential relationship between the number of cycles and the accumulated pile rotation. However, the research reveals opposing conclusions regarding the effect of the relative density on the exponent relating the pile rotation with the number of cycles.

The effect of continouos long-term cyclic loading on the pile behaviour has been investigated through numerical modelling in which the soil stiffness is degraded based on triaxial tests (Lesny and Hinz, 2007; and Achmus et al., 2009b). The prospect of degrading the soil stiffness in the constitutive models on the basis of triaxial testing is an interesting idea. However, validation against experimental work (preferably field tests) is needed.

Only few experimental pile tests have been conducted regarding the accumulated pile rotation for random long-term cyclic loading. LeBlanc et al. (2010b) found that the accumulated pile rotation is independent of the loading sequence, which disagrees with the findings of Peralta and Achmus (2010). The influence of loading sequence needs to be further investigated. LeBlanc et al. (2010b) proposed a method for determination of the accumulated pile rotation based on the extended rainflow method proposed by Rychlik (1987) and Miner's rule.

Research regarding the variation of the stiffness of the soil-pile interaction with long-term cyclic loading is needed. Results from LeBlanc et al. (2010a) indicate that the stiffness increases logarithmically with the number of cycles and that the increase is independent of the relative density. However, the tests were only conducted in loose to medium dense soil, and hence a further investigation is needed for dense to very dense soil.

4.11 Scour effect on the soil-pile interaction

Around a vertical pile placed on the seabed the water-particle flow from currents and waves will undergo substantial changes causing erosion of soil material. Hence, local scour holes around these piles will form. When large wind farms are built, scouring can also take place on a more global scale. The scour depth of local scour holes can according to DNV (2010) be up to 1.3 times the pile diameter. Scour protection consisting of rock infill can be employed to avoid the development of scour. However, scour protection is very expensive and on some locations it can be hard to deploy due to the sea conditions. Det Norske Veritas provide regulations for the possible depths of global and local scour holes (DNV, 2010). Further, they require that the p–y curves are modified for the presence of scour. However, they do not provide any regulations on how to modify the p–y curves for the presence of global and local scour.

The International Organization for Standardization, ISO, and the American

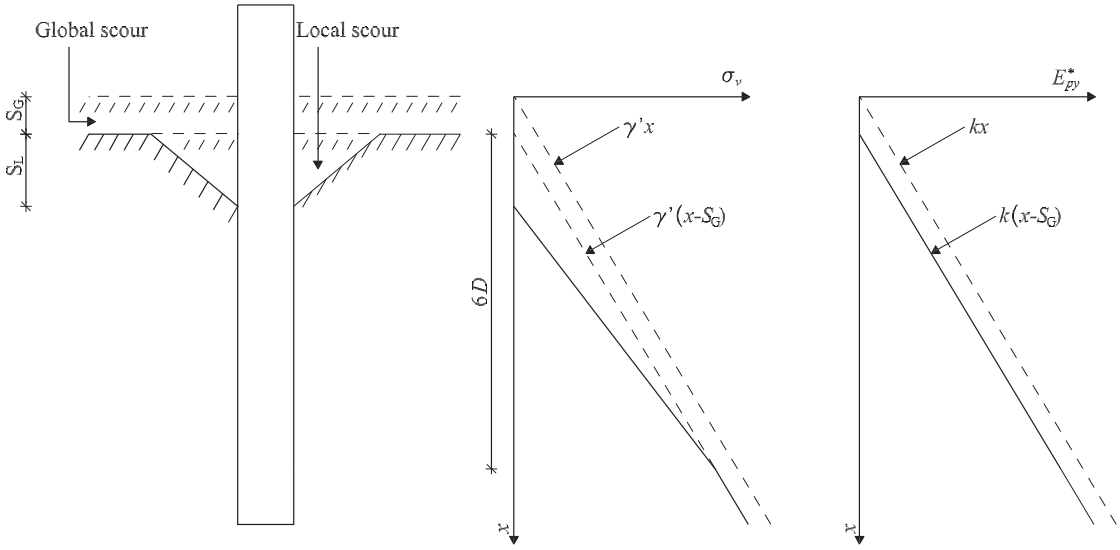

Figure 29: Reduction in effective vertical stresses and initial stiffness of the p–y curves due to global and local scour, after ISO (2007).

Petroleum Institute, API, provides a simple method to account for local and global scour in the p–y curve formulation (ISO, 2007; API, 2008) in which the effective vertical stresses are assumed to vary with depth as shown in fig. 29. The change in effective vertical stress changes the value of the ultimate soil resistance, cf. (28). They only reduce the initial stiffness of the p–y curves due to the presence of global scour. In ISO (2007) and API (2008) it is stated that the method shown in fig. 29 is not generally accepted.

When local and global scour takes place, the effective soil stresses decrease. Hence, the soil becomes slightly overconsolidated, with the largest overconsolidation ratio in the upper soil layers. As the soil becomes overconsolidated the soil strength increases. Hence, it is conservative not to take the overconsolidation effect into account. Lin et al. (2010) modified the p–y curve formulation proposed by Reese et al. (1974) to account for the effect of overconsolidation. Due to the overconsolidation the coefficient of horizontal earth pressure increases, and further, the friction angle increases. These changes in the soil properties were incorporated in the expression of p_u, cf. (12) and (13). They compared the pile behaviour calculated by means of a Winkler model approach for the test piles at Mustang Island, cf. Cox et al. (1974), for two conditions: one in which the original friction angle and coefficient of horizontal earth pressure were used; and one in which the overconsolidated parameters were used. They found a significant increase in p_u when the soil is considered to be overconsolidated. Further, the maximum bending moment in the pile decreased with 7 % when assuming overconsolidated soil. Hence, for piles installed without scour protection, the effect of overconsolidation should be incorporated in the design.

Achmus et al. (2010b) conducted a numerical study of the effect of scour on the lateral pile behaviour of non-slender large-diameter piles. They employed the commercial program ABAQUS and the Mohr-Coulomb constitutive model. They incorporated cyclic soil behaviour by means of the degradation stiffness method (Achmus et al., 2007; Kuo, 2008). They varied parameters such as the pile diameter, the scour depth, and the loading eccentricity. They concluded that, the effect of scour increases for decreasing pile slenderness ratio. Further, they found that scour is more

unfavourable for small loading eccentricities.

Due to changing sea conditions the scour depth around unprotected monopile foundations will vary with time. The process in which the scour depth is decreasing is termed backfilling. Currently, there is no knowledge regarding the properties of the backfilled soil material and how to incorporate this in a Winkler approach. Knowledge regarding these issues are important for the fatigue design of the steel material used for the monopile.

5 Conclusion

Monopiles are an often used foundation concept for offshore wind energy converters. They are usually designed by use of the p–y curve method which is a versatile and practical design method. Furthermore, the method has a long history of approximately 50 years of experience.

The p–y curve method was originally developed to be used in the offshore oil and gas sector and has been verified for flexible piles with pile diameters up to approximately 2 m. However, for offshore wind turbines, monopiles with diameters of 4 to 6 m and a slenderness ratio around 5 are not unusual.

In the present review a number of the assumptions and not clarified parameters associated with the p–y curve method have been described. The analyses considered in the review state various conclusions of which some are rather contradictory. Important findings of this paper are summarised as follows:

- When employing the Winkler model approach, the soil response at a given depth is assumed to be independent of the deflections above and below that given depth. Pasternak (1954) proposed a modification of the Winkler model approach in which the shear stress between soil layers is accounted for. However, the effect of involving the shear stress between soil layers seems to be rather small, and from the analysis it is not clear whether the results are dependent on pile properties.

- The failure modes assumed when dealing with the ultimate soil resistance at shallow depth seems rather unrealistic. In the traditionally employed methods the surface of the pile is assumed smooth. Furthermore, the method does not take the pile deflection pattern into account, which seems critical for rigid piles.

- Soil dilatancy affects the soil response such that a large value of the dilatancy angle leads to large values of the ultimate soil resistance. The effect of soil dilatancy is neglected in the p–y curve formulations. However, a relationship between the soil dilatancy and the friction angle exists. Hence, the influence of soil dilatancy is implicitly accounted for in the expressions for p_u.

- Determining the ultimate soil resistance by the method proposed by Hansen (1961), seems to give more reasonable results than the method associated with the design codes. Prasad and Chari (1999) presented an expression for the ultimate soil resistance which accounts for the deflection pattern for non-slender piles. Zhang et al. (2005) modified the expression of Prasad and Chari (1999) such that side friction is included. Large-scale tests are needed to further validate the expressions for the ultimate soil resistance.

- In current practice, piles are analysed separately for vertical and horizontal behaviour. The effect on combined loading has untill now primarily been

investigated by means of numerical modelling. From this numerical work it can be concluded that vertical loading affects the horizontal pile stiffness and capacity. Compressional vertical loading has a minor positive effect on the horizontal stiffness and capacity, while tensile vertical loading decrease the lateral pile capacity moderately. The effect of combined loading on the vertical stiffness and capacity is more significant.

- Analyses of the sensitivity of p–y curves to pile bending stiffness, E_pI_p, gives rather contradictory conclusions. According to the Strain Wedge model, the formulations of p–y curves are highly affected by the pile bending stiffness. This is in contradiction to the existing p–y curve formulation and the numerical analyses performed by Fan and Long (2005) as well as Kim and Jeong (2011).
- The initial stiffness is independent of pile diameter according to the existing p–y curves. This agrees with analytical investigations by Terzaghi (1955), and Vesic (1961). Similarly, Ashford and Juirnarongrit (2005) concluded that initial stiffness is independent of the pile diameter based upon an analysis of a finite element model and tests on large scale concrete piles. Carter (1984) and Ling (1988), however, found that the initial stiffness is linear proportional to pile diameter.
- Based upon a numerical model, Lesny and Wiemann (2006) found that the initial stiffness is over-predicted at large depths when considering non-slender large-diameter piles.
- More research is needed regarding the initial stiffness of p–y curves.
- Fan and Long (2005) found from numerical analyses that the initial stiffness of the p–y curves as well as the ultimate soil resistance increases with an increase in the coefficient of horizontal earth pressure. This effect is not taken into consideration in the existing p–y curve formulations.
- A pile which behaves rigidly will have a negative deflection at the pile toe causing shear stresses at the pile toe. Further, pile rotation at the pile toe will impose a moment on the pile caused by vertical stresses acting on the pile toe. These effects are not taken into consideration in the existing p–y curve formulations.
- For non-slender, large-diameter piles the research regarding the shape of the p–y curves is limited.
- The p–y curves are developed for homogeneous soils. Few analyses have been made on layered soils. Further these analyses have been conducted on flexible piles. Georgiadis (1983) proposed a method to adjust the p–y curve formulations for layered soils in which an equivalent depth is determined for the soil layers beneath the upper layer. McGann et al. (2012) investigated the effect of layered soil on the p–y curves and found that both the soil layers above and below an intermediate layer affect the p–y curves of the intermediate layer. Based on the numerical analyses McGann et al. (2012) proposed a modification of the p–y curves due to layered soil. Both the findings of Georgiadis (1983) and McGann et al. (2012) needs furhter validation against tests on non-slender piles.
- Cyclic loading is only in a very simplified manor incorporated in the current p–y curve formulations. The accumulation of pile deflection due to long-term cyclic loading have been investigated by means of both numerical modelling and small-scale tests. Most researchers conclude that the

pile deflection accumulates exponentially with the number of cycles. Further, factors such as the relative density, ζ_b and ζ_c affects the accumulation.

- For random cyclic loading LeBlanc et al. (2010b) found that the accumulation of pile deflection is independent of the loading sequency, which is in contrast to the findings of Peralta and Achmus (2010).

- The variation of the stiffness of the soil-pile interaction with cyclic loading needs further investigation. LeBlanc et al. (2010a) suggested that the stiffness increases logarithmically with the number of cycles independently of the relative density of the soil. However, they only considered piles in loose to medium dense sand. Hence, further investigations are needed for piles in dense to very dense sand.

- For piles installed offshore without scour protection both global and local scour will take place. This changes the soil-pile interaction. ISO (2007) suggests a simplified method for modification of p–y curves due to scouring. However, the method needs validation. Lin et al. (2010) pointed out that the soil becomes overconsolidated when scouring takes place. Hence, the coefficient of horizontal earth pressure and the friction angle increases.

- Due to changing sea conditions the depth of the scour holes around unprotected offshore piles will vary with time. Knowledge is needed regarding the properties of backfilled soil material. Such knowledge can be essential for optimising the fatigue design for monopiles designed unprotected against scour development.

References

Abdel-Rahman K., and Achmus M., 2005. Finite element modelling of horizontally loaded Monopile Foundations for Offshore Wind Energy Converters in Germany. *International Symposium on Frontiers in Offshore Geotechnics*, Perth, Australia, Sept. 2005.

Abdel-Rahman K., and Achmus M., 2006. Numerical modelling of the combined axial and lateral loading of vertical piles. *Proceedings of Numerical Methods in Geotechnical Engineering*, Graz, Austria, Sept. 2006.

Achmus M., and Thieken K., 2006. Behavior of piles under combined lateral and axial loading. *2nd Internaltional Symposium on Frontiers in Offshore Geotechnics*, Perth, Australia, Nov. 2010.

Achmus M., Abdel-Rahman K., Kuo Y.-S., 2007. Numerical modelling of large diameter steel piles under monotonic and cyclic horizontal loading. *Proceedings of the 10th International Symposium on Numerical Models in Geomechanics*, NUMOG 10, pp. 453-459.

Achmus M., Abdel-Rahman K., and Thieken K., 2009a. Behavior of Piles in Sand Subjected to Inclined Loads. *Proceedings of International Symposium on Computational Geomechanics*, Juan-Les-Pins, France, May 2009.

Achmus M., Kuo Y.-S., and Abdel-Rahman K., 2009b. Behavior of monopile foundations under cyclic lateral load. *Computers and Geotechnics*, **36**(5), pp. 725-735.

Achmus M., Albiker J., and Abdel-Rahman K., 2010a. Investigations on the behavior of large diameter piles under cyclic lateral loading. *Proceeding of Frontiers in Offshore Geotechnics II*, Perth, Western Australia, Australia, pp. 471-476.

Achmus M., Kuo Y.-S., and Abdel-Rahman K., 2010b. Numerical Investigation of Scour Effect on Lateral Resistance of Windfarm Monopiles. *Proceedings of the Twentieth International Offshore and Polar Engineering Conference*, Beijing, China, June 2010.

Achmus M., and Thieken K., 2010. Behavior of piles under combined lateral and axial loading. *Proceedings of Frontiers in Offshore Geotechnics II*, Perth, Western Australia, Australia, Nov. 2010, pp. 465-470.

Alizadeh M., and Davisson M. T., 1970. Lateral load test on piles - Arkansas River project. *Journal of Soil Mechanics and Foundation Engineering Division*, **96**(5), pp. 1583-1604.

API, 2000. *Recommended practice for planning, designing, and constructing fixed offshore platforms - Working stress design, API RP2A-WSD*, American Petrolium Institute, Washington, D.C., 21. edition.

API, 2008. *Errata and Supplement 3 for: Recommended Practice for Planning, Designing and Constructing Fixed Offshore Platforms - Working Stress Design*, American Petrolium Institute, Washington, D.C.

Ashford S. A., and Juirnarongrit T., March 2003. Evaluation of Pile Diameter Effect on Initial Modulus of Subgrade Reaction. *Journal of Geotechnical and Geoenvironmental Engineering*, **129**(3), pp. 234-242.

Ashford S. A., and Juirnarongrit T., 2005. Effect of Pile Diameter on the Modulus of Subgrade Reaction. *Report No. SSRP-2001/22, Department of Structural Engineering, University of California, San Diego.*

Ashour M., Norris G., and Pilling P., April 1998. Lateral loading of a pile in layered soil using the strain wedge model. *Journal of Geotechnical and Geoenvironmental Engineering*, **124**(4), paper no. 16004, pp. 303-315.

Ashour M., and Norris G., May 2000. Modeling lateral soil-pile response based on soil-pile interaction. *Journal of Geotechnical and Geoenvironmental Engineering*, **126**(5), paper no. 19113, pp. 420-428.

Ashour M., Norris G., and Pilling P., August 2002. Strain wedge model capability of analyzing behavior of laterally loaded isolated piles, drilled shafts and pile groups. *Journal of Bridge Engineering*, **7**(4), pp. 245-254.

Ashour M., and Norris G., 2003. Lateral loaded pile response in liquefiable soil, *Journal of Geotechnical and Geoenvironmental Engineering*,**129**(5), pp. 404-414.

Banerjee P. K., and Davis T. G., 1978. The behavior of axially and laterally loaded single piles embedded in non-homogeneous soils. *Geotechnique*, **28**(3), pp. 309-326.

Barton Y. O., and Finn W. D. L., 1983. Lateral pile response and *p–y* curves from centrifuge tests. *Proceedings of the 15th Annual Offshore Technology Conference* , Houston, Texas, paper no. OTC 4502, pp. 503-508.

Belkhir S., Mezazigh S., and Levacher, D., December 1999. Non-Linear Behavior of Lateral-Loaded Pile Taking into Account the Shear Stress at the Sand. *Geotechnical Testing Journal*, GTJODJ, **22**(4), pp. 308-316.

Bhattacharya S., Lombardi D., and Wood D. M., 2011. Similitude relationships for physical modelling of monopile-supported offshore wind turbines. *International Journal of Physical Modelling in Geotechnics*, **11**(2), pp. 58-68.

Bogard D., and Matlock H., 1980. Simplified Calculation of p-y Curves for Laterally Loaded Piles in Sand. *Unpublished Report,*

The Earth Technology Corporation, Inc., Houston, Texas, USA.

Briaud J. L., Smith T. D., and Meyer, B. J., 1984. Using pressuremeter curve to design laterally loaded piles. *In Proceedings of the 15th Annual Offshore Technology Conference*, Houston, Texas, paper no. OTC 4501.

Broms B. B., 1964. Lateral resistance of piles in cohesionless soils. *Journal of Soil Mechanics and Foundation Division*, **90**(3), pp. 123-156.

Brødbæk, K. T., Augustesen, A. H., Møller, M., and Sørensen, S. P. H., 2011. Physical modelling of large diameter piles in coarse-grained soil. *Proceedings of the 21. European Young Geotechnical Engineers' Conference (XXI EYGEC)*, 4.-7. September, Rotterdam, The Netherlands.

Budhu M., and Davies T., 1987. Nonlinear Analysis of Laterally loaded piles in cohesionless Soils. *Canadian geotechnical journal*, **24**(2), pp. 289-296.

Carter D. P., 1984. A Non-Linear Soil Model for Predicting Lateral Pile Response. *Rep. No. 359, Civil Engineering Dept,. Univ. of Auckland, New Zealand.*

Comodromos E. M., 2003. Response prediction for horizontally loaded pile groups. *Journal of the Southeast Asian Geotechnical Society*, **34**(2), pp. 123-133.

Cox W. R., Reese L. C., and Grubbs B. R., 1974. Field Testing of Laterally Loaded Piles in Sand. *Proceedings of the Sixth Annual Offshore Technology Conference*, Houston, Texas, paper no. OTC 2079.

Das B. M., Seeley G. R., and Raghu D., 1976. Uplift capacity of model piles under oblique loads. *Journal of the Geotechnical Engineering Division*, ASCE, **102**(9), pp. 1009-1013.

Davisson M. T., and Gill L. C., 1963. Laterally Loaded Piles in a Layered Soil System. *Journal of the Soil Mehcanics and Foundation Engineering Division*, ASCE, **89**(SM3), pp. 63-94.

Davisson M. T. and Salley J. R., 1970. Model study of laterally loaded piles. *Journal of Soil Mechanics and Foundation Engineering Division*, ASCE, **96**(5), pp. 1605-1627.

Desai C. S., Sharma K. G., Wathugala G. W., and Rigby D. B., 1991. Implementation of hierarchical single surface δ_0 and δ_1 models in finite element procedure. *International Journal for Numerical & Analytical Methods in Geomechanics*, **15**(9), pp. 649-680.

DNV, 2010. *Design of Offshore Wind Turbine Structures, DNV-OS-J101.* Det Norske Veritas, Det Norske Veritas Classification A/S.

Dobry R., Vincente E., O'Rourke M., and Roesset J., 1982. Stiffness and Damping of Single Piles. *Journal of geotechnical engineering*, **108**(3), pp. 439-458.

Dordi C. M., 1977. Horizontally Loaded Piles in Layered Soils. *Proceedings of Specialty Session 10, The effect of Horizontal Loads on Piles due to Surcharge of Seismic Effects, Ninth International Conference on Soil Mechanics and Foundation Engineering*, Tokyo, Japan, July 1977, pp. 65-70.

Dunnavant T. W., and O'Neill M. W., 1985. Performance analysis and interpretation of a lateral load test of a 72-inch-diameter bored pile in overconsolidated clay. *Report UHCE 85-4*, Dept. of Civil Engineering., University of Houston, Texas, p. 57.

Fan C. C., and Long J. H., 2005. Assessment of existing methods for predicting soil response of laterally loaded piles in sand. *Computers and Geotechnics* **32**, pp. 274-289.

Georgiadis M., 1983. Development of p-y curves for layered soils. *Proceedings of*

the Conference on Geotechnical Practice in Offshore Engineering, ASCE, pp. 536-545.

Georgiadis M., Anagnostopoulos C., and Saflekou S., 1992. Centrifugal testing of laterally loaded piles in sand. *Canadian Geotechnical Journal*, **29**(2), pp. 208-216.

Gudehus G., and Hettler A., 1983. Model Studies of Foundations in Granular Soil, *In Development in Soil Mehcanics and Foundation Engineering 1*, pp. 29-63.

Hansen B. J., 1961. The ultimate resistance of rigid piles against transversal forces. *Danish Geotechnical Institute, Bull. No. 12*, Copenhagen, Denmark, 5-9.

Harremoës P., Ovesen N. K., and Jacobsen H. M., 1984. *Lærebog i geoteknik 2*, 4. edition, 7. printing. Polyteknisk Forlag, Lyngby, Danmark.

Hetenyi M., 1946. *Beams on Elastic Foundation.* Ann Arbor: The University of Michigan Press.

Huurman M., 1996. Development of traffic induced permanent strain in concrete block pavements. *Heron*, **41**(1), pp. 29-52.

ISO, 2007. Petroleum and natural gas industries - Fixed steel offshore structures. *International Organization for Standardization*, ISO 19902:2007 (E).

Jeong S., Kim Y., and Kim J., 2011. Influence on lateral rigidity of offshore piles using proposed p-y curves. *Ocean Engineering*, **38**(), pp. 397-408.

Kagawa T., and Kraft L. M., 1980. Lateral load-deflection relationships of piles subjected to dynamic loadings. *Soils and Foundations*, **20**(4), pp. 19-34.

Karasev O. V., Talanov G. P., and Benda S. F., 1977. Investigation of the work of single situ-cast piles under different load combinations. *Journal of Soil Mechanics and Foundation Engineering*, translated from Russian, **14**(3), pp. 173-177.

Karthigeyan S., Ramakrishna V. V. G. S. T., and Rajagopal K., May 2006. Influence of vertical load on the lateral response of piles in sand. *Computers and Geotechnics* **33**, pp. 121-131.

Khadilkar B. S., Chandrasekaran V. S., and Rizvi I. A., 1973. Analysis of Laterally Loaded Piles in Two-Layered Soils. *Proceedings of the Eigth International Conference on Soil Mechanics and Foundation Engineering*, Moscow, Russia, pp. 155-158.

Kim Y., and Jeong S., 2011. Analysis of soil resistance on laterally loaded piles based on 3D soil-pile interaction. *Computers and Geotechnics*, **38**(2), pp. 248-257.

Klinkvort R. T., and Hededal O., 2010. Centrifuge modelling of offshore monopile foundations, *Proceedings of International Symposium Frontiers in Offshore Geotechnics 2*, Perth, Western Australia, November 8 to November 10 2010.

Kuo Y.-S., 2008. On the behavior of large-diameter piles under cyclic lateral load, *Ph.D. thesis Vol. 65*, Leibniz University Hannover, Hannover, Germany.

LeBlanc C., 2009. Design of offshore wind turbine support structures: Selected topics in the field of geotechnical engineering, *DCE Thesis, Department of Civil Engineering, Aalborg University, Denmark*, (18).

LeBlanc C., Houlsby G. T., and Byrne B. W., 2010a. Response of Stiff Piles to Long-term Cyclic Loading, *Geotechnique*, **60**(2), pp. 79-90.

LeBlanc C., Houlsby G. T., and Byrne B. W., 2010b. Response of stiff piles to random two-way lateral loading, *Geotechnique*, **60**(9), pp. 715-721.

Lesny K., and Wiemann J., 2006. Finite-Element-Modelling of Large Diameter Monopiles for Offshore Wind Energy Converters. *Geo Congress 2006, February 26*

to March 1, Atlanta, GA, USA.

Lesny K., and Hinz P., 2007. Investigation of monopile behaviour under cyclic lateral loading. *Proceedings of Offshore Site Investigation and Geotechnics*, London, England, pp. 383-390.

Lesny K., Paikowsky S. G., and Gurbuz A., 2007. Scale effects in lateral load response of large diameter monopiles. *Geo-Denver 2007 February 18 to 21*, Denver, USA.

Lesny K., and Hinz P., 2009. *Contemporary Topics in Deep Foundations - Proceedings of selected papers of the 2009 International Foundation Congress and Equipment Expo*, pp. 512-519.

Lin S.-S., and Liao J.C., 1999. Permanent Strains of Piles in Sand due to Cyclic Lateral Loads, *Journal of Geotechnical and Geoenvironmental Engineering*, **125**(9), pp. 798-802.

Lin C., Bennett C., Han J., and Parsons R. L., 2010. Scour effects on the response of laterally loaded piles considering stress history of sand, *Computers and Geotechnics*, **37**, pp. 1008-1014.

Ling L. F., 1988. Back Analysis of Lateral Load Test on Piles. *Rep. No. 460, Civil Engineering Dept., Univ. of Auckland, New Zealand.*

Little R. L., and Briaud J. L., 1988a. Cyclic Horizontal Load Test on 6 Piles in Sands at Houston Ship Channel. *Research Report 6540 to USAE Waterways Experiment Station*, Civil Engineering, A&M University, Texas, USA.

Little R. L., and Briaud J. L., 1988b. Full scale cyclic lateral load tests on six single piles in sand. *Miscellaneous Paper GL-88-27*, Geotechnical Division, Texas A&M University, College Station, Texas, USA.

Long J. H., and Vanneste G., 1994. Effects of Cyclic Lateral Loads on Piles in Sand. *Journal of Geotechnical Engineering*, **120**(1), pp. 225-244.

Matlock H., and Reese L. C., 1960. Generalized Solutions for Laterally Loaded Piles. *Journal of the Soil Mechanics and Foundations Division*, **86**(5), pp. 63-91.

Matlock H., 1970. Correlations for Design of Laterally Loaded Piles in Soft Clay. *Proceedings, Second Annual Offshore Technology Conference*, Houston, Texas, paper no. OTC 1204, pp. 577-594.

McClelland B., and Focht J. A. Jr., 1958. Soil Modulus for Laterally Loaded Piles. *Transactions.* ASCE 123: pp. 1049-1086.

McGann C. R., Arduino P., and Mackenzie-Helnwein P. (2012). Simplified Procedure to Account for a Weaker Soil Layer in Lateral Load Analysis of Single Piles. *Journal of Geotechnical and Geoenvironmental Engineering*, ASCE, accepted December 14. 2011, posted ahead of print December 17 2011.

Meyerhof G. G., Mathur S. K., and Valsangkar A. J., 1981. Lateral resistance and deflection of rigid wall and piles in layered soils, *Canadian Geotechnical Journal*, **18**, pp. 159-170.

Meyerhof G. G., and Sastry V. V. R. N., 1985. Bearing capacity of rigid piles under eccentric and inclined loads. *Canadian Geotechnical Journal*, (22), pp. 267-276.

Miner M. A., 1945. Cumulative Damage in Fatigue. *Journal of Applied Mechanics*, **12**, pp.A159-A164.

Murchison J. M., and O'Neill M. W, 1984. Evaluation of *p–y* relationships in cohesionless soils. *Analysis and Design of Pile Foundations. Proceedings of a Symposium in conjunction with the ASCE National Convention*, pp. 174-191.

Naik T. R., and Peyrot A., 1976. Analysis and Design of Laterally Loaded Piles and Caissons in a Layered Soil System. *Methods of Structural Analysis, Proceedings of*

the National Structural Engineering Conference, ASCE, Madison, Wisconsin, USA, Aug. 1976, pp. 589-606.

Norris G. M., 1986. Theoretically based BEF laterally loaded pile analysis. *Proceedings, Third Int. Conf. on Numerical Methods in offshore piling*, Editions Technip, Paris, France, pp. 361-386.

O'Neill M. W., Murchison J. M., 1983. An Evaluation of p-y Relationships in Sands. *Research Report No. GT-DF02-83*, Department of Civil Engineering, University of Houston, Houston, Texas, USA.

O'Neill M. W., and Dunnavant T. W., 1984. A study of effect of scale, velocity, and cyclic degradability on laterally loaded single piles in overconsolidated clay. *Report UHCE 84-7*, Dept. of Civ. Engrg., University of Houston, Texas, p. 368.

Pasternak P. L., 1954. On a New Method of Analysis of an Elastic Foundation by Means of Two Foundation Constants, *Gosudarstvennoe Izadatelstro Liberatuni po Stroitelstvui Arkhitekture*, Moskow, pp. 355-421.

Peck R. B., Hanson W. E., and Thornburn T. H., 1953. *Foundation Engineering*, John Wiley and Sons, Inc. New York.

Pender M. J., 1993. Aseismic Pile Foundation Design Analysis. *Bull. NZ Nat. Soc. Earthquake Engineering.*, **26**(1), pp. 49-160.

Pender J. M., Carter D. P., and Pranjoto S., 2007. Diameter Effects on Pile Head Lateral Stiffness and Site Investigation Requirements for Pile Foundation Design. *Journal of Earthquake Engineering*, **11**(SUPPL. 1), pp. 1-12.

Peng J.-R., Clarke B. G., and Rouainia M., 2006. A Device to Cyclic Lateral Loaded Model Piles, *Geotechnical Testing Journal*, **29**(4), pp. 1-7.

Peralta P., and Achmus M., 2010. An experimental investigation of piles in sand subjected to lateral cyclic loads, *Physical Modelling in Geotechnics*, Taylor& Francis Group, London.

Petrosowitch G., and Award A., 1972. Ultimate lateral resistance of a rigid pile in cohesionless soil, *Proceedings of the 5th European Conference on SMFE*, Madrid, **3**, pp. 407-412.

PHRI, 1980. Port and Harbour Research Institute. *Technical Standards for Port and Harbour Facilities in Japan.*, Office of Ports and Harbours, Ministry of Transport.

Poulos H. G., 1971. Behavior of laterally loaded piles: I - Single piles. *Journal of the Soil Mechanics and Foundations Division*, **97**(5), pp. 711-731.

Poulos H. G., and Davis E. H., 1980. *Pile foundation analysis and design*, John Wiley & Sons.

Poulus H., and Hull T., 1989. The Role of Analytical Geomechanics in Foundation Engineering. *Foundation Eng.: Current principles and Practices*, **2**, pp. 1578-1606.

Prakash S., 1962. Behavior of pile groups subjected to lateral loads. *Thesis*, University of Illinois, Urbana, Illinois, USA.

Prasad Y. V. S. N., and Chari T. R., 1999. Lateral capacity of model rigid piles in cohesionless soils, *Soils and Foundations*, **39**(2), pp. 21-29.

Reese L. C., and Matlock H., 1956. Non-dimensional Solutions for Laterally Loaded Piles with Soil Modulus Assumed Proportional to Depth. *Proceedings of the eighth Texas conference on soil mechanics and foundation engineering.* Special publication no. 29.

Reese L. C., Cox W. R., and Koop, F. D., 1974. Analysis of Laterally Loaded Piles in Sand. *Proceedings of the Sixth Annual*

Offshore Technology Conference, Houston, Texas, **2**, paper no. OTC 2080.

Reese L. C., and Welch R. C., 1975. Lateral loading of deep foundation in stiff clay. *Journal of Geotechnic Engineering.*, Div., **101**(7), pp. 633-649.

Reese L. C., and Van Impe W. F., 2001. *Single Piles and Pile Groups Under Lateral Loading*, Taylor & Francis Group plc, London.

Remaud D., Garnier J., and Frank R. (1998). Laterally loaded piles in dense sand - group effects. *Proceedings of the International Conference Centrifuge*, Tokyo, Japan, pp. 533-538.

Rycklik I., 1987. A new definition of the rainflow cycle counting method. *International Journal of Fatigue*, **9**(2), pp. 119-121.

Scott R. F., 1980. Analysis of Centrifuge Pile Tests: Simulation of Pile Driving. *Research Report, American Petroleum Institute OSAPR Project 13*, California Institute of Technology, Pasedena, California, USA.

Stevens J. B., and Audibert J. M. E., 1979. Re-examination of p-y curve formulation. *Proceedings Of the XI Annual Offshore Technology Conference*, Houston, Texas, OTC 3402, pp. 397-403.

Stewart H. E., 1986. Permanent strains from cyclic variable-amplitude loadings. *Journal of Geotechnical Engineering*, ASCE, **112**(6), pp. 646-661.

Sørensen, S. P. H., Brødbæk, K. T., Møller, M., Augustesen, A. H., and Ibsen, L. B., 2009. Evaluation of Load-Displacement Relationships for Large-Diameter Piles. *Proceedings of the twelft International Conference on Civil, Structural and Environmental Engineering Computing (eds. Topping, Costa Neves and Barros), 1.-4. September, Madeira, Portugal*, paper 244.

Sørensen, S. P. H., Ibsen, L. B., and Augustesen, A. H., 2010. Effects of diameter on initial stiffness of *p–y* curves for large-diameter piles in sand. *Proceedings of the seventh European Conference on Numerical Methods in Geotechnical Engineering (eds Benz &Nordal eds), 2.-4. June, Trondheim, Norway*, pp. 907-912

Terashi M., 1989. Centrifuge modeling of a laterally loaded pile. *Proceedings of the Twelfth International Conference of Soil Mechanics and Foundation Engineering*, Rio de Janeiro, Brazil, pp. 991-994.

Terzaghi K., 1955. Evaluation of coefficients of subgrade reaction. *Geotechnique*, **5**(4), pp. 297-326.

Timoshenko S. P., 1941. Strength of materials, part II, advanced theory and problems, 2nd edition, 10th printing. New York: D. Van Nostrand.

Verdue L., Garnier J., and Levacher D., 2003. Lateral cyclic loading of single piles in sand. *International Journal of Physical Modelling in Geotechnics*, **3**(3), pp. 17-28.

Vesic A. S., 1961. Beam on Elastic Subgrade and the Winkler's Hypothesis. *Proceedings of the 5th International Conference on Soil Mechanics and Foundation Engineering*, Paris, **1**, pp. 845-850.

Winkler E., 1867. Die lehre von elasticzitat and festigkeit (on elasticity and fixity), Prague, 182 p.

Yang Z., and Jeremic B. (2005). Study of Soil Layering Effects on Lateral Loading Behavior of Piles. *Journal of Geotechnical and Geoenvironmental Engineering*, ASCE, **131**(6), pp. 762-770.

Zhang L., Silva F., and Grismala R., January 2005. Ultimate Lateral Resistance to Piles in Cohesionless Soils. *Journal of Geotechnical and Geoenvironmental Engineering*, **131**(1), pp. 78-83.

Title:

Testing of Laterally Loaded Rigid Piles with Applied Overburden Pressure.

Authors:

Sørensen, S. P. H., Ibsen, L. B., and Foglia, A.

Year of publication:

2012

Published in:

Submitted for publication.

Number of pages:

7

Testing of Laterally Loaded Rigid Piles with Applied Overburden Pressure

Søren P. H. Sørensen, Lars B. Ibsen and Aligi Foglia
Department of Civil Engineering, Aalborg University
Aalborg, Denmark

ABSTRACT

Small-scale tests have been conducted for the purpose of investigating the quasi-static behaviour of laterally loaded, non-slender piles installed in cohesionless soil. For that purpose, a new and innovative test setup has been developed. The tests have been conducted in a pressure tank such that it was possible to apply an overburden pressure to the soil. Hereby, the traditional uncertainties related to low effective stresses for small-scale tests has been avoided. A scaling law for laterally loaded piles has been proposed based on dimensional analysis. The novel testing method has been validated against the test results by means of the scaling law.

KEY WORDS: Pile foundations; Model tests; Overburden pressure; Earth pressure; Dimensional analysis; Sand.

INTRODUCTION

For offshore wind turbines, the monopile foundation concept is often employed. Typically, the monopile foundation concept consists of an open-ended steel tube, which is either drilled or driven into the seabed. The pile diameter, D, and the embedded pile length, L_p, are usually in the range of 4-6 m and 15-30 m, respectively. Hence, the slenderness ratio, L_p/D, is in the order of four to seven, and therefore the piles exhibit a rather rigid body motion.

The Winkler model approach is traditionally employed in the design of offshore monopiles. In this approach, the interaction between the soil and the pile is modelled by means of uncoupled non-linear springs. The stiffness of the nonlinear springs is described by means of *p-y* curves. These curves describe the soil resistance acting on the pile wall as a function of the pile deflection. Design regulations of the American Petroleum Institute, API (2000), and Det Norske Veritas, DNV (2010), recommend the use of the *p-y* curve formulation proposed by O'Neill and Murchison (1983) for piles situated in cohesionless soils. The formulation has been validated by Murchison and O'Neill (1984) through tests on piles with diameters up to approximately 2 m and length to diameter ratios larger than 10. The formulation has, however, not been validated for piles with $L_p/D \approx 5$ and D = 4-6 m. Therefore, further research is needed regarding the behaviour and design of large-diameter, non-slender piles.

An extensive test programme has been conducted at Aalborg University in order to investigate the behaviour of non-slender piles in sand exposed to quasi-static lateral loading. Piles with diameters of 60 to 100 mm, embedded pile lengths of 240 to 500 mm and slenderness ratios of 3 to 6 have been tested. Hence, the scale in comparison with real monopiles is between 1:40 and 1:100. Traditionally, when small-scale tests are conducted, the low effective stresses in the soil cause significant scale-effects. The internal friction angle, φ, and the Young's modulus of elasticity for the soil, E_s, depend heavily on the effective stresses in the soil. Therefore, the average values of these parameters for traditional 1-g small-scale tests deviate from the average values of these parameters in the soil around full-scale foundations. To avoid this, it is necessary to increase the effective stresses in the soil. This can be accomplished by either testing in a centrifuge or by testing in a pressure tank. The tests presented in this paper have been conducted in a pressure tank in which an overburden pressure of P_0 = 0-100 kPa has been applied to the soil. For P_0 = 100 kPa, the average vertical stress in the small-scale tests is slightly higher than 100 kPa and similar to the average vertical effective stress in the soil around a foundation with $L_p \approx$ 20-25 m.

When applying an overburden pressure to the soil, the effective stress distribution with depth becomes trapezoidal instead of triangular. Hereby, the stress distribution for the small-scale tests with applied overburden pressure is significantly different from the stress distribution around full-scale piles. However, this difference can be overcome by means of scaling.

In the present paper, the pile behaviour of non-slender piles is assessed on the basis of small-scale tests in a pressure tank. The test setup is thoroughly described. A scaling law relating the pile rotation to the applied overturning moment is presented. The new and innovative test method is validated against test results by means of the scaling law.

TEST SETUP

23 quasi-static tests were conducted on laterally loaded piles. The tests were conducted in a pressure tank such that it was possible to apply an overburden pressure to the soil.

Aluminium piles with diameters of 60 to 100 mm were tested. The behaviour of both closed-ended and open-ended piles was investigated. A wall thickness, *wt*, of 5 mm was used for all the test piles. The ratio between the wall thickness and the pile diameter is approximately three times higher for the test piles than for real monopiles. However, since aluminium is approximately three times softer than steel, the ratio between the pile bending stiffness, E_pI_p, and the pile diameter, D, is similar for the test piles and for typical monopiles used as foundation for offshore wind turbines.

Pressure Tank

The small-scale tests were conducted in a pressure tank at Aalborg University. The pressure tank had an inner diameter of approximately 2.1 m and a height of approximately 2.5 m. It contained trap doors enabling access into the tank. Further, wiring from measurement devices could be led out of the tank through openings.

A cross-sectional view of the test setup is shown in Fig. 1. It was possible to let water into and out of the tank through a pipe located at the bottom of the tank. At the bottom of the tank, a saturated gravel layer was positioned which ensured an even distribution of the water coming from the inlet. A layer of saturated sand was placed on top of the gravel layer.

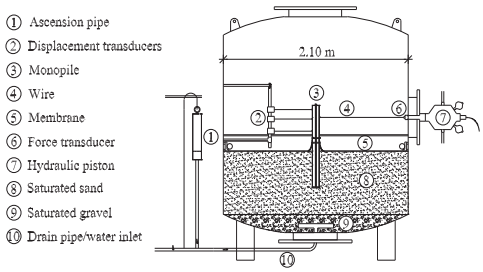

Fig. 1. Cross-sectional view of the test setup.

In order to increase the effective stresses in the soil, an elastic membrane was placed on top of it. The membrane hermetically sealed off the air on top of the membrane from the water in the voids of the soil material. To ensure a hermetic seal, rubber mouldings were attached to the sides of the membrane. Further, an inflated fire hose was employed to press the membrane out against the walls of the pressure tank. A retainer clamp was used to seal the gap between the pile and the membrane. It was not possible to make a perfect seal between the membrane and the tank wall as well as between the membrane and the pile wall. Approximately 15 cm of water was therefore placed on top of the membrane. This ensured that the soil remained saturated in spite of a minor leakage through the membrane. Moreover, the minor leakage was minimised, because, at a temperature of 20 °C, the dynamic viscosity of water is approximately 50 times larger than the dynamic viscosity of air. Therefore, when water was placed on top of the membrane instead of air, the volumetric leakage through gaps in the membrane was approximately 50 times slower. The water flow through the membrane varied between 20 and 50 l/hour. The test results are not expected to be influenced by this minor water flow through the membrane. The drain pipe located at the bottom of the pressure tank was connected to an ascension pipe so that, a hydrostatic pore pressure could be maintained throughout the tests.

The test piles were loaded by means of a hydraulic piston which was connected to the test piles with use of a thin steel wire.

Measuring System

The lateral load and the lateral pile displacement were measured as shown in Fig. 2. The pile displacement was measured by means of wire transducers of the type WS10-1000-R1K-L10 from ASM GmbH at three levels along the piles: respectively 200 mm, 370 mm and 480 mm above the soil surface. A force transducer was connected in series between the hydraulic piston and the steel wire. A force transducer of the type HBM U2B 20 kN was employed. An absolute pressure transducer of the type HBM P6A 10 bar was employed to measure the air pressure in the pressure tank.

In order to ensure drained soil conditions, the loading of the test piles was displacement-controlled with a loading velocity of 0.01 mm/s. In Pedersen and Ibsen (2009) a detailed description of the data acquisition is presented.

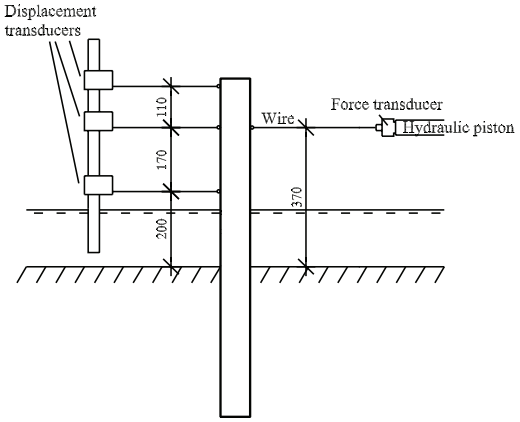

Fig. 2. Positioning of displacement and force transducers.

Soil Properties and Preparation of Soil

All the tests were conducted on Aalborg University Sand No. 1 (Baskarp Sand No. 15) which is a graded sand type. The largest grains are round while the smallest grains have sharp edges. The sand has been tested thoroughly by Larsen (2008) and Ibsen et al. (2009). The soil properties are summarised in Table 1. Ibsen et al. (2009) proposed an expression, valid for Aalborg University Sand No. 1, relating the secant internal friction angle, φ, with the relative density, I_D, and the minor effective stress, σ'$_3$:

$$\varphi = 0.152 I_D + 27.39 {\sigma'_3}^{-0.2807} + 23.21[°] \quad (1)$$

In Eq. 1, the relative density should be inserted in per cent and the confining pressure should be inserted in kPa.

Prior to each test, the soil was prepared by means of a two-step procedure. At first an upward gradient of 0.91 was applied to the soil, and afterwards the soil was vibrated mechanically in a standardised pattern. For a detailed description of the soil preparation see Sørensen and Ibsen (2011).

Table 1. Properties of Aalborg University Sand No. 1, after Larsen (2008).

Specific grain density, d_s	2.64
Maximum void ratio, e_{max}	0.858
Minimum void ratio, e_{min}	0.549
50 % - quantile, d_{50}	0.14 mm
$U = d_{60}/d_{10}$	1.78

Cone penetration tests (CPT) were conducted prior to each test. The relative density, determined based on the CPT's, varied from 0.75 to 0.91 throughout the test programme. Hence, the soil was classified as dense to very dense sand which is similar to typical compactions of offshore sand.

DIMENSIONAL ANALYSIS

Scope of the Dimensional Analysis

Dimensional analysis is essential to geotechnical physical modelling. Only by means of that, the small-scale effects can be understood and the test results used for prototype design. Generally, the friction angle, φ, and the Young's modulus of elasticity for the soil, E_s, are effective stress dependent such that the friction angle is high and the Young's modulus of elasticity is low for low effective stresses. Hence, the average values of the soil parameters for traditional small-scale tests conducted at normal stress level differ from the average values of the soil parameters in the soil around full-scale foundations. In order to overcome this, an overburden pressure was applied in the small-scale tests presented in this paper.

Several researchers have proposed scaling laws for laterally loaded piles (e.g. Gudehus and Hettler, 1983; Peralta and Achmus, 2010; and Bhattacharya et al., 2011). However, these scaling laws do not account for an applied overburden pressure. A scaling law accounting for an applied overburden pressure has therefore been developed. The purpose of such scaling law is to enable comparison between tests conducted at different overburden pressures and to scale up the results to full-scale foundations. For the design of monopile foundations for offshore wind turbines accurate determination of the pile rotation, θ, is essential. The pile rotation is expected to be a function of the relative density of the sand, I_D, the loading eccentricity, e, the embedded pile length, L_p, the pile diameter, D, the overburden pressure, P_0, and the friction angle of the soil, φ. These properties are in the following derivation shown to be included within the moment pile capacity, R_M, and the applied overturning moment, M_R.

Derivation of the Scaling Law

According to Rankine, the total passive earth pressure per unit length, $E^p_{Rankine}$, acting on a retaining wall is given as follows:

$$E^p_{Rankine} = \frac{1}{2}\gamma h^2 K^p_\gamma + phK^p_p + chK^p_c \quad (2)$$

h is the height of the retaining wall, p is the overburden pressure, c is the cohesion of the soil and $K^p{}_\gamma$, $K^p{}_p$ and $K^p{}_c$ are passive earth pressure coefficients. The expression in Eq. 2 is based on a deformation pattern consisting of rigid body lateral translation. Further, the retaining wall is assumed to have an infinite length and the interaction between wall and soil is assumed to be smooth. In contrast, offshore monopiles are loaded eccentrically, causing the pile deformation pattern to primarily consist of rotation, and furthermore, the piles are circular, resulting in a three-dimensional deformation pattern in the soil surrounding them. For piles it should be noted that side friction also contributes to the pile capacity and pile stiffness. Although the behaviour of retaining walls and laterally loaded piles are significantly different, the capacity of both types of structures arises primarily from lateral soil pressures acting against the structures. It is assumed that the lateral pile capacity, R_H, can be calculated as:

$$R_H = k_1 k_2 E^p_{Rankine} D = k_1 k_2 \left(\frac{1}{2}\gamma {L_p}^2 K^p_\gamma + P_0 L_p K^p_p + cL_p K^p_c\right) D \quad (3)$$

where the factor k_1 adjusts for the rotation of the pile, and the factor k_2 adjusts for the change from two- to three-dimensional soil-structure interaction. The factor k_1 is expected to depend on the ratio between the loading eccentricity and the embedded pile length, e/L_p, since this ratio affects the depth to the point of rotation. k_1 is also expected to depend on the slenderness ratio, L_p/D, since this ratio governs the pile flexibility and, therefore, also governs the depth to the point of rotation. Reese et al. (1974) suggested that the lateral extent of the wedge forming in front of a laterally loaded pile depends on the friction angle and the relative density of the soil. Therefore, the factor k_2 is expected to depend on these parameters. The last term in Eq. 3, $cL_pK^p{}_c$, can be disregarded, since a cohesionless soil material was employed in the experimental tests. The passive earth pressure coefficients, $K^p{}_\gamma$ and $K^p{}_p$, can be calculated as:

$$K^p_\gamma = K^p_p = \tan^2\left(45° + \frac{\varphi}{2}\right) \quad (4)$$

The loading eccentricity was 0.37 m for all the tests, which corresponds to between $0.74L_p$ and $1.54L_p$. For offshore wind turbines, the design load from wind and waves often has an eccentricity between $0.5L_p$ and $2.0L_p$. Therefore, the applied overturning moment around the point of rotation, M_R, has a large influence on the pile behaviour of both the test piles and full-scale piles. M_R is calculated as:

$$M_R = H\left(e + k_3 L_p\right) \quad (5)$$

where H is the applied lateral load and k_3L_p is the depth of the point of rotation. The depth to the point of rotation depends on e/L_p and L_p/D. Hereby, k_3 depends on both e/L_p and L_p/D. Because both the test piles and full-scale piles behave rigidly and are eccentrically loaded, the value of k_3 has been chosen to 0.8. This value agrees well with the point of zero deflection determined from the centrifuge tests of non-slender laterally loaded piles reported by Klinkvort and Hededal (2010), and the small-scale tests on rigid piles reported by Christensen (1961).

The overturning moment capacity around the point of zero deflection, R_M, can be estimated as a dimensionless factor, k_4, multiplied by the embedded pile length and the lateral pile capacity:

$$R_M = k_4 L_p R_H = k_1 k_2 k_4 L_p E^p_{Rankine} D \quad (6)$$

The factor k_4 primarily depends on the depth to the point of rotation. k_4 is therefore dependent on e/L_p and L_p/D.

The pile rotation, θ, depends on the ratio between the applied overturning moment around the point of rotation and the moment capacity:

$$\theta = f\left(\frac{M_R}{R_m}\right) = f\left(\frac{H\left(e+k_3 L_p\right)}{k_1 k_2 k_4 L_p E^p_{Rankine} D}\right) \quad (7)$$

where f is, as yet, an unknown function. All the experiments conducted were designed such that the test piles had a slenderness ratio comparable to the slenderness ratio used for full-scale foundations for offshore wind turbines. Further, the ratio between the loading eccentricity and the embedded pile length was also comparable to the ratio for full-scale foundations. The test piles were installed in dense to very dense sand, similar to typical sand deposits in the offshore environment. Therefore, the values of the factors k_1, k_2, k_3 and k_4 are expected to deviate only slightly between different scales. Thus, for small- and full-scale tests of typical monopiles used as the foundation of offshore wind turbines, Eq. 7 can be reduced to:

$$\theta = f\left(\frac{H\left(e+0.8L_p\right)}{L_p E^p_{Rankine} D}\right), \quad \text{for } L_p/D \approx 5 \text{ and } e/L_p \approx 0.5\text{-}2.0 \quad (8)$$

The normalised overturning moment, M_{norm}, is defined as:

$$M_{norm} = \frac{H(e+0.8L_p)}{L_p E^p_{Rankine} D} \quad (9)$$

RESULTS

The load-displacement relationship for a test with D = 100 mm, L_p = 500 mm and P_0 = 0 kPa and a test with D = 100 mm, L_p = 500 mm and P_0 = 100 kPa are shown in Fig. 3 and Fig. 4, respectively. Significant fluctuations can be observed in the measured lateral load for the test with P_0 = 0 kPa while the fluctuations of the measured lateral load are small for the test with P_0 = 100 kPa. The reason for this is that the capacity of the hydraulic piston is large compared to the applied load for the test with P_0 = 0 kPa. These fluctuations were observed for all the tests conducted at normal stress level. The fluctuations are only considered to exhibit a minor influence on the load-displacement relationships. In the following figures, the lateral load shown for the tests at normal stress level is smoothed as a running average calculated over 10 s. Since a loading velocity of 0.01 mm/s was used, the lateral displacement increased 0.1 mm within 10 s. When comparing the load-displacement relationships shown in Fig. 3 and Fig. 4, it can be observed that the application of an overburden pressure dramatically increases the pile stiffness and pile capacity. The observed increase is as expected.

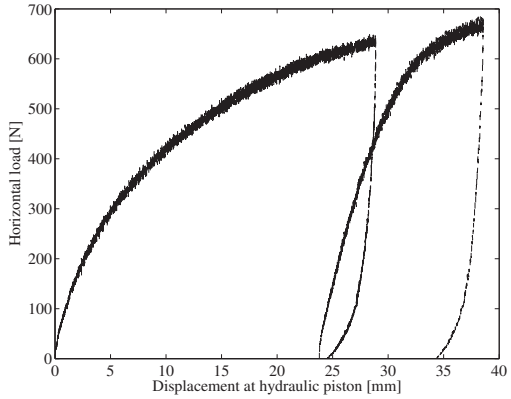

Fig. 3. Load-displacement relationship for a test with D = 100 mm, L_p = 500 and P_0 = 0 kPa.

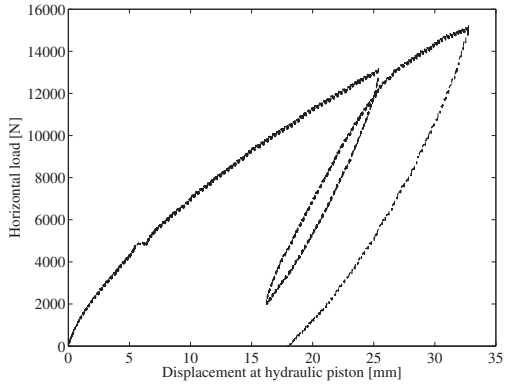

Fig. 4. Load-displacement relationship for a test with D = 100 mm, L_p = 500 mm and P_0 = 100 kPa.

For a pile diameter of 80 mm both open- and closed-ended piles were tested. In Fig. 5, the load-displacement relationships obtained for open- and closed-ended piles are compared. No significant difference in the load-displacement relationship can be observed. This corroborates the fact that the pile stiffness and pile capacity originate primarily from lateral bedding and that the shear and normal stress acting at the pile toe merely has a secondary influence on the pile behaviour for lateral loading.

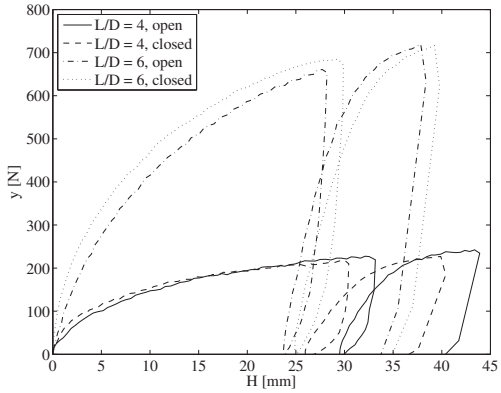

Fig. 5. Comparison of load-displacement relationships for open-/closed-ended piles, P_0 = 0 kPa.

The normalised overturning moment, M_{norm}, is in Fig. 6 plotted against the pile rotation, θ. The pile rotation was determined as an average rotation:

$$\tan(\theta) = \frac{y(x=-e)}{e+0.8L_p} \quad (10)$$

where y is the pile deflection and x is the depth below soil surface.

Fig. 6 show some scatter in the normalised plot. The scatter is however minimised heavily when only the tests with overburden pressure applied are considered. The figure illustrates that the relationship between the pile rotation and the normalised overturning moment are comparable for varying P_0, L_p/D and e/L_p. Hence, the test results validate the scaling law.

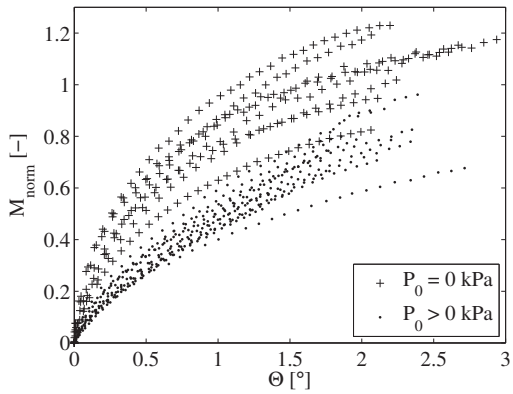

Fig. 6. M_{norm} versus θ for all the conducted tests.

In Fig. 7, the normalised overturning moment is plotted against the pile rotation for the tests with pile diameters of 80 mm slenderness ratios of 5 and with applied overburden pressures varying from 0 to

100 kPa. The curves for the tests with overburden pressure applied to the soil are almost identical in the normalised plot, although, the normalised pile stiffness, M_{norm}/θ, seems to decrease slightly for increasing P_0. The two tests without overburden pressure seem to reach the pile capacity at a smaller value of pile rotation than the tests with overburden pressure. From consolidated drained triaxial tests on Aalborg University Sand No. 1, Hokkesund Sand, Santa Monica Beach Sand and Sacramento River Sand, Ibsen and Lade (1999) found that the vertical strain at failure increases for increasing values of confining pressure. Kolymbas and Wu (1990) found a similar result from consolidated drained triaxial tests on Karlsruhe medium dense sand. A correlation exists between the pile rotation and the strain in the soil. Hence, the effect of the applied overburden pressure on the pile rotation at failure is analogue to the effect of the confining stress on the vertical strain at failure. The mean values of the effective stresses in the soil are comparable for the small-scale tests with an overburden pressure of 100 kPa applied to the soil and full-scale foundations. Test with overburden pressure applied might therefore capture the relationship between the pile rotation and the normalised overturning moment for full-scale foundations. Although, in order to validate this statement, validation against full-scale tests is needed.

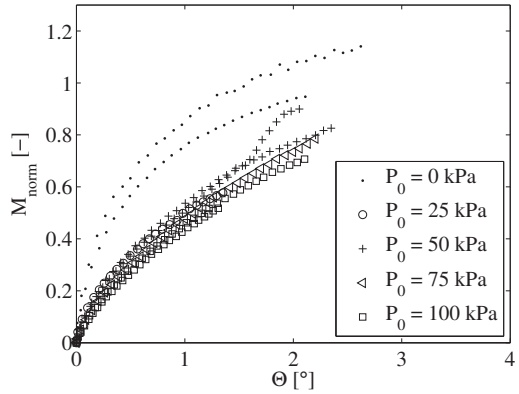

Fig. 7. M_{norm} versus θ for varying P_0, D = 80 mm, L_p = 400 mm.

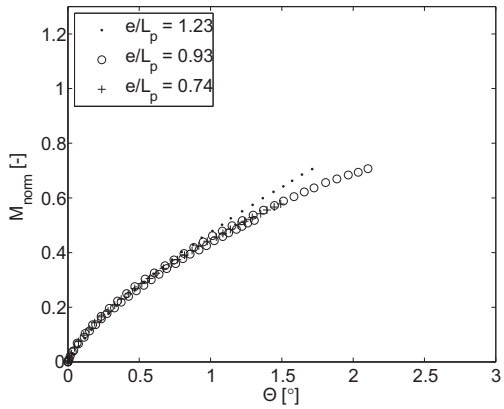

Fig. 8. M_{norm} versus θ for the tests with L_p/D = 5, P_0 = 100 kPa.

Fig. 8 and Fig. 9 indicate that the scaling law proposed in Eq. 8 is robust in such a way that it captures a variation of e/L_p and L_p/D within 0.74-1.54 and 4-6, respectively. Hence, the small-scale tests corroborate the proposed scaling law.

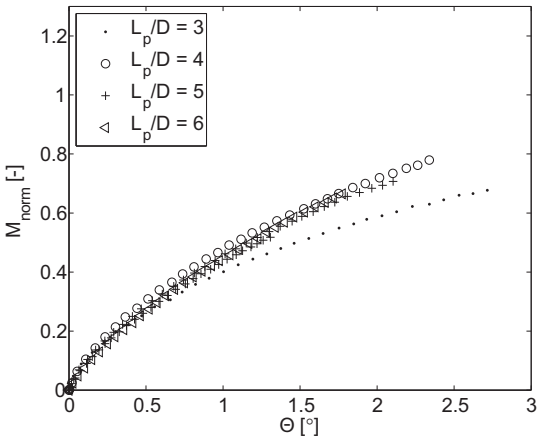

Fig. 9. M_{norm} versus θ for the tests with D = 80 mm, P_0 = 100 kPa.

POTENTIAL IMPLICATION FOR DESIGN

Gudehus and Hettler (1983) suggested the following expression for the displacement of a rigid pier:

$$\frac{u}{D} = A_u C_e \left(\frac{H}{\gamma D^3}\right)^{\mu} \tag{11}$$

where A_u depends on e/L_p and L_p/D, C_e depends on the void ratio, e, and μ is a dimensionless constant. Similar to the proportionality between the pile displacement and the horizontal loading raised to the power of μ as suggested by Gudehus and Hettler (1983), it is assumed that the pile rotation is proportional to the normalised overturning moment raised to the power of μ:

$$\theta = C M_{norm}^{\mu} \tag{12}$$

C is a dimensionless constant. The parameters C and μ should be fitted to test results. It should be emphasised that Eq. 11 and 12 show no maximum for H/M_{norm}. These, equations are therefore not able to predict H/M_{norm} for very large displacements/rotations.

In Fig. 10, Eq. 12 is fitted to the test results for the small-scale tests with overburden pressure applied. The least squares fitting method has been used for the fitting. It can be observed that the fitted function provides a reasonable fit with the test results for pile rotations up to 1.5-2.0°. For pile rotations larger than 1.5-2.0°, the fitted function starts to overestimate the normalised overturning moment. Since, Eq. 12 is not bounded by an upper limit for M_{norm}, the poor fit for large values of the pile rotation is as expected.

A typical monopile foundation for offshore wind turbines has a pile diameter of 4 m, an embedded pile length of 20 m and a loading eccentricity of 30 m corresponding to 1.5 times the pile length. Hence, the slenderness ratio and the ratio between the eccentricity and the pile length are in the same order as for the small-scale tests. Typically, the soil is medium dense to dense. Therefore, a friction angle of 40° has been assumed. When scaling up the results from the small-scale tests to a full-scale foundation with the above mentioned parameters, the load-rotation relationship shown in Fig. 11 is found. It should be emphasised that the scaling law needs validation against large- or full-scale tests before small-scale testing with overburden pressure applied

to the soil can be applied in the design of monopile foundations for offshore wind turbines.

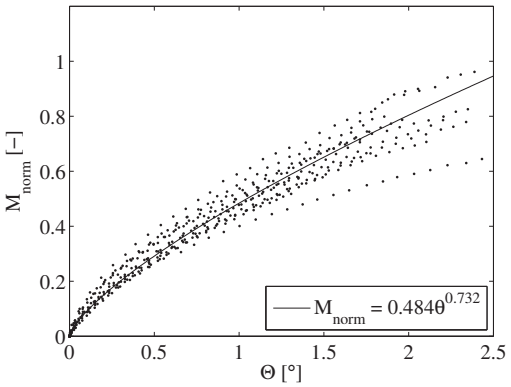

Fig. 10. Eq. 12 fitted to the test results for the tests with overburden pressure, L_p/D = 3-6, e/L_p = 0.74-1.54, P_0 = 25-100 kPa.

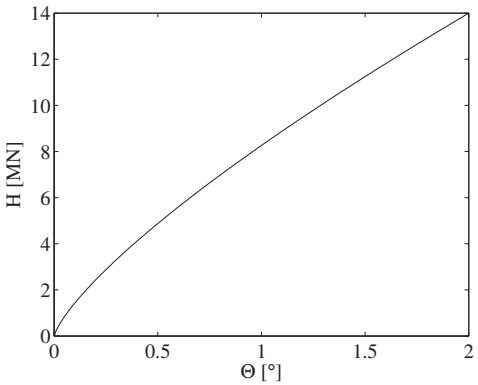

Fig. 11. Load-rotation relationship for a full-scale monopile with D = 4 m, L_p = 20 m, e = 30 m situated in a cohesionless soil with φ = 40°.

CONCLUSIONS

The behaviour of non-slender laterally loaded piles was investigated by means of small-scale tests conducted with varying ratios between the loading eccentricity and the embedded pile length, varying slenderness ratios and varying overburden pressures. A scaling law relating the pile rotation with the normalised overturning moment was proposed. The major conclusions of the experimental work are:

- A new and innovative test setup for small scale testing was developed in which the effective stresses in the soil can be increased. The test setup worked as planned.
- The pile capacity and pile stiffness for open- and closed-ended piles were found to be rather similar. Therefore, the shear and normal stresses acting at the pile toe only slightly affects the pile behaviour for non-slender laterally loaded piles.
- A scaling law of the relationship between the overturning bending moment and the pile rotation was proposed. The scaling law was found to be very accurate for the conducted tests and it hereby proved to be valid for eccentricities between 0.74L_p and 1.54L_p and for slenderness ratios of 3 to 6.
- The pile rotation at failure was found to depend on the mean value of the effective soil stresses. This finding is analogue to the relationship between the strain at failure and the confining stress in triaxial tests.
- The small-scale tests results were scaled up to a typical full-scale foundation. Regarding the scaling from small-scale to full-scale it should be noted that the scaling law needs validation against large- or full-scale tests.

ACKNOWLEDGEMENTS

The experimental work has only been possible with the financial support from the Energy Research Programme administered by the Danish Energy Authority. The experimental work is associated with the ERP programme "Physical and numerical modelling of monopile for offshore wind turbines", journal no. 033001/33033-0039. The funding is sincerely acknowledged. Appreciation is extended to Kristian T. Brødbæk, Martin Møller, Hanne R. Roesen, Kristina Thomassen, Alejandro B. Moreno, Linas Mikalauskas and Jose L. T. Diaz for helping with the experimental work. Furthermore, the authors would like to thank the staff at the laboratory at the Department of Civil Engineering, Aalborg University, for their immeasurable help with the test setup.

REFERENCES

API (2000). "Recommended practice for planning, designing, and constructing fixed offshore platforms - Working stress design", *API RP2A-WSD. American Petroleum Institute*, Washington, D.C., USA, 21. edition.

Bhattacharya, S., Lombardi, D. & Wood, D. M. (2011). "Similitude relationships for physical modelling of monopile-supported offshore wind turbines". *International Journal of Physical Modelling in Geotechnics*, Vol. 11, No.2, pp. 58-68.

Christensen, N. H. (1961). "Model tests with transversally loaded rigid piles in sand". *Danish Geotechnical Institute*, Copenhagen, Denmark, Bulletin No. 12, pp. 10-16.

DNV (2010). "Design of Offshore Wind Turbine Structures", *DNV-OS-J101*. Det Norske Veritas, Det Norske Veritas Classification A/S.

Gudehus, G. & Hettler, A. (1983). "Model Studies of Foundations in Granular Soil". *In Development in Soil Mechanics and Foundation Engineering*, Vol. 1, pp. 29-63.

Ibsen, L. B., Hanson, M., Hjort, T. H. & Thaarup, M. 2009. "MC parameter calibration for Aalborg University Sand No. 1". *DCE Technical Report no. 62*, Department of Civil Engineering, Aalborg University, Denmark.

Ibsen, L. B. & Lade, P. V. 1999. "Effects of nonuniform stresses and strains on measured characteristic state". *Proceedings of the second International Symposium on Pre-Failure Deformation Characteristics of Geomaterials*, Torino, Italy.

Klinkvort, R. T. & Hededal, O. 2010. "Centrifuge modelling of offshore monopile foundations". *Proceedings of International Symposium Frontiers in Offshore Geotechnics 2*, Perth, Western Australia, November 8 to 10 2010.

Kolymbas, D. & Wu, W (1990). "Recent results of triaxial tests with

granular materials". *Powder Technology*, Vol. 60, pp. 99-119.

Larsen, K. A. (2008). "Static behaviour of bucket foundations". *DCE Thesis no. 7*, Department of Civil Engineering, Aalborg University, Denmark.

Murchison, J. M. & O'Neill, M. W. (1984). "Evaluation of p-y relationships in cohesionless soils. Analysis and design of pile foundations". *Proceedings of a Symposium in conjunction with the ASCE National Convention*, New York, New York, USA, pp. 174-191.

O'Neill, M.W. & Murchison, J. M. (1983). "An Evaluation of p-y Relationships in Sands". *Research Report No. GT-DF02-83*, Department of Civil Engineering, University of Houston, Houston, Texas.

Pedersen, T. S. & Ibsen, L. B. 2009. "Manual for dynamic triaxial cell". *DCE Technical Report no. 75*, Department of Civil Engineering, Aalborg University, Denmark.

Peralta, P. & Achmus, M. (2010). "An experimental investigation of piles in sand subjected to lateral cyclic loads". *Physical Modelling in Geotechnics*, Taylor & Francis Group, London.

Reese, L. C., Cox., W. R. & Koop, F. D. (1974). "Analysis of Laterally Loaded Piles in Sand". *Proceedings of the Sixth Annual Offshore Technology Conference*, Houston, Texas, Paper no. 2080, pp. 473-483.

Sørensen, S. P. H. & Ibsen, L. B. (2011). "Small-scale quasi-static tests on non-slender piles situated in sand - Test results". *DCE Technical Report no. 112*, Department of Civil Engineering, Aalborg University, Denmark.

Title:

Experimental Comparison of Non-Slender Piles under Static Loading and under Cyclic Loading in Sand.

Authors:

Sørensen, S. P. H., and Ibsen, L. B.

Year of publication:

2012

Published in:

Accepted at the 22nd International Ocean and Polar Engineering Conference, XXII ISOPE, Rhodes, Greece.

Number of pages:

7

Title:

Revised expression for the static initial part of p–y curves for piles in sand.

Authors:

Sørensen, S. P. H., Augustesen, A. H., and Ibsen, L. B.

Year of publication:

2012

Published in:

Submitted for publication.

Number of pages:

40

Date of submission: 26th of April 2012

Title: Revised expression for the static initial part of *p-y* curves for piles in sand

Authors: Søren Peder Hyldal Sørensen[1]

Anders Hust Augustesen[2]

Lars Bo Ibsen[3]

Affiliations: [1] Ph.D. fellow, Master of Science in Civil Engineering, Department of Civil Engineering, Aalborg University, Denmark.

[2] Chief specialist in Geotechnical Engineering, Ph.D., Master of Science in Civil Engineering, COWI A/S.

[3] Professor in Civil Engineering, Department of Civil Engineering, Aalborg University, Denmark.

Contact address: Søren Peder Hyldal Sørensen, Sohngaardsholmsvej 57, 9000 Aalborg, Denmark

Telephone: +45 60755884

E-mail: sphs@civil.aau.dk

Number of words: 4945

Number of tables: 2

Number of illustrations: 18

Abstract: Monopile foundations with diameters of 4 to 6 m are often employed for offshore wind turbines. The Winkler model approach, where the soil pressure acting against the pile wall is provided by uncoupled springs with stiffnesses provided by *p*-*y* curves, is traditionally used in the design of monopiles. However, the method is developed for slender piles with diameters up to approximately 2 m when considering piles in sand. Hence, the method is not validated for piles employed for wind turbines used nowadays.

The aim of the paper is to modify the *p*-*y* curve formulation proposed by the American Petroleum Institute to large-diameter non-slender piles in sand. A modified expression for the static part of the *p*-*y* curves for piles in sand is proposed in which the initial slope of the *p*-*y* curves depends on the depth below the soil surface, the pile diameter and Young's modulus of elasticity of the soil. The reassessment of the *p*-*y* curves recommended by the American Petroleum Institute is based on three-dimensional numerical analyses conducted by means of the commercial program *FLAC*^{3D} incorporating a Mohr-Coulomb failure criterion.

List of notations:

a, b, c and d:	Dimensionless factors
A:	Dimensionless correction factor for the ultimate soil resistance
A_p:	Shear area of the pile
C_1, C_2 and C_3:	Dimensionless factors
D:	Pile diameter
D_{ref}:	Reference pile diameter
e:	Loading eccentricity
$E_{0.1}$:	Young's modulus of elasticity for the soil at a strain level of 0.1 %
E_p:	Young's modulus of elasticity of the pile
E_{py}:	Secant stiffness of *p*-*y* curves
E^*_{py}:	Initial stiffness of *p*-*y* curves, $E^*_{py} = \left.\frac{dp}{dy}\right\|_{y=0}$
E_s:	Young's modulus of elasticity of the soil
$E_{s,ref}$:	Reference value of Young's modulus of elasticity for the soil
G_p:	Shear modulus of the pile
H:	Horizontal force
I_p:	Second moment of area of the pile
L_p:	Embedded pile length
k:	Initial modulus of subgrade reaction
M:	Overturning bending moment
p:	Lateral soil resistance
p_u:	Ultimate soil resistance
P_0:	Overburden pressure
V:	Vertical force
wt:	Pile wall thickness
x:	Depth below soil surface
x_{ref}:	Reference depth below soil surface
y:	Pile deflection
γ/γ':	Unit weight/effective unit weight
δ:	Wall friction angle
ν:	Poisson's ratio
φ:	Internal friction angle
ψ:	Dilatancy angle

Keywords: Piles, soil/structure interaction, stiffness

Revised expression for the static initial part of *p-y* curves for piles in sand

1. Introduction

The monopile foundation concept is often employed in the design of offshore wind turbines. Monopiles are welded steel pipe piles driven open-ended into the soil. In order to be able to sustain the large forces and moments, the outer pile diameter, D, is typically four to six meters with an embedded pile length, L_p, in the range of 15 to 30 m. Hence, the slenderness ratio, L_p/D, is around five.

The American Petroleum Institute (API, 2000) and Det Norske Veritas (DNV, 2010), recommend to employ the Winkler model approach in the design of monopiles, i.e. the pile is considered as a beam on an elastic foundation. The elastic foundation consists of a discrete number of springs with stiffness's determined by means of *p-y* curves (Figure 1). *p-y* curves describe the variation of soil resistance, p, acting against the pile wall as a function of the lateral pile displacement, y.

For piles in sand, API (2000) and DNV (2010) recommend a *p-y* curve formulation, which is based on full-scale tests at Mustang Island (Cox et al. 1974). Two identical circular piles with diameters of 0.61 m and embedded pile lengths of 21 m were tested. This corresponds to a slenderness ratio of 34.4. A total of seven load cases were conducted; 2 static and 5 cyclic. The *p-y* curve formulation has in addition to these tests been validated for slender piles with diameters up to approximately 2 m (Murchison and O'Neill 1984). The formulation has, however, not been validated for piles with diameters of 4 to 6 m and $L_p/D \approx 5$. Hereby, the influence of pile properties such as the pile diameter, the pile bending stiffness and the pile slenderness ratio on the soil response still needs to be investigated.

In the serviceability state, only small rotations of the monopiles are allowed. Further, strict demands are set to the total stiffness of the foundation in order to avoid resonance with the wind and wave loading.

Hereby, the initial stiffness, e.g. the initial slope of the *p-y* curves, is of high importance in the design of monopile foundations for offshore wind turbines.

In the present paper, the *p-y* curve formulation recommended by API (2000) and DNV (2010) is re-evaluated for static loading conditions. The main focus is on the initial part of the *p-y* curves. In the design of offshore wind turbine foundations, the cyclic behaviour is of high interest due to the cyclic behaviour of wind and wave loads. However, the trend of the initial part of the *p-y* curves is expected to be similar for static and cyclic loading. According to Kramer (1996) the backbone curve of a soil can be described by two parameters: the initial (low-strain) stiffness and the (high-strain) shear strength. It is assumed that the soil-structure interaction similarly can be described by an initial slope, *dp*/*dy*, and an ultimate resistance. An expression of the initial slope of the *p-y* curves is proposed aiming at accurate predictions of the pile behaviour when the pile is exposed to serviceability limit state (SLS) loads. The expression is determined based on a numerical study. The effect on the pile behaviour by incorporating the modified expression for the initial slope of the *p-y* curves in a Winkler model is illustrated for a monopile foundation situated at Horns Rev, Denmark.

2. *p-y* curve formulation

API (2000) and DNV (2010) recommend the *p-y* curve formulation given in Equation 1 for piles located in sand.

$$p(y) = Ap_u \tanh\left(\frac{kx}{Ap_u} y\right) \tag{1}$$

p_u is the ultimate soil resistance, k is the initial modulus of subgrade reaction and x is the depth below the soil surface. A is a dimensionless factor depending on the loading scenario, i.e. static or cyclic:

$$A=\begin{cases}\left(3.0-0.8\dfrac{x}{D}\right)\geq 0.9 & \text{, Static loading}\\ 0.9 & \text{, Cyclic loading}\end{cases} \tag{2}$$

Based on lateral pile translation the ultimate soil resistance can in accordance with Bogard and Matlock (1980) be estimated as:

$$p_u=\min\begin{pmatrix}(C_1x+C_2D)\gamma' x\\ C_3D\gamma' x\end{pmatrix} \tag{3}$$

C_1, C_2 and C_3 are dimensionless factors varying with the internal friction angle, φ. k depends on the relative density/internal friction angle of the soil. The initial slope of the *p-y* curves denoted E^*_{py} is thereby:

$$E^*_{py}=\left.\frac{dp}{dy}\right|_{y=0}=Ap_u\left.\frac{\dfrac{kx}{Ap_u}}{\cosh^2\left(\dfrac{kx}{Ap_u}y\right)}\right|_{y=0}=kx \tag{4}$$

Hence, E^*_{py} is considered to be independent of the pile properties, e.g. the pile diameter, D, the slenderness ratio, L_p/D, and the pile bending stiffness, E_pI_p. E^*_{py} varies linearly with depth below the soil surface.

Several authors have investigated the influence of the pile diameter on E^*_{py} with contradictory conclusions. Terzaghi (1955), Ashford and Juirnarongrit (2003) and Fan and Long (2005) conclude that the pile diameter has no significant effect on the initial slope of the *p-y* curves. In contrast, Carter (1984) and Ling (1988) propose a linear dependency between pile diameter and initial stiffness.

Based on numerical investigations and a linear variation of $E_{py}{}^*$ with depth as given in Equation 4, Lesny and Wiemann (2006) conclude that the stiffness is overestimated for large depths. Instead, they propose a nonlinear variation of E^*_{py} with depth, i.e. $E_{py}{}^*$ is proportional with $x^{0.6}$.

The pile-soil interaction and pile response are affected by the flexibility of the pile. The slenderness ratio for monopiles for modern offshore wind turbines is significantly lower than the slenderness ratio for the piles

tested at Mustang Island. Therefore, monopiles used for offshore wind turbine foundations exhibit a rather stiff behaviour in contrast to the rather flexible piles tested at Mustang Island. Several authors have proposed criteria for flexible/stiff pile behaviour, i.e. Poulus and Hull (1989), Dobry et al. (1982) and Budhu and Davies (1987). According to Poulus and Hull (1989), a pile behaves as stiff or flexible when the embedded pile length, L_p, fulfils the criteria given in Equation 5 and Equation 6, respectively.

$$L_p < 1.48\left(\frac{E_p I_p}{E_s}\right)^{0.25} \qquad \text{stiff pile behaviour} \qquad (5)$$

$$L_p > 4.44\left(\frac{E_p I_p}{E_s}\right)^{0.25} \qquad \text{flexible pile behaviour} \qquad (6)$$

The Young's modulus of elasticity for the pile and the soil are denoted E_p and E_s, respectively. I_p denotes the second moment of area for a cross-section of the pile. Hence, a monopile typically employed for offshore wind turbine foundations (pile diameter, D = 4 m, wall thickness, wt = 0.05 m, and embedded pile length, L_p = 20 m) behaves rigidly when E_s < 7.6 MPa and flexible when E_s > 617 MPa. The Young's modulus of elasticity is even for dense sands normally less than 100 - 130 MPa implying more rigid pile behaviour than flexible. In contrast, the piles tested at Mustang Island behave flexible when E_s > 0.34 MPa. The sand at Mustang Island was, according to Cox et al. (1974), medium dense to dense. Hence, the two test piles clearly satisfy the criteria for flexible pile behaviour.

In conclusion, the *p-y* curve formulation currently recommended by API (2000) and DNV (2010) is at first sight not well-suited for the design of monopile foundations for offshore wind turbines due to scale effects. Knowledge is especially needed regarding the initial part of the *p-y* curves. A concise state-of-the-art review of *p-y* curves for piles in sand is presented by Sørensen et al. (2012).

3. Numerical modelling

3.1 *Establishing the numerical model*

A numerical model has been constructed in the commercial program *FLAC*^{3D} (FLAC^{3D} 3.1 manual, 2006), with the objective of determining the behaviour of monopiles exposed to static lateral loading.

Due to symmetry, only half of the soil and pile is modelled (Figure 2). The pile and the soil are divided into zones each consisting of five 4-noded constant strain-rate sub-elements of tetrahedral shape. An outer diameter of 40*D,* as proposed by Abbas et al. (2008), is used whereas the bottom boundary is placed 15 m below the pile toe. This ensures that the model boundaries do not influence the results.

For practical reasons the pile is modelled as a solid pile. Therefore, the Young's modulus of elasticity and the density of the solid pile are scaled to ensure that the bending stiffness and the weight including soil are identical to the properties of a tubular pile. The plug ratio is assumed equal to unity. The shear stiffness, A_pG_p, is not scaled correctly, which is of minor importance since bending is governing in the design of monopiles. Analyses, not presented here, show that the difference in the maximum deflections at the seabed is for a pile with L_p/D = 5 less than 2 % when comparing the results based on the solid pile model with the results obtained by means of a shell pile model reflecting the tubular pile.

The Mohr-Coulomb material model is employed for the sand. The reason for using such a simple model is that the soil parameters employed in the model can be determined from few experimental tests. Further, it is convenient to have few model parameters in a parametric study. Hence, it seems naturally to incorporate a material model with only one stiffness parameter. Achmus et al. (2009), Chik et al. (2009) and Kim and Jeong (2011) have successfully modelled horizontally loaded piles in clay and sand, respectively, by employing the Mohr-Coulomb material model for the soil. The interface between the pile and the soil is modelled by means of a linear Coulomb shear strength criterion allowing gapping and slipping between the pile and the soil.

A displacement-controlled horizontal loading is applied as a velocity to the centre nodes of the pile head. Hereby, a number of steps are prescribed in order to reach the desired pile deflection. To ensure a quasi-static behaviour of the pile-soil system, the velocity of the pile is set to 10^{-6} m/s. For piles with slenderness ratios larger than 10, numerical instability arises if displacement controlled loading is employed. Instead, the load for these piles has been applied as a load distributed evenly to all nodes at the pile head.

Damping is introduced since FLAC^{3D} is a dynamic, explicit finite difference solver. Combined damping is employed since it, according to FLAC^{3D} 3.1 manual (2006), is preferable for uniform motions. When using combined damping both the velocity and the derivative of the unbalanced force contribute to the damping force. Due to the small velocities applied, it has not been necessary to introduce absorbing model boundaries.

The numerical simulations are executed in stages. First, the initial stresses in the soil are generated using a K_0-procedure. Secondly, an equilibrium state is established for the pile and the soil in which the soil properties are employed for the pile material. At this stage, the interface between the soil and the pile is assumed smooth. Thirdly, a new equilibrium state is calculated in which the pile and the interface are given the correct properties. After reaching equilibrium, the horizontal load is applied as described.

In order to investigate the convergence of the numerical model, a pile with D = 4 m, L_p = 20 m, t = 0.05 m situated in a soil with φ = 40° and E_s = 53 MPa has been simulated. The simulation has been carried out with respectively 2660, 8022, 18828 and 67480 zones in the model. The load-displacement relationships are shown in Figure 3. It can be observed that with 18828 and 67480 elements similar results are obtained. Approximately 20000 elements are therefore used in the numerical simulations.

3.2 *Validation*

The numerical model has been validated against 23 laboratory tests conducted in a so-called pressure tank, cf. Sørensen et al. (2009) and Sørensen and Ibsen (2011). The cross-sectional view of the test setup is

shown in Figure 4. Aluminium piles with diameters of 40-100 mm and embedded pile lengths of 200-500 mm were exposed to lateral loading. The piles were embedded in saturated sand. Aalborg University Sand No. 1 (Baskarp Sand No. 15) was used for the testing and it has been rigorously tested (Ibsen et al. 2009). Prior to each test the sand was prepared by mechanical vibration. Cone penetration tests were conducted prior to each test by means of a laboratory CPT-cone. The relative density was for all the tests found to be approximately 80 %. Hence, the soil was classified as dense to very dense sand which is similar to typical compactions of offshore sand.

A rubber membrane was placed on top of the soil material sealing off the air on top of the membrane hermetically from the water in the voids of the soil material. Hereby, it was possible to increase the effective soil stresses homogeneously. The increase in effective vertical soil stresses corresponds to the application of an overburden pressure. Traditionally, significant scale-effects are present for small-scale tests at normal stress level, for instance, the friction angle of the soil is very large and the Young's modulus of elasticity for the soil is low. Further, the soil parameters will vary strongly with depth. These uncertainties are avoided when applying an overburden pressure. Application of an overburden pressure to the soil causes an unrealistic stress distribution with depth as the effective vertical stress is nonzero at the soil surface. The small-scale tests are therefore not directly scalable. When calibrating the numerical model against the small-scale tests, the actual model dimensions are employed as input to the numerical model. Further, the applied overburden pressure is also applied to the soil in the numerical model. Soil parameters determined from cone penetrations tests and triaxial tests have directly been employed in the numerical model.

Results from two tests (L_p/D = 5 and P_0 = 100 kPa in both cases but D equalling 40 mm and 100 mm, respectively) as well as load-settlement curves established by means of the FLAC^{3D} model are shown in Figure 5. A reasonable concordance between the numerical simulations and the test results has been

found, especially for y/D less than 0.25. The same tendency has been observed when comparing numerical simulations with 21 other laboratory tests (L_p/D = 5, D = 40-100 mm and P_0 = 0-100 kPa).

3.3 *Pile and soil properties*

Steel piles with pile diameters of D = 1-7 m and length of L_p = 20 m have been studied. Hence, the slenderness ratio, L_p/D, varies between 3 and 20. For practical purposes the pile wall thickness, *wt,* is assumed constant and equal to 0.05 m. This leads to bending stiffnesses, E_pI_p, varying between 3.5 GNm^2 and 1384 GNm^2. According to the criteria by Poulus and Hull (1989) the pile with D = 1 m behaves flexibly for E_s > 8.6 MPa and rigidly for E_s < 0.1 MPa and the pile with D = 7 m behaves flexibly for E_s > 3362 MPa and rigidly for E_s < 41.5 MPa. Hence, for D = 1 m flexible pile behaviour is expected while a rather rigid pile behaviour is expected for D = 7 m.

According to Klinkvort et al. (2010) the location of the force resultant, e with respect to the embedment length, L_p, influences the shape of the *p-y* curves. Normally, e/L_p is in the interval of 0.5 to 2.0 for the design load of monopiles for offshore wind turbines. In this study, e/L_p = [0.50; 0.75; 1.00; 1.50; 2.00] have been applied.

A Young's modulus of elasticity, E_p, a Poisson's ratio, ν, and a unit weight, γ, of 210 GPa, 0.3 and 77 kN/m^3, respectively, have been assumed for the steel material. A homogeneous soil is employed. The internal friction angle of the sand has been varied between φ = 30-43°. The wall friction angle, δ, between the soil and the pile is as proposed by Brinkgreve and Swolfs (2007) set to:

$$\delta = \arctan\left(\frac{2\tan(\varphi)}{3}\right) \tag{7}$$

Hereby, the wall friction angle takes values from 21° to 32°. The dilatancy angle, ψ, of the soil material is given in Equation 8 (Brinkgreve and Swolfs, 2007):

$$\psi = \varphi - 30 \ [°] \tag{8}$$

Hence, the dilatancy angle assumes values varying from zero to thirteen degrees. Young's modulus of elasticity for the soil has been varied in the range 21 to 93 MPa. For sand, Young's modulus of elasticity for the soil is typically within this range.

Generally the stiffness of sand is effective stress dependent. However, in order to decouple the influence of soil stiffness and depth below soil surface on E^*_{py}, the Young's modulus of elasticity for the soil, E_s, has been assumed constant with depth in the parametric study of parameters influencing the initial slope of the *p-y* curves.

4. Results

4.1 *Effects of L_p/D, E_pI_p, e/L_p and soil properties on the pile response*

Figure 6 and Figure 7 present pile deflections and bending moment distributions for piles with D = 1-7 m and φ = 37°, respectively. For D = 7 m the pile behaves very stiffly. In contrast, the pile with D = 1 m behaves rather flexibly. The depth to the point of zero deflection increases for increasing pile diameter. Furthermore, the depth of the maximum bending moment increases for increasing pile diameter. Since the length has been kept constant at 20 m, the slenderness ratio, L_p/D, varies as the pile diameter is varied. It can, hereby, be concluded that the slenderness ratio has a significant effect on the pile behaviour. A similar tendency has been observed for other combinations of φ, E_s and e/L_p.

Figure 8 illustrate the variation of the initial slope of the *p-y* curves, E_{py}^* with pile diameter, D, and depth below soil surface. In practice E^*_{py} has been estimated as the secant stiffness for a pile displacement of 1.5 mm. E^*_{py} is therefore considered as a parameter capturing the initial part of the *p-y* curves and not as the small strain stiffness which should be employed when considering dynamic loading. A non-linear increase of E_{py}^* can be observed for increasing depths, which is in contrast to the linear dependency proposed by API (2000) and DNV (2010). Further, E_{py}^* is found to increase for increasing pile diameter (Figure 8). In contrast, API (2000) and DNV (2010) propose that E_{py}^* is independent of the pile diameter. The rotation of the pile

causes discontinuities in the values of E_{py}^* at depths between approximately 8-17 m as the point of rotation changes with the size of loading. Therefore, values of E_{py}^* at these depths are left out in the following figures.

Figure 9, Figure 10 and Figure 11 illustrate the variation of the initial slope of the *p-y* curves, E_{py}^* with friction angle, φ, Young's modulus of elasticity for the soil, E_s, and loading eccentricity, e/L_p,, respectively. According to Figure 9, E^*_{py} is insignificantly influenced by the internal friction angle. Furthermore, Figure 10 indicates that E_{py}^* increases with increasing values of Young's modulus of the soil, E_s. However, API (2000) and DNV (2010) suggest that E^*_{py} is independent on the Young's modulus of elasticity of the soil and instead dependent on the internal friction angle. However, it should be noted that Young's modulus of elasticity of the soil and the internal friction angle are interrelated via the relative density of the sand. Figure 11 indicates that E^*_{py} is independent of the loading eccentricity for e/L_p = 0.5-2.0. The above mentioned trends have also been observed for other combinations of *D*, φ and E_s.

Figure 12 presents the influence of bending stiffness, E_pI_p, on the *p-y* curves. It can be concluded that the *p-y* curves are not influenced by E_pI_p. This is in agreement with Fan and Long (2005), but in contrast to Ashour and Norris (2000).

4.2 *Modified expression for the initial slope of the p-y curves*

Figure 8 and Figure 10 indicate that the initial slope of the *p-y* curves, E_{py}^*, depends on the depth below the soil surface, *x*, Young's modulus of elasticity for the soil, E_s, and the pile diameter, *D*. A modified expression for the initial stiffness is proposed in Equation 9.

$$E^*_{py} = a \cdot \left(\frac{x}{x_{ref}}\right)^b \cdot \left(\frac{D}{D_{ref}}\right)^c \cdot \left(\frac{E_s}{E_{s,ref}}\right)^d \tag{9}$$

b, c, and d are dimensionless constants whereas a is a constant specifying the initial stiffness for $D = D_{ref} = 1$ m, $x = x_{ref} = 1$ m and $E_s = E_{s,ref} = 1$ MPa. Further, x and D should both be inserted in meters and E_s in MPa. Values of a, b, c and d have been found to 1000 kPa, 0.3, 0.5 and 0.8, respectively.

The constants a, c and d have been determined based on least squares fitting. The constant b has due to the discontinuity of the initial stiffness around the point of zero deflection been determined by visual fitting of Equation 9 with the *FLAC*^{3D} simulations.

Figure 13 shows E^*_{py} normalized with respect to $(E_s/E_{s,ref})^{0.8}$ for varying values of Young's modulus of elasticity for the soil and $D = 4$ m. It can be observed that Equation 9 provides a reasonable description of the dependency of the internal friction angle when using $d = 0.8$. Similar results have been obtained for D = 1-7. The linear variation of E_{py}^* with depth, $b = 1$, and the non-linear expression proposed be Lesny and Wiemann (2006), $b = 0.6$, overestimates E^*_{py} for large depths.

In Figure 14, the normalised E^*_{py} for an internal friction angle of 40°, $E_s = 74$ MPa, and varying pile diameters is presented as function of depth. A constant bending stiffness has been employed. The proposed expression for E^*_{py} (Equation 9), produces a reasonable fit. The same tendency has been observed for other combinations of D, e/L_p and E_s.

The expression of E^*_{py} presented in Equation 9 is based on a parametric study in which the soil stiffness, E_s, has been assumed constant with depth. In Figure 15, the initial slope of the p-y curves determined by means of *FLAC*^{3D} and Equation 9 is compared for a situation in which the Young's modulus of elasticity for the soil is stress-dependent. Young's modulus of elasticity, E_s, has been varied with confining stress and relative density according to Equation 10 in which $\sigma'_{3,ref}$ is a reference minor effective stress of 100 kPa and E_s is given in kPa. The equation is valid for Aalborg University Sand No. 1 and it has been determined based on triaxial tests (Ibsen et al. 2009).

$$E_s = (1.15 I_D + 20000) \cdot \left(\frac{\sigma_3'}{\sigma_{3,ref}'} \right)^{0.58} \tag{10}$$

The proposed expression of E^*_{py} (Equation 9) is found to produce a reasonable fit. Hence, Equation 9 is also valid for sands with effective stress dependent stiffness.

When using Equation 9 for the initial slope of *p-y* curves for investigations of the serviceability limit state, the authors would recommend employing the initial Young's modulus of elasticity for the soil, $E_s \approx E_{0.1}$, as monopiles used as foundation for offshore wind turbines are exposed to small displacements/rotations.

5. Example - Horns Rev 1

The wind turbine considered in this example is a part of Horns Rev 1 Offshore Wind Farm, built during 2003 and located in the North Sea approximately 30 km west of Esbjerg in Denmark. The wind turbines at the site are all of the Vestas V80-2.0 MW type with a total assembly weight of 105.6 t. The hub height is 70 m above MSL and the site is dominated by westerly winds. The foundations are monopiles having a diameter of 4.0 m. A transition piece with outer diameter of 4.34 m constitutes the transition from the tower to the monopile, cf. Hald et al. (2009).

5.1 *Pile and loads conditions*

The steel monopile considered is the foundation for wind turbine 14. The outer diameter is 4 m, the length is 31.6 m and the wall thickness, wt, and thereby the bending stiffness, E_pI_p, varies along the pile as shown in Figure 16. E_p denotes Young's modulus, and I_p is the second moment of area around a horizontal axis perpendicular to the pile axis. The monopile has been driven to its final position 31.8 m below the mean sea level leading to an embedded depth of 21.9 m.

The pile behaviour is investigated corresponding to the serviceability limit state (SLS): the horizontal load H = 2.0 MN and the overturning bending moment M = 45 MNm, both acting at seabed level, whereas the vertical load is V = 5.0 MN. The SLS-loads are generated from wind and wave loading.

5.2 *Soil conditions*

The soil profile consists primarily of sand with the stratification and properties summarized in Table 1. φ is the angle of internal friction and ψ is the dilation angle. The friction angle φ is determined from cone penetration tests according to the procedure proposed by Schmertmann (1978). Apart from the silt/sand layer with organic material all other layers have relatively high angles of internal friction (36.6° < φ < 45.4°). Further, it is assumed that $\psi = \varphi - 30°$. The unit weight γ and the submerged unit weight γ' of the soil are, except in the layer including the organic material, 20 kN/m^3 and 10 kN/m^3, respectively. In the organic sand layer, γ/γ' yields 17/7 kN/m^3.

For the *FLAC*^{3D} analyses the classical Mohr-Coulomb criterion and a linear elastic material model have been combined to describe the elasto-plastic material behaviour of the soil. It is assumed that the stiffness of the soil can be represented by the secant Young's modulus E_s corresponding to an average axial strain of 0.1 % as well as Poisson's ratio v. According to Lunne et al. (1997), this level of strain is reasonably representative for many well-designed foundations. E_s is stress-dependent and it is determined according to Lengkeek (2003). Apart from the silt/sand layer with organic material, all soil layers have relatively high stiffness (100 MPa < E_s < 168.8 MPa).

The increase in effective soil stresses caused by the scour protection has not been considered in the numerical analysis.

5.3 *Results and discussion*

In Figure 17, the calculated deflections are shown for the case in which the pile is subjected to the static SLS-loads. The pile behaviour has been determined by means of *FLAC*^{3D} and the Winkler model approach

employing, respectively, the original API *p-y* curves given by Equations 1-4 (in the following denoted the API method) and the API *p-y* curves employing the modified expression for the initial stiffness given in Equation 9 (in the following denoted the modified API method). The deflection patterns predicted by *FLAC*^{3D} and the modified API method have similar shapes. The monopile behaves relatively rigid implying that a "toe kick" occurs; this is especially pronounced when considering the deflection behaviour predicted by means of *FLAC*^{3D} and the modified API method. Below 14 m the deflection pattern estimated by the API method and *FLAC*^{3D} deviate significantly. *FLAC*^{3D} estimates, for example, greater horizontal deflections at the pile toe compared to the API method (Table 2). The deviation in deflection pattern may be due to the fact that the initial stiffness, E^*_{py}, provided by the API method is overestimated at great depths. Since the API method overestimates the stiffness with depth compared to *FLAC*^{3D} and the modified API method, the depth for zero deflection predicted by the API method is located closer to the seabed (Table 2). Furthermore, the maximum horizontal deflection at seabed level determined by means of the API method is much lower compared to the deflections predicted by the other methods (Table 2). The above mentioned observations also apply for other load levels.

The three approaches predict similar distributions of the moment with depth. However, *FLAC*^{3D} estimates slightly lesser and higher moments at moderate and deep depths, respectively, compared to the API method and the modified API method. The maximum moments determined by the three approaches are almost identical (Table 2). The depths to the maximum moment are 3.4 m and 2.1 m, respectively, with *FLAC*^{3D} giving rise to the latter value.

The *p-y* curves at different depths are shown in Figure 18. Except for the depth x = 2.1 m the API method has a tendency to overestimate the soil resistance, p, at a given deflection, y, compared to the other two approaches. The pressures, estimated by means of *FLAC*^{3D}, mobilised at the depth x = 7.4 m are less than the pressures at both x = 2.1 m and x = 3.9 m for a given deflection y. This is due to the lower angle of

internal friction and the lower Young's modulus of elasticity of the third layer compared to the first layer (Table 1). The above mentioned observations also apply for other load levels and depths.

Generally, the modified API method predicts the results obtained by *FLAC*^{3D} better than the API method. The deviations, however, in the results determined by means of *FLAC*^{3D} and the modified API method may be caused by: the traditional uncertainties related to numerical modelling; shortcomings in the method proposed by Georgiadis (1983), in which layered soil profiles have been taken into account; shortcomings in the general shape of the *p-y* curves; and shortcomings in the definition of the ultimate soil resistance.

6. Conclusions

This paper considers large-diameter non-slender monopiles in sand for offshore wind turbines. In design of such piles the initial part of the *p-y* curves are especially important. A modified expression for the initial slope of the *p-y* curves has been proposed, in which the slope depends on the depth below the soil surface, the pile diameter and Young's modulus of elasticity of the soil. This is in contrast to the method recommended by the American Petroleum Institute (API) in which the initial part of the *p-y* curves is independent of Young's modulus of elasticity and the diameter. The reassessment of the *p-y* curves recommended by the API is based on three-dimensional numerical analyses and the reassessment is aiming for a better prediction of the pile behaviour, especially when exposed to SLS loads.

The differences in pile behaviour by employing a Winkler model incorporating the current *p-y* curves recommended by API and a modified version in which the expression for the initial slope of the *p-y* curves proposed in this paper is employed, respectively, has been evaluated. The assessment is based on a monopile for an offshore wind turbine at Horns Rev, Denmark. A three-dimensional numerical model of the pile at Horns Rev has also been established by means of the commercial software package *FLAC*^{3D}. Generally, the modified API method predicts the results obtained by *FLAC*^{3D} considerably better than the API method.

7. References

Abbas, J.M., Chik, Z.H. & Taha, M.R. (2008). Single pile simulation and analysis subjected to lateral load. *Electronic Journal of Geotechnical Engineering,* **13E**, 1–15.

Achmus, M., Kuo, Y.-S. & Abdel-Rahman, K. (2009). Behavior of monopile foundations under cyclic lateral load. *Computers and Geotechnics*, **36**, No. 5, 725-735.

API (2000). *Recommended practice for planning, designing, and constructing fixed offshore platforms – Working stress design, API RP2A-WSD*. American Petroleum Institute, Washington, D.C., USA, 21. Edition.

Ashford, S. A., & Juirnarongrit, T. (2003). Evaluation of pile diameter effect on initial modulus of subgrade reaction. *Journal of Geotechnical and Geoenvironmental Engineering* **129**, No. 3, 234-242.

Ashour, M., & Norris, G. (2000). Modeling lateral soil-pile response based on soil-pile interaction. *Journal of Geotechnical and Geoenvironmental Engineering* **126**, No. 5, 420-428.

Bogard, D. & Matlock, H. (1980). Simplified Calculation of p-y Curves for Laterally Loaded Piles in Sand, *Unpublished Report, The Earth Technology Corporation, Inc.,* Houston, Texas.

Brinkgreve, R. B. J. & Swolfs, W (2007). *PLAXIS 3D FOUNDATION, Material Models manual, Version 2*. PLAXIS b.v.

Budhu, M. & Davies, T. (1987). Nonlinear analysis of laterally loaded piles in cohesionless soils. *Canadian Geotechnical Journal* **24**, No. 2, 289-296.

Carter, D. P. (1984). *A non-linear soil model for predicting lateral pile response.* Civil Engineering Dept., Univ. of Auckland, New Zealand, Rep. No. 359.

Chik, Z. H., Abbas, J. M., Taha, M. R. & Shafiqu, Q. S. M. (2009). Lateral behavior of single pile in cohesionless soil subjected to both vertical and horizontal loads. *European Journal of Scientific Research* **29**, No. 2, 194-205.

Cox, W. R., Reese, L. C. & Grubbs, B. R. (1974). Field testing of laterally loaded piles in sand. *Proceedings of the Sixth Annual Offshore Technology Conference, Houston, Texas, USA,* pp. 459-464.

DNV (2010). *Design of Offshore Wind Turbine Structures, DNV-OS-J101*. Det Norske Veritas, Det Norske Veritas Classification A/S.

Dobry, R., Vincente, E., O'Rourke, M. & Roesset, J. (1982). Stiffness and damping of single piles. *Journal of Geotechnical Engineering*, **108,** No. 3, 439-458.

Fan, C. C. & Long, J. H. (2005). Assessment of existing methods for predicting soil response of laterally loaded piles in sand. *Computers and Geotechnics* **32**, 274-289.

FLAC^{3D} 3.1 manual (2006). *Fast langrangian analysis of continua in 3 dimensions*. Itasca Consulting Group Inc., Minneapolis, Minnesota, USA.

Georgiadis, M (1983). Development of p-y curves for layered soils. In *Proc. of the Conference on Geotechnical Practice in Offshore Engineering*, pp. 536–545.

Hald, T., Mørch, C., Jensen, L., Bakmar, C. L. & Ahle, K (2009). Revisiting monopile design using *p-y* curves – Results from full scale measurements on Horns Rev. *European Offshore Wind 2009, Stockholm, Sweden*. Ibsen, L. B., Hanson, M., Hjort, T. H. & Thaarup, M. (2009). MC parameter calibration for Baskarp Sand No. 15. *DCE Technical Report No. 62, Department of Civil Engineering, Aalborg University, Denmark.*

Kim, Y. & Jeong, S. (2011). Analysis of soil resistance on laterally loaded piles based on 3D soil-pile interaction. *Computers and Geotechnics* **38**, 248-257.

Klinkvort, R. T, Leth, C. T. & Hededal, O. (2010). Centrifuge modelling of a laterally cyclic loaded pile. *Proceedings of International Conference on Physical Modelling in Geotechnics, Zürich, Switzerland*, pp. 959-964.

Kramer, S. L. (1996). *Geotechnical Earthquake Engineering.* Prentice-Hall International Series in Civil Engineering and Engineering Mechanics, William J. Hall (eds.), ISBN0-13-374943-6.

Lengkeek, H.J. (2003). Estimation of sand stiffness parameters from cone resistance. *PLAXIS Bulletin No. 13*, 15–19.

Lesny, K. & Wiemann, J. (2006). Finite-element-modelling of large diameter monopiles for offshore wind energy converters, *Geo Congress 2006, Atlanta, Georgia, USA*.

Ling, L. F. (1988). *Back analysis of lateral load test on piles*. Civil Engineering Dept., Univ. of Auckland, New Zealand, Rep. No. 460.

Lunne, T., Robertson, P.K. & Powell, J.J.M. (1997). *Cone penetration testing in geotechnical practice.* Blackie Academic & Professional.

Murchison, J. M. & O'Neill, M. W. (1984). Evaluation of *p-y* relationships in cohesionless soils. Analysis and design of pile foundations. *Proceedings of a Symposium in conjunction with the ASCE National Convention, New York, New York, USA*, pp. 174-191.

Poulus, H. & Hull, T. (1989). The Role of Analytical Geomechanics in Foundation Engineering. *In Foundation Eng.: Current principles and Practices* **2**, pp. 1578-1606.

Schmertmann, J.H. (1978). *Guidelines for cone penetration test, performance and design*. US Federal Highway Administration, Washington, DC, USA , Report, FHWA-TS-78-209, 145.

Sørensen, S. P. H., Brødbæk, K. T., Møller, M., Augustesen, A. H. & Ibsen, L. B. (2009). Evaluation of the load-displacement relationships for large-diameter piles in sand. *Proceedings of the Twelfth International Conference on Civil, Structural and Environmental Engineering Computing, Funchal, Madeira, Portugal*, paper no. 244.

Sørensen, S. P. H. & Ibsen, L. B. (2011). Small-scale Quasi-static tests on non-slender piles situated in sand – Test results. *DCE Technical Report No. 112, Department of Civil Engineering, Aalborg University, Denmark.*

Sørensen, S. P. H., Brødbæk, K. T., Møller, M. & Augustesen, A. H. (2012). Review of laterally loaded monopiles employed as the foundation for offshore wind turbines. *DCE Technical Report No. 137, Department of Civil Engineering, Aalborg University, Denmark.*

Terzaghi, K. (1955). Evaluation of coefficients of subgrade reaction, *Geotechnique* **5**, No. 4, 297-326.

Table 1. Soil conditions including average values of the strength and stiffness parameters for each soil layer.

	Depth [m]	φ [°]	E_s [MPa]	ν [-]
Sand	0 - 4.5	45.4	130	0.28
Sand	4.5 - 6.5	40.7	114.3	0.28
Sand(silty)	6.5 - 11.9	38.0	100	0.28
Sand(silty)	11.9 - 14.0	36.6	104.5	0.28
Sand/silt/organic	14.0 - 18.2	27.0	4.5	0.28
Sand	18.2 →	38.7	168.8	0.28

Table 2. Comparison of the distribution of bending moment, pile deflection and pile rotation calculated by means of *FLAC*^{3D}, the API method, and the modified API method, respectively.

	FLAC^{3D}	API	Mod. API
Max. moment [MNm]	47.1	48.8	48.3
Depth max. moment [m]	2.5	3.0	2.8
Pile deflection, seabed [mm]	14.8	11.4	13.7
Pile deflection, toe [mm]	-1.0	-0.6	-2.5
Rotation, seabed [°]	0.12	0.12	0.13
Depth to zero deflection [m]	13.2	9.4	9.8

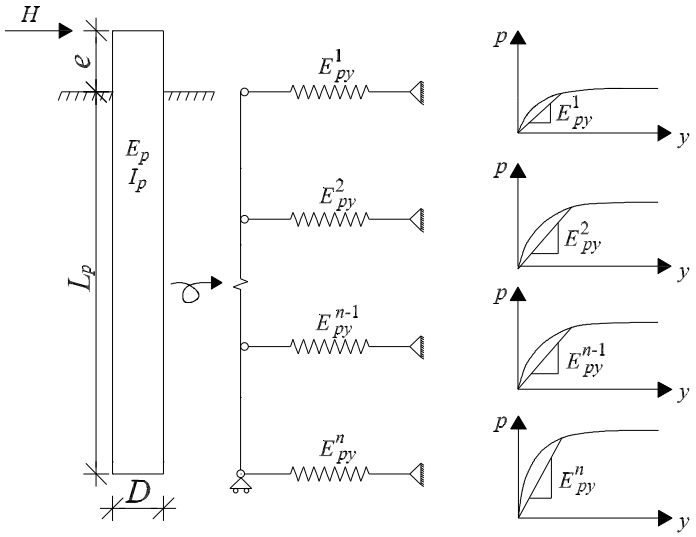

Figure 1. Winkler model approach in which a pile is modelled as a beam on an elastic foundation with spring stiffnesses given by *p*-*y* curves. The circles illustrate hinges.

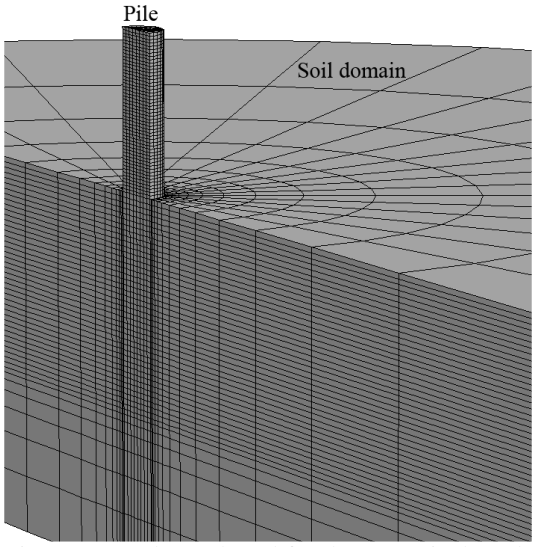

Figure 2. Mesh employed for the numerical model.

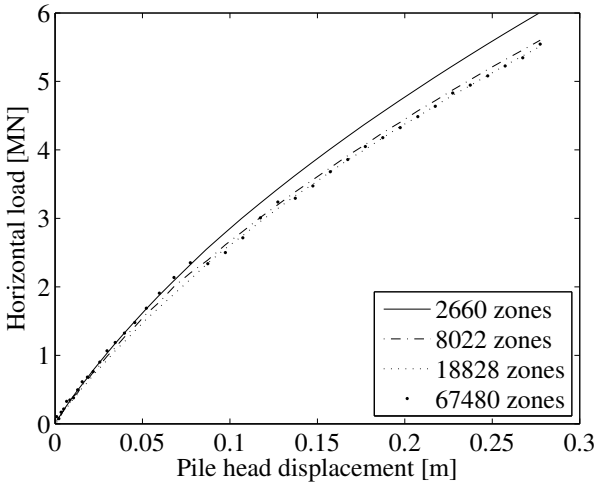

Figure 3. Load-displacement relationship for D = 4 m, L_p = 20 m, t = 0.05 m, E_s = 53 MPa and φ_{tr} = 40° obtained with 2660, 8022, 18828, and 67480 zones.

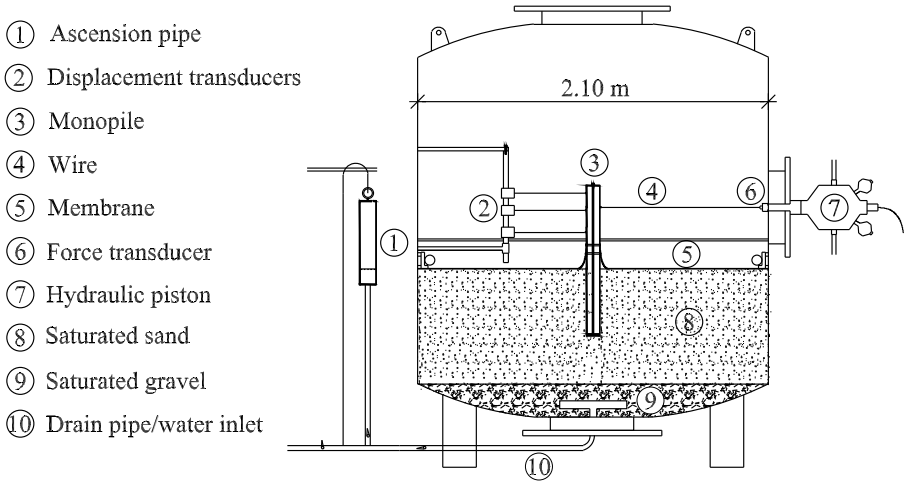

Figure 4. Cross-sectional view of the test setup, after Sørensen and Ibsen (2011).

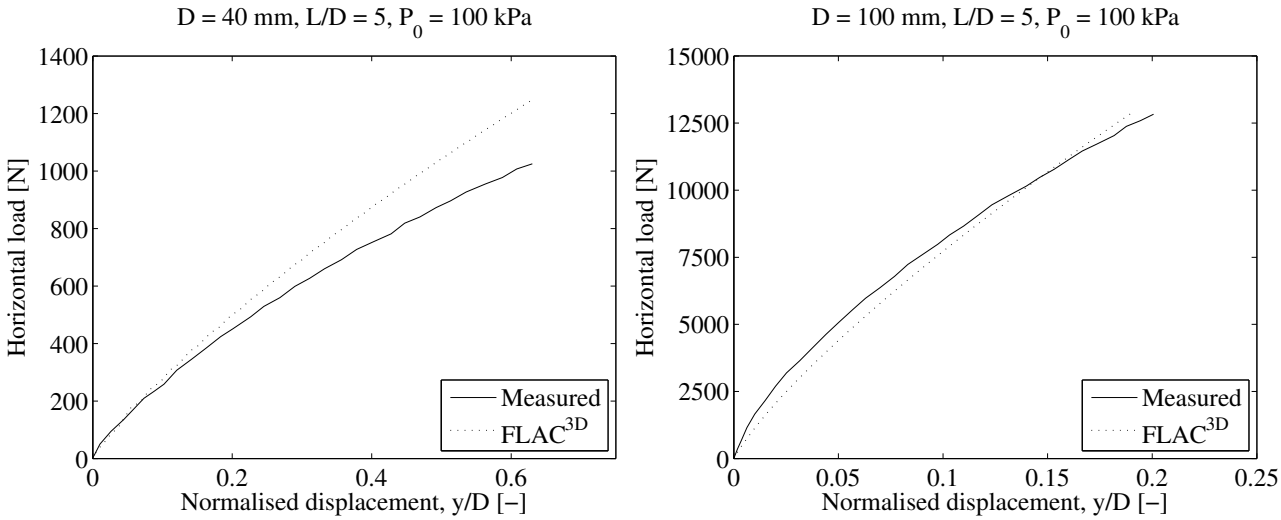

Figure 5. Comparison of numerical simulations and laboratory tests.

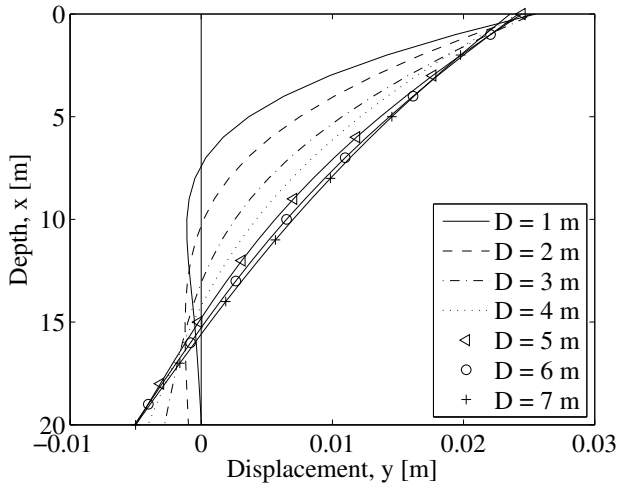

Figure 6. Pile displacement along the pile for φ_{tr} = 37°, E_s = 59 MPa, D = 1-7 m, wt = 0.05 m, L_p = 20 m and e/L_p = 0.75. The lateral pile deflection at the soil surface is for all the piles approximately 0.025 m.

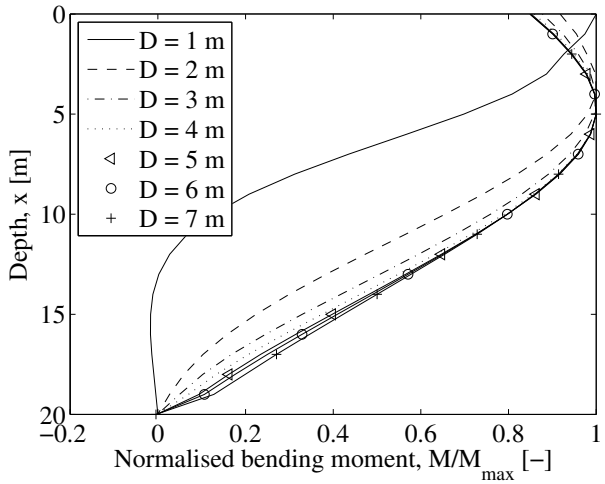

Figure 7. Distribution of bending moment. D = 1-7 m, φ = 37°, E_s = 59 MPa, wt = 0.05 m, L_p = 20 m and e/L_p = 0.75.

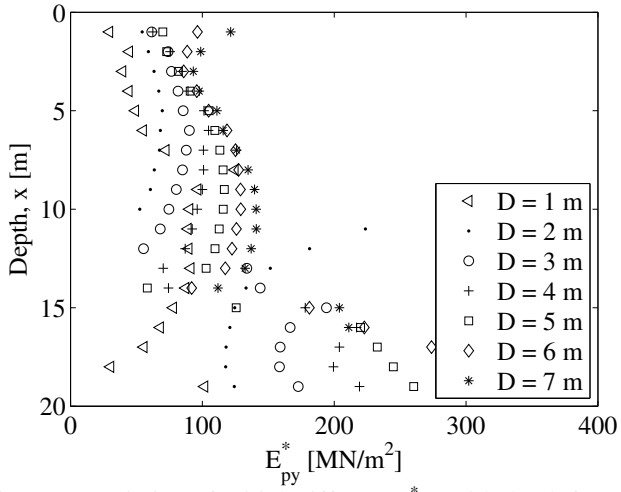

Figure 8. Variation of Initial stiffness, E^*_{py}, with depth for D = 1-7 m, φ = 37°, E_s = 59 MPa, L_p = 20 m and e/L_p = 0.75.

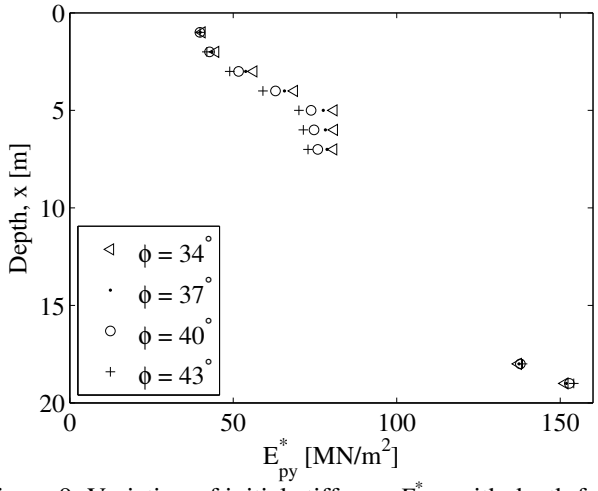

Figure 9. Variation of initial stiffness, E^*_{py}, with depth for varying internal friction angles. D = 5 m, E_s = 59 MPa, L_p = 20 m, e/L_p = 0.75.

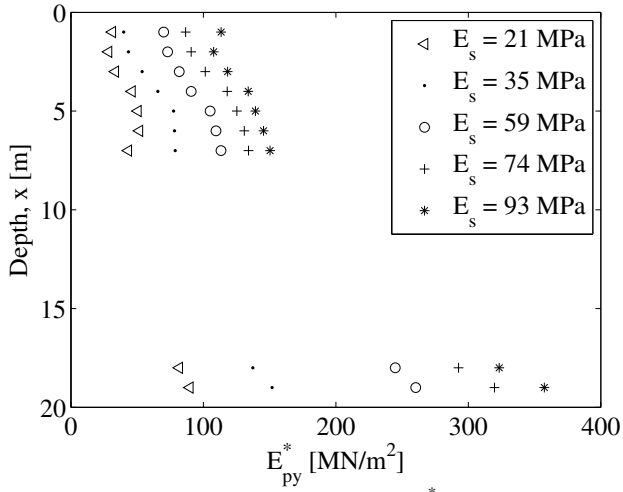

Figure 10. Variation of initial stiffness, E^*_{py}, with depth for varying values of the Young's modulus of elasticity for the soil. D = 5 m, L_p = 20 m, e/L_p = 0.75 and φ = 37°.

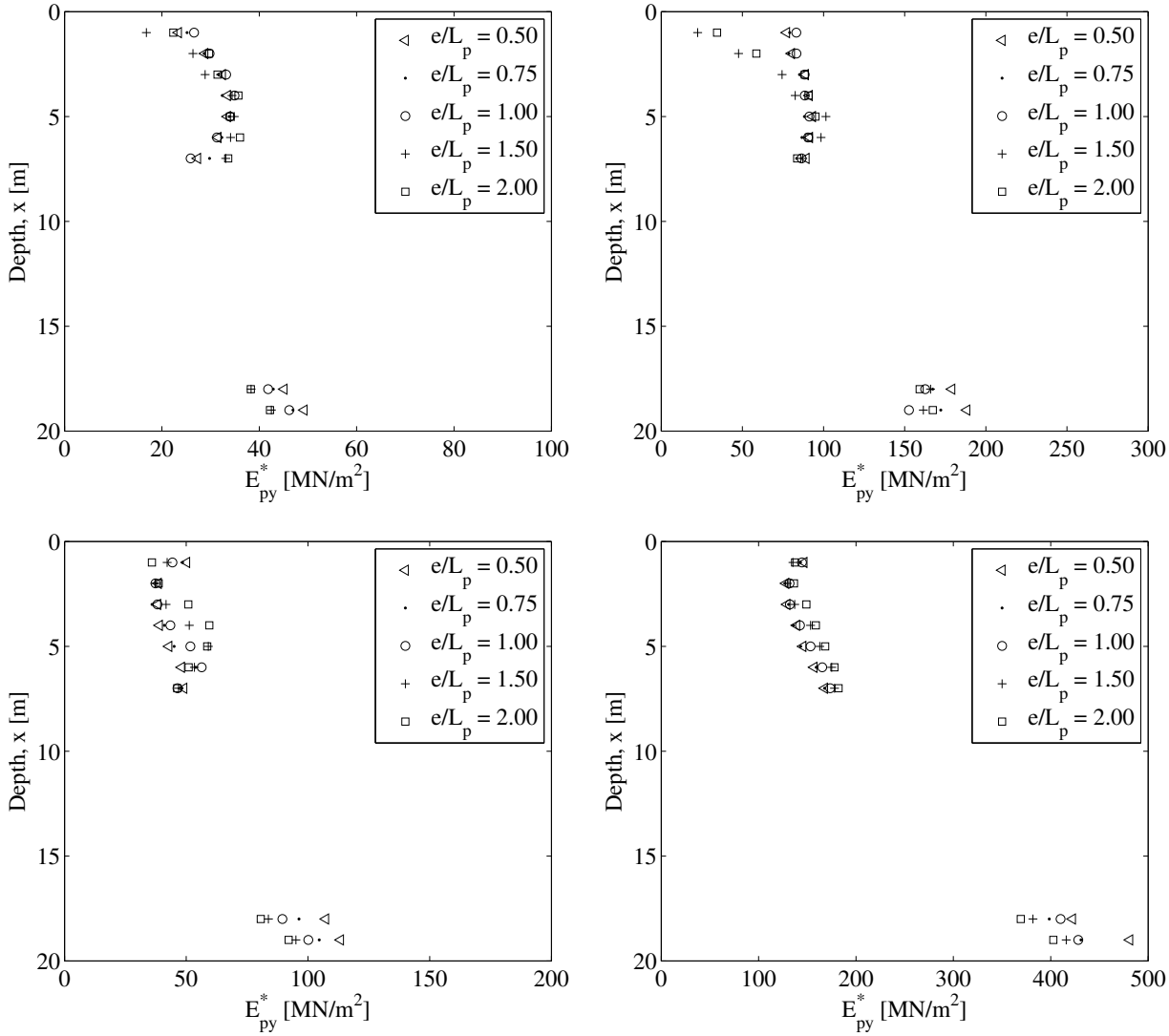

Figure 11. Variation of Initial stiffness, E^*_{py}, with depth for varying e/L_p. Top left – D = 2 m, E_s = 21 MPa, L_p = 20 m, φ = 37°. Top right – D = 2 m, E_s = 93 MPa, L_p = 20 m, φ = 37°. Bottom left – D = 6 m, E_s = 21 MPa, L_p = 20 m, φ = 37°. Bottom right – D = 6 m, E_s = 93 MPa, L_p = 20 m, φ = 37°.

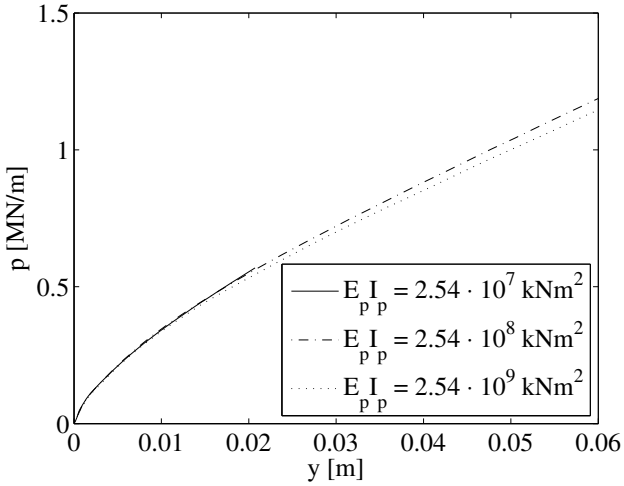

Figure 12. Comparison of *p*-*y* curves for varying pile bending stiffness. D = 4 m, φ = 40°, x = 4 m, E_s = 74 MPa, L_p = 20 m and e/L_p = 0.75.

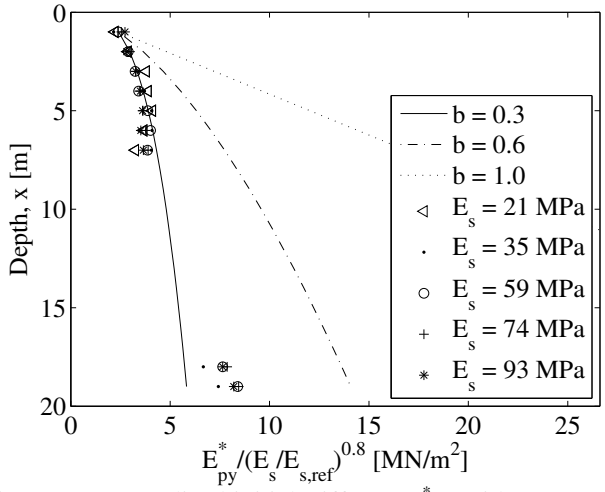

Figure 13. Normalized initial stiffness, E^*_{py}, with respect to $(E_s/E_{s,ref})^{0.8}$ for E_s = 21-93 MPa, L_p = 20 m, e/L_p = 0.75 and D = 4 m. Three continuous curves describing the variation of initial stiffness with depth are shown, b = 0.3, b = 0.6, and b = 1. All curves have been forced through the average normalised initial stiffness in a depth of 1 m.

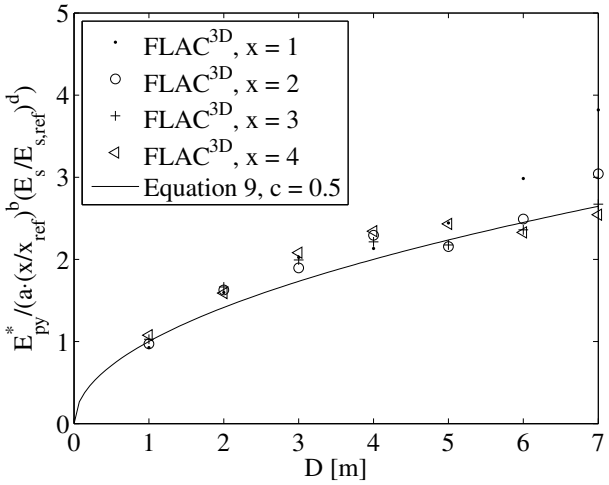

Figure 14. Normalised initial stiffness for varying pile diameter and for φ = 40°, E_s = 74 MPa, L_p = 20 m and e/L_p = 0.75. Further, the bending stiffness has been kept constant for all piles with a bending stiffness corresponding to a steel pile with a pile diameter of 4 m and a wall thickness of 0.05 m.

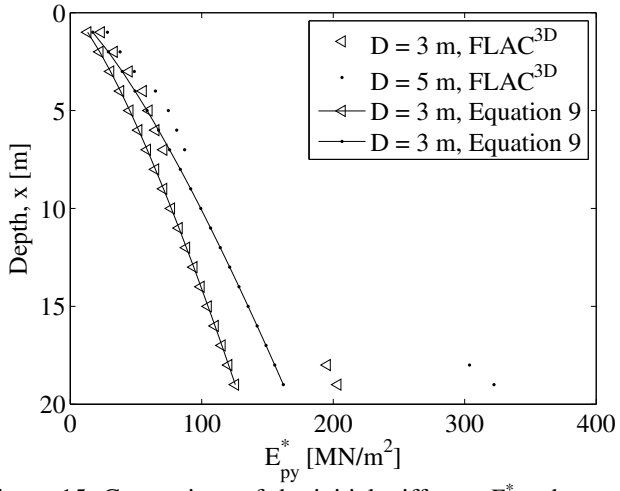

Figure 15. Comparison of the initial stiffness, E^*_{py}, determined by means of *FLAC*^{3D} and Equation 9. L_p = 20 m, *wt* = 0.05 m, e/L_p = 0.75, φ = 37° and I_D = 80 %.

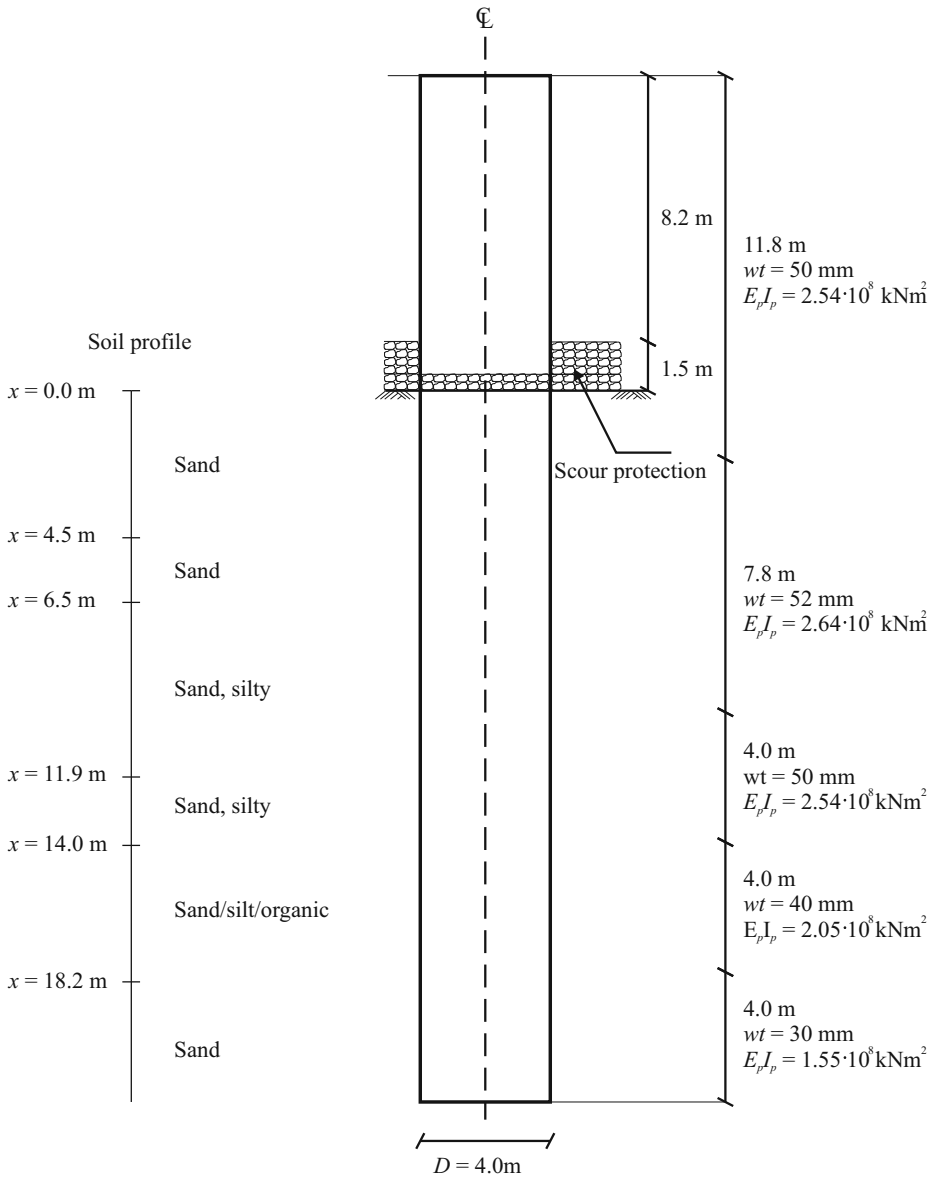

Figure 16. Geometry and pile properties of a monopile foundation employed at Horns Rev 1 offshore wind farm.

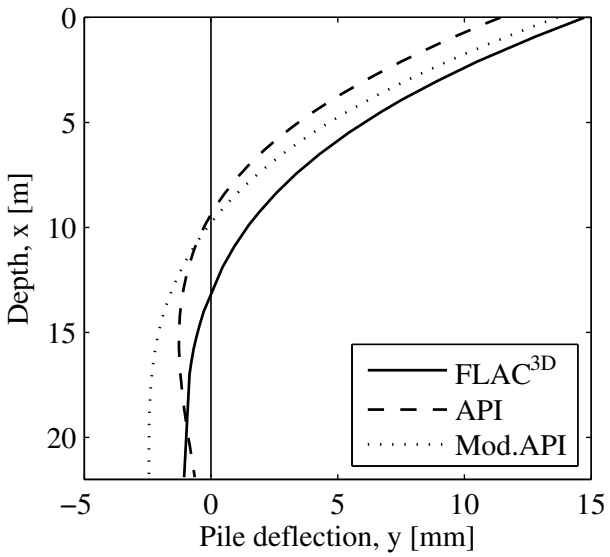

Figure 17. Pile deflections at maximum horizontal load for the monopile foundation of Wind Turbine 14 at Horns Rev 1.

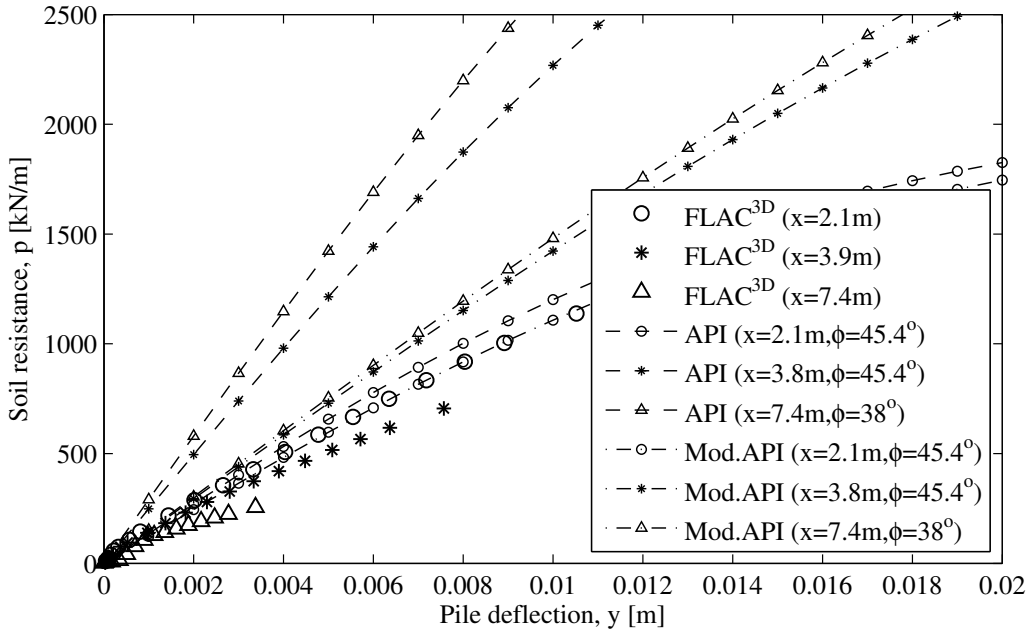

Figure 18. Soil resistance as a function of pile deflection and depth for the monopile foundation of Wind Turbine 14 at Horns Rev 1.

Title:

Experimental Evaluation of Backfill in Scour Holes around Offshore Monopiles.

Authors:

Sørensen, S. P. H., Ibsen, L. B., and Frigaard, P.

Year of publication:

2010

Published in:

In Proceedings of the 2nd International Symposium on Frontiers in Offshore Geotechnics, II ISFOG, Perth, Australia, 8-10 November 2010, Balkema Publishers, A.A. / Taylor & Francis, The Netherlands, pp. 617-622.

Number of pages:

6

Title:

Assessment of Scour Design for Offshore Monopiles Unprotected Against Scour.

Authors:

Sørensen, S. P. H., and Ibsen, L. B.

Year of publication:

2012

Published in:

Submitted for publication.

Number of pages:

42

Assessment of Scour Design for Offshore Monopiles Unprotected Against Scour

Søren Peder Hyldal Sørensen[a,*], Lars Bo Ibsen[b]

[a]*Department og Civil Engineering, Aalborg University, Sohngaardsholmsvej 57, 9000 Aalborg, Denmark, email: sphs@civil.aau.dk, tlf: +45 6075 5884, fax: +45 9940 8552*
[b]*Department og Civil Engineering, Aalborg University, Sohngaardsholmsvej 57, 9000 Aalborg, Denmark, email: lbi@civil.aau.dk*

Abstract

When designing offshore monopiles without scour protection, the stiffness of the foundation will vary with time due to the dependency of sea conditions on the scour depth. Currently, design regulations of organizations such as Det Norske Veritas (DNV) and the International Organization for Standardization (ISO) recommend the use of the most extreme local scour depth as the design scour depth. This is a conservative approach, because the scour depth depends on the sea conditions and because the equilibrium scour depth is low during moderate to extreme wave loading. In this paper the effect of using expected scour depths when designing for the ultimate limit state and the fatigue limit state are illustrated by means of a desk study.

Keywords: Scour, backfill, pile, wind turbine foundation, fatigue

1. Introduction

The monopile foundation concept is often employed as the foundation for offshore wind turbines. The monopile foundation concept consists of a steel

*Corresponding author

cylinder driven or drilled open-ended into the seabed. Typical dimensions are: pile diameters of $D = 4 - 5$ m; pile wall thicknesses of $wt \approx 50 - 120$ mm; and embedded pile lengths of $L_p = 15 - 30$ m. The monopile foundation concept has for offshore wind turbines mainly been employed in shallow waters with water depths ranging from approximately 10-25 m supporting 2-5 MW wind turbines.

Offshore wind turbine foundations are exposed to large lateral loads and overturning bending moments due to among others waves and wind. Ubilla et al. (2006) state that the design loading on a 3.5 MW offshore wind turbine is approximately 6 MN in vertical loading, 4 MN in horizontal loading and 120 MNm in overturning moment. Of these the vertical loading is considered a static load originating from the selfweight of the wind turbine and the foundation, while the horizontal loads in contrast are cyclic. The wave frequency of extreme waves is typically 0.07-0.14 Hz while the energy rich wind turbulence typically has a frequency less than 0.1 Hz. Monopile foundations for offshore wind turbines are therefore designed such that the first natural frequency lies within the rotor frequency, 1P, and the blade passing frequency, 3P. Typically, 1P lies within 0.17-33 Hz, and 3P lies within 0.5-1.0 Hz. Therefore, the first natural frequency of offshore wind turbine is required to be within a narrow range. Hence, offshore wind turbines are heavily affected of changes in the first natural frequency. Offshore wind turbines are traditionally designed for a lifetime of 20 years. During the lifetime of an offshore wind turbine approximately 100 cycles with a large load amplitude are expected and further $10^6 - 10^8$ cycles with low or intermediate load amplitude are expected. Therefore, the wind turbines and the foundation of

the wind turbines should be designed such that fatigue failure of the steel material is prevented.

Around offshore piles installed in sandy or silty soil erosion of soil material can occur leading to local scour holes. The scour depth relative to the pile diameter is primarily dependent on the Keulegan-Carpenter number. However, Shield's parameter, Froude's number, the water depth, the bed shape and the sediment dimensions also influence the scour depth. Generally, the scour depth, S, is large when currents are dominating and small when waves are dominating. Several authors have investegated scour around piles (Breuser et al., 1977; Sumer et al., 1992a,b, 1993; Whitehouse, 1998; Richardson and Davis, 2001; den Boon et al., 2004). To avoid the generation of scour holes, scour protection consisting of rock infill can be deployed around offshore monopile foundations. Deployment of scour protection is however costly. Furthermore, the deployment requires calm sea conditions. The economic feasibility of deployment of scour protection, therefore, depends on the site conditions.

When designing an offshore monopile foundation without scour protection, scour will occur and the depth of the scour hole will vary with time. Therefore, the stiffness and capacity of the foundation as well as the natural frequency of the offshore wind turbine will vary with time. DNV (2010) suggests the use of the local extreme scour depth for all investigations of the wind turbine. This seems to be a conservative estimate for both the fatigue limit state (FLS) as well as the ultimate limit state (ULS), since the scour depth generally is small when waves are dominating and large when currents are dominating. The stiffness of the foundation is hereby large when the

foundation is exposed to major loads and small when minor loads act on the foundation.

In this paper a review of the scour/backfilling phenomena is presented. Current knowledge regarding the equilibrium scour depth, the timescale of scour and backfilling, and the properties of backfilled soil material is assessed. An adaptive scour design approach is presented in which the time variation of scour depth is included in the FLS- and ULS-design. The potential savings are illustrated for a design example. The objective of the adaptive scour design approach is not to provide design methods for offshore monopiles unprotected against scour, but merely to illustrate potential savings by accounting for the variation of scour depth with the sea conditions in the design.

2. Review of scour/backfilling phenomena

Installing a vertical cylinder in the offshore environment causes significant changes to the waterflow resulting in one or more of the following phenomena: contraction of flow at the side edges of the pile; formation of a horse-shoe vortex at the base in front of the pile; formation of lee-wake vortices behind the pile; generation of turbulence; occurance of wave breaking; occurance of wave reflection; and occurence of wave diffraction. These phenomena increase the capacity of the local sediment transport causing the formation of local scour holes. Scour occurs when the near bed shear stress exceeds the critical shear stress at which sediment starts to move.

In addition to local scour natural instabilities can cause rise and fall of the seabed level, for instance, sand waves. Furthermore, scour can also occur

over a large area. These phenomena are typically denoted general scour. The present paper focuses on changes in the seabed level arising from local scour.

2.1. Equilibrium scour depth

The scour depth around offshore piles depends on the sea condition. Generally currents leads to large scour holes while waves leads to smaller scour holes. For a given sea state an equilibrium scour depth exists. The process in which the scour depth increases is denoted scouring, while the process in which the scour depth decreases is denoted backfilling.

Current induced scour has been studied extensively. Breuser et al. (1977) presented the following equation for the equilibrium scour depth, $S_{\infty,c}$, around a circular cylindar in steady currents:

$$\frac{S_{\infty,c}}{D} = \alpha \tanh\left(\frac{h}{D}\right) \tag{1}$$

where α is the depth independent equilibrium scour depth and h is the water depth. To obtain expected values of the scour depth $\alpha = 1.3$ should be employed. Høgedal and Hald (2005) suggests $\alpha = 1.75$ as a conservative design value of the current generated equilibrium scour depth. Based on physical experiments for the Q7 Offshore Wind Farm in The Netherlands, den Boon et al. (2004) adjusted Eq. (1):

$$\frac{S_{\infty,c}}{D} = \alpha K_1 \tanh\left(K_2 \frac{h}{D}\right) \tag{2}$$

where K_1 and K_1 are correction factors accounting for depth limitation and sediment grading.

Sumer et al. (1992b) determined the mean value and the standard deviation of the equilibrium scour depth from the experimental data from Breuser et al. (1977):

$$\frac{S_{\infty,c}}{D} = 1.3 \tag{3}$$

$$\sigma_{S_{\infty,c}/D} = 0.7 \tag{4}$$

Det Norske Veritas has in their design regulation DNV (2010) adopted the mean value of the equilibrium scour depth, cf. Eq. (3). The International Organization for Standardization has adopted a scour depth of $1.5D$ in their recommendations, cf. ISO (2007).

Sumer et al. (1992b) investigated scour around piles under the presence of waves. They found that the existence and the extension of both the vortex shedding at the lee side of a pile as well as the horseshoe vortex at the upstream side of the pile are governed primarily by the Keulegan-Carpenter number. The Keulegan-Carpenter number is defined as:

$$KC = \frac{U_m T}{D} \tag{5}$$

where U_m denotes the maximum value of the outer oscillatory flow velocity and T is the wave period. Sumer and Fredsøe (2001) indicate that the peak wave period, T_p, should be used for irregular waves.

The horseshoe vortex and the vortex shedding at the lee side of the pile increase the capacity of the local sediment transport. Hereby, these vortices lead to the formation of local scour holes, and the Keulegan-Carpenter number, KC, is governing for the equilibrium scour depth. Based on several

small-scale tests, Sumer et al. (1992b) proposed the following dependency between the equilibrium scour depth around a pile in waves, $S_{\infty,w}$, and the Keulegan-Carpenter number:

$$\frac{S_{\infty,w}}{D} = S_{\infty,c}\left(1 - \exp\left(-0.03(KC - 6)\right)\right), \qquad KC \geq 6 \tag{6}$$

The equilibrium scour depth increases for increasing values of KC and approaches a constant value equal to the current generated scour depth for large values of KC.

Sumer and Fredsøe (2001) investigated scour around piles in combined waves and current through experimental modelling. From their study they introduced the dimensionless parameter U_{cw}:

$$U_{cw} = \frac{U_c}{U_c + U_m} \tag{7}$$

where U_c is the undisturbed current velocity at a distance $y = D/2$ from the bed. The dimensionless parameter U_{cw} describes whether currents or waves are dominating. For a current only condition, U_{cw} takes a value of 1, and for a waves only condition, U_{cw} takes a value of 0. Based on their tests, they proposed the following expression for the equilibrium scour depth in combined waves and current:

$$\frac{S_{\infty,cw}}{D} = \frac{S_{\infty,c}}{D}\left(1 - \exp\left(-A(KC - B)\right)\right), \qquad KC \geq B \tag{8}$$

where $S_{\infty,c}$ is the equilibrium scour depth for a current dominated sea state

and A and B are constants depending on U_{cw}:

$$A = 0.03 + \frac{3}{4}U_{cw}^{2.6} \tag{9}$$

$$B = \exp\left(-4.7U_{cw}\right) \tag{10}$$

Høgedal and Hald (2005) compared data for the scour depth around existing unprotected monopiles for offshore wind turbines at the Scroby Sands Offshore Wind Farm with the expressions of Breuser et al. (1977), den Boon et al. (2004) and Sumer et al. (1992b), cf. Eq. (1), (2) and (6). They found that the equilibrium scour depth proposed by Sumer et al. (1992b) overestimates the scour depth for shallower water (h/D <3). Further, they concluded that the expressions for the equilibrium scour depth proposed by Breuser et al. (1977) and den Boon et al. (2004) provides accurate estimates of the scour depth.

2.2. Prediction of scour depth

In order to predict the scour depth accurately based on a time series with given wave and current conditions, it is necessary to have an accurate estimation of the equilibrium scour depth and further an accurate estimation of the time scale, T, of both the scour and the backfilling process. Sumer et al. (1992a) investigated the timescale of scour in waves and current through physical modelling. For currents, they presented 18 tests with pile diameters varying from 30-510 mm, while they presented 28 tests with pile diameters of 10-40 mm on the timescale for piles in waves. Based on their experiments they found that the scour depth during the scour process varies with time,

t, as follows:

$$S = S_\infty \left(1 - \exp(-t/T)\right) \tag{11}$$

where T is the time scale of scour. Sumer et al. (1992a) found that the timescale in currents is dependent on the ratio between the boundary-layer thickness, δ, and the pile diameter as well as the Shields parameter, Θ, while the time scale in waves is dependent on the Keulegan-Carpenter number and the Shields parameter:

$$T = T^* \frac{D^2}{\left(g(s-1)d\right)^{0.5}} \tag{12}$$

$$T^* = \frac{1}{2000}\frac{\delta}{D}\Theta^{-2.2} \quad , \qquad \text{current} \tag{13}$$

$$T^* = 10^-6 \left(\frac{KC}{\Theta}\right)^3 , \qquad \text{waves} \tag{14}$$

T^* denotes the normalised time scale, g denotes the acceleration due to gravity, s denotes the specific grain density and d denotes the sediment grain size. Shields parameter can be determined by:

$$\Theta = \frac{U_f^2}{(s-1)gd}, \qquad \text{current} \tag{15}$$

$$\Theta = \frac{U_{fm}^2}{(s-1)gd}, \qquad \text{waves} \tag{16}$$

where U_f is the undisturbed friction velocity and U_{fm} is the maximum value of the undisturbed bed shear velocity.

Hartvig et al. (2010) investigated both the scour and the backfilling process around piles in the offshore environment through physical modelling. Initially, they proposed Eq. (17) and (18) for the development of the scour

depth, S, with time and the scour voloume, V, with time, respectively.

$$S = S_\infty + (S_0 - S_\infty) \exp(-t/T_S) \tag{17}$$

$$V = V_\infty + (V_0 - V_\infty) \exp(-t/T_V) \tag{18}$$

S_0 denotes the initial scour depth at $t = 0$, V_0 denotes the initial scour volume at $t = 0$, V_∞ denotes the equilibrium scour volume, T_S denotes the time scale for the change in scour depth and T_V denotes the time scale for the change in scour volume. The equations account for both the scour and the backfilling process. From the physical modelling they found that initially the scour depth decreases slowly while the scour volume decreases quickly during the backfill process of a minor scour hole. In contrast, the scour depth decreases quickly while the scour volume decreases slowly during the backfill process of a large scour hole. These findings illustrate that the shape of the scour hole changes during the backfilling process. The change of the scour shape is not included in Eq. (17) and (18). In spite that Eq. (17) and (18) do not include the change of the scour shape, the equations can be a useful tool to predict the variation of scour depth or scour volume with time due to their simple structure. Hartvig et al. (2010) found that backfilling is faster for combined waves and current than for waves only. For $KC = 3$, $\Theta = 0.2$ and $D = 0.1$ m, they determined the normalised time scale for the change in scour volume, V, during backfilling in waves to 3.9. By means of Eq. (14) which was developed for the scour process, the normalised time scale, t_V, of backfilling should be 0.0034. This illustrates that the equations for the time scale of scour cannot be employed for the backfilling process. Similarly,

Fredsøe et al. (1992) found for pipelines that the time scale for the backfilling process is different from the time scale for the scour process. Hartvig et al. (2010) conducted a rather limited number of tests regarding the time scale of backfill with only one type of waves only sea condition, one type of combined waves and current sea condition and one size of pile diameter. Hence, further tests are needed for investigation of the time scale of backfill.

Sørensen et al. (2010) conducted a large-scale tests on the time scale of backfilling around a pile in waves. The pile had a diameter of 0.55 m. An irregular wave series with $KC = 9$ and $\Theta = 0.4$ was generated. The normalised time scale was found to 0.015. The Keulegan-Carpenter number and Shields Parameter for the test by Hartvig et al. (2010) and Sørensen et al. (2010) are in the same order of magnitude. However, the normalised time scale is approximately 260 times larger for the small-scale test by Hartvig et al. (2010) than for the large-scale test of Sørensen et al. (2010). This illustrates that the scaling of small scale tests on the backfilling process might be subject to uncertainties and that more research is needed regarding the backfilling process.

2.3. Properties of backfilled soil material

Sørensen et al. (2010) investigated the relative density of backfilled soil material around a pile in waves based on physical modelling. A scour hole with a scour depth of $1.3D$ was manually prepared around a pile with a diameter of 0.55 m. After the preparation of the scour hole an irregular wave series with $KC = 9$ and $\Theta = 0.4$ was generated causing backfilling. After reaching a new equilibrium scour depth, the relative density, I_D, of the backfilled soil material was determined to 65-80 % corresponding to dense

sand. Only one test concerning the relative density of backfill was conducted. Hence, the result is only indicative since the influence of several parameters needs investigation: the Shields parameter, the Keulegan-Carpenter number, the dimensionless parameter U_{cw}, the time period of backfilling, etc. The relative density of offshore sand near the mudline is often very dense, mainly due to compaction from waves (Augustesen et al., 2009). Therefore, it is expected that the relative density of the backfilled soil material compacts with time. However, the time frame needed for such a compaction is currently not known. For sand, the strength and stiffness increases for increasing values of the relative density. Therefore, the findings of Sørensen et al. (2010) indicate a significant stiffness and strength of the backfilled soil material.

3. Adaptive scour design

When designing offshore monopile foundations unprotected against scour, design regulations such as DNV (2010) and ISO (2007) recommend that the local extreme scour depth is employed as design scour depth. This, however, seems to be a conservative assumption due to the following reasons:

- Extreme local scour normally occurs for a current only situation.
- For combined waves and current and for waves only, the local equilibrium scour depth is considerably less than for current only.
- The hydrodynamic loads in ULS and FLS are mainly governed by waves.

Therefore, the local scour depth is small when the hydrodynamic loads are large, and the local scour depth is large when the hydrodynamic loads are

small.

Høgedal and Hald (2005) conducted a desk study on appropriate scour depths for the fatigue limit state (FLS) and the ultimate limit state (ULS). The Scroby Sands Offshore Wind Farm was used as reference for their desk study. They determined the equilibrium scour depth for possible combinations of the significant wave height, H_s, and the undisturbed current velocity, U_C, by means of Eq. (2) and Eq. (8). From statistical analyses they found that the scour depth should be $0.63D$, $0.05D$ and $0.61D$ for respectively FLS, ULS with extreme waves and ULS with other extreme loads. In their analyses they assumed that changes in the scour depth occured immediately. This assumption is non-conservative, which Høgedal and Hald (2005) also recognised. The large-scale test on backfill presented by Sørensen et al. (2010), however, illustrate that the backfilling process is fast for a large-scale monopile in a sea state with extreme waves. The error of not accounting for the time scale of scour and backfilling might therefore be minor. The desk study conducted by Høgedal and Hald (2005) was based on the sea conditions at the Scroby Sands Offshore Wind Farm. Hence, the design scour depths can not be employed directly for other offshore wind farms.

Combining the findings of Sørensen et al. (2010) regarding the relative density of backfilled soil material with the desk study of Høgedal and Hald (2005), the following assumptions might be reasonable for respectively FLS- and ULS-design:

- FLS - A local extreme scour hole has been developed and afterwards the scour depth has been reduced due to backfilling. The design scour depth depends on the site characteristics and can be expected to be in

the order of $0.63D$. The backfilled soil material has a relative density of 65-80 %.

- ULS, extreme waves - A local extreme scour hole has been developed and afterwards the scour depth has been reduced due to backfilling. The design scour depth depends on the site characteristics and can be expected to be in the order of $0.05D$. The backfilled soil material has a relative density of 65-80 %.

- ULS, other extreme load - A local extreme scour hole has been developed and afterwards the scour depth has been reduced due to backfilling. The design scour depth depends on the site characteristics and can be expected to be in the order of $0.61D$. The backfilled soil material has a relative density of 65-80 %.

4. Example - Design of monopile foundations for offshore wind turbines based on revised scour adaptive design approach

The potential savings by accounting for the variation of scour depth with time is illustrated for a wind turbine foundation at the Horns Rev 1 Offshore Wind Farm. The Horns Rev 1 Wind Farm is located in the North Sea west of Esbjerg, Denmark. The Wind Farm was built in 2002 and consists of 80 Vestas V80/2 MW wind turbines. Wind turbine 14 is used as example. The mean water level is 9.0 m at the location of wind turbine 14. The following five scour/backfilling conditions have been considered:

- Condition 1 - No scour has yet occured.

- Condition 2 - A local extreme scour depth of $1.3D$ is assumed for both FLS and ULS design. This assumption follows the guidelines of DNV (2010).

- Condition 3 - A local extreme scour hole with a depth of $1.3D$ has been backfilled to a scour depth of $0.63D$ and $0.05D$ for respectively FLS and ULS. The relative density of the backfilled soil material is assumed to be 0 %.

- Condition 4 - A local extreme scour hole with a depth of $1.3D$ has been backfilled to a scour depth of $0.63D$ and $0.05D$ for respectively FLS and ULS. The relative density of the backfilled soil material is assumed to be 65 %.

- Condition 5 - A local extreme scour hole with a depth of $1.3D$ has been backfilled to a scour depth of $0.63D$ and $0.05D$ for respectively FLS and ULS. The relative density of the backfilled soil material is assumed to be 80 %.

For condition 3–5 the design scour depths reported by Høgedal and Hald (2005) for the Scroby Sands Offshore Wind Farm has been adopted. These design scour depths are based on the conditions at Scroby Sands and they are therefore not applicable for the Horns Rev 1 Offshore Wind Farm. However, since the objective of the current study is merely to illustrate potential savings by accounting for the time variation of scour/backfilling they have been adopted.

The first and second natural frequency are determined for condition 1-5. Accurate predictions of especially the first and second natural frequency are

important in order to predict the magnitude of the dynamic load amplification. The fatigue life and the maximum pile stresses in the ultimate limit state during extreme waves is compared for condition 2-5.

4.1. Geometry of pile and tower

Monopiles have been employed as the foundation of the wind turbines at the Horns Rev 1 Offshore Wind Farm. These monopiles have an outer diameter of 4.0 m, a total length of 30.0-32.7 m and embedded lengths of approximately 20-25 m. Transition pieces with outer diameters of 4.34 and wall thicknesses of 0.09 m constitutes the transition between pile and tower. The wall thickness, wt, of the monopile for wind turbine 14 varies with depth as shown in fig. 1. Hereby also the pile bending stiffness, E_pI_p, varies with depth. The monopile foundation for wind turbine 14 has a length of 31.6 m and the embedded length is 21.9 m.

[Figure 1 about here.]

4.2. Soil properties

The soil properties has been determined based on an extensive test programme including geotechnical borings, cone penetration tests and triaxial tests. The soil profile at wind turbine 14 consists primarily of sand. The soil conditions and parameters are summarised in tab. 1, where φ_p denotes the peak friction angle, ψ denotes the angle of dilation and ν denotes Poisson's ratio. The friction angle has been determined based on the CPT's according to the procedure proposed by Schmertmann (1978). The dilatancy angle has been determined as:

$$\psi = \varphi_p - \varphi_c \tag{19}$$

where $\varphi_c = 30°$ denote the critical state friction angle. The effective unit weight has for all the sand layers been assumed to be $\gamma' = 10$ kN/m^3. For the organic soil layer the effective unit weight is $\gamma' = 7$ kN/m^3.

[Table 1 about here.]

4.3. Loading conditions

For an offshore wind turbine foundation, several load combinations needs to be investigated. This paper adresses two of these load combinations: the ultimate limit state with a 50-year wave height and the fatigue limit state. These two load combinations are shown in tab. 2 where N denotes the number of load cycles, M denotes the overturning bending moment, H denotes the horizontal load and V denotes the vertical load.

[Table 2 about here.]

4.4. Winkler model approach

The Winkler model approach, originally formulated by Winkler (1867), has been employed to determine the pile behaviour. In the Winkler model approach, the pile is modelled as a beam on an elastic foundation in which the interaction between pile and soil is modelled as a series of uncoupled springs. The stiffnesses of these springs is governed by the so-called p–y curves, describing the soil resistance acting on the pile wall, p, against the pile deflection, y. The Winkler model approach is illustrated in fig. 2.

[Figure 2 about here.]

The p–y curve formulation proposed by O'Neill and Murchison (1983) and validated against a database of field tests on piles in sand by Murchison and O'Neill (1984) has been employed. The formulation is a modification of the p–y curve formulation originally proposed by Reese et al. (1974). Both formulations are based on the field tests presented by Cox et al. (1974) on flexible piles. Design regulations such as API (2000), ISO (2007) and DNV (2010) has adopted the p–y curve formulation proposed by O'Neill and Murchison (1983). The p–y curve formulation is given in eq. (20)

$$p(y) = Ap_u \tanh(\frac{kx}{Ap_u}y) \tag{20}$$

A is a dimensionless correction factor depending on the type of loading and the ratio between the depth and the pile diameter. p_u is the theoretical ultimate soil resistance, k is the initial modulus of subgrade reaction and x is the depth below seabed. The initial slope of the p–y curves is governed by:

$$E^*_{py} = \frac{dp}{dy}|_{y=0} = kx \tag{21}$$

Hereby, the initial slope of the p–y curves is proportional to the depth below seabed. The initial modulus of subgrade reaction, k, and the ultimate soil resistance, p_u, both depends on the friction angle of the soil. Furthermore, p_u depends on the depth below seabed and the effective vertical stress.

The soil stratification at wind turbine 14 consists of layered soil. The p–y curve formulation proposed by O'Neill and Murchison (1983) is valid for homogeneous soils. According to Georgiadis (1983) and Yang and Jeremic (2005), the p–y curves should be modified to account for layered soils. The p–

y curves has been modified due to layered soil based on the method proposed by Georgiadis (1983) in which equivalent depths are determined for all layers beneath the upper soil layer.

The presence of scour holes is in the p–y curves accounted for by reduction of the effective soil stresses as suggested by ISO (2007) and API (2008). Hereby, the ultimate soil resistance, p_u, is reduced. The initial slope of the p–y curves is not reduced for local scouring. The reduction of the effective soil stresses is illustrated in fig. 3. Lin et al. (2010) emphasized that the soil beneath a scour hole will be overconsolidated. Taking this into account when calculating p–y curves for the interaction between pile and soil would increase the ultimate soil resistance, p_u. This phenomena has not been accounted for in the current study.

[Figure 3 about here.]

4.5. Natural frequency

The first and second undamped natural frequency has been determined for wind turbine 14 by means of the Winkler model approach. The initial slope of the p–y curves has been employed as stiffness of the soil-pile interaction. This assumption seems valid for minor vibrations of the wind turbine. For large vibrations the non-linear soil behaviour should be accounted for. In the p–y curve formulation proposed by O'Neill and Murchison (1983) cyclic loading only affects the correction factor A. Hence, the initial slope of the p–y curves does not change due to cyclic loading. LeBlanc et al. (2010) found based on small-scale tests on non-slender piles that the secant stiffness of the unloading path increases with the number of cycles. They conducted tests

on piles situated in sand with a relative density of 4-38 %. Whether their findings are valid for dense to very dense sands has not been clarified. The effect of the number of cycles on the stiffness of the soil-pile interaction has not been accounted for in the current study.

The first and second undamped natural frequency of wind turbine 14 is in tab. 3 and 4 shown for varying scour/backfilling conditions. The first natural frequency decreases with approximately 5 % when a scour hole of $1.3D$ has been formed while the second natural frequency decreases with approximately 10 %. With a scour depth of $0.63D$ corresponding to a typical scour depth during fatigue loads the first natural frequency is approximately 3 % lower than the natural frequency prior to scour, while the first natural frequency decreases with approximately 1.5 % when the scour depth is $0.05D$ corresponding to the estimate on the design scour depth for the ultimate limit state with extreme wave loads. The relative density of the backfilled soil material has a significant effect on the first and second natural frequency of the wind turbine. An increase in relative density give rise to an increase of the natural frequencies of the wind turbine.

[Table 3 about here.]

[Table 4 about here.]

4.6. ULS-design

The ultimate limit state design has been investigated for wind turbine 14 for extreme wave loading by means of the Winkler model approach. The soil parameters from tab. 1 have been implemented directly.

The pile bending moment and the maximum cross-sectional von Mises stress is in fig. 4 and fig. 5 shown for varying scour/backfilling conditions. Further, the results are summarised in tab. 5. The von Mises stresses, σ_m, is determined as:

$$\sigma_m = \sqrt{3J_2} \tag{22}$$

where J_2 is the second deviatoric stress invariant.

[Figure 4 about here.]

[Figure 5 about here.]

[Table 5 about here.]

Scour increases the maximum pile bending moment and the depth below original seabed to the maximum pile bending moment significantly. Further, the maximum cross-sectional von Mises sresses increases significantly for depths larger than 5 m due to the presence of scour. Backfilling significantly decreases the maximum cross-sectional von Mises stresses. For a depth of 10 m below the original seabed the maximum cross-sectional von Mises stress is 105.2 MPa prior to scouring, 202.3 MPa for a scour depth of $1.3D$ and 120.0 MPa when a scour hole with a depth of $1.3D$ has been beckfilled with sand material with a relative density of 80 % to a new scour depth of $0.05D$. This illustrates that the stresses in the monopile is significantly lower when employing the design scour depth proposed by Høgedal and Hald (2005) than when employing a design scour depth of $1.3D$ as recommended by DNV (2010).

4.7. FLS-design

The fatigue limit state is investigated for a longitudinal welding along the monopile. Hence, the welding is parallel to the direction of the applied stress. The welding is categorised as a category C1 welding.

In the current study on the fatigue limit state design, the dynamic amplification of stresses due to resonance has not been included. Normally, dynamic stress amplifications has a significant influence on the fatigue limit state. However, since the purpose of the study is merely to illustrate the effect on the FLS-design by adopting a design scour depth accounting for the actual variations in scour depth, the wind turbine dynamics have not been included. DNV (2011) proposes the use of S–N curves when investigating the fatigue life. S–N curves describe the number of cycles, N, at which failure occurs versus the stress level, $\Delta\sigma$. The following S–N curve can be employed for steel:

$$\log(N) = \log(\overline{a}) - m \log\left(\Delta\sigma \left(\frac{t}{t_{ref}}\right)^{k}\right) \tag{23}$$

where N is the number of cycles, $\log(\overline{a})$ is the intercept of the $\log N$ axis, m is the negative inverse slope of the S–N curve, $\Delta\sigma$ is the stress range inserted in MPa, t is the thickness through which a crack will most likely grow and t_{ref} is a reference thickness. For a steel welding of category C1 located in seawater, with cathodic protection and exposed to more than 10^6 cycles the following parameters can be adopted: $m = 5.0$, $\log(\overline{a}) = 16.081$, $t_{ref} = 25$ mm and $k = 0.15$. For the considered welding, t can be taken as the wall thickness of the pile. In the current study the stress range at failure has not

been reduced by resistance factors.

In fig. 6 and tab. 6 the maximum cross-sectional von Mises stress relative to the fatigue capacity at $N = 10^7$ cycles, $\sigma_m/\sigma_{N=10^7}$, is shown for varying scour/backfill conditions. It can be observed that for $x > 5$ m, $\sigma_m/\sigma_{N=10^7}$ is significantly affected by the scour/backfill conditions. Adopting a design scour depth of $0.063D$ and a relative density of the backfilled soil material of $I_D = 80$ % instead of adopting the extreme local scour depth of $1.3D$ in the fatigue limit state design causes a decrease in $\sigma_m/\sigma_{N=10^7}$ of 0 %, 2 %, 24 % and 37 % at depths below the original seabed of 2 m, 5 m, 10 m and 15 m, respectively.

[Figure 6 about here.]

[Table 6 about here.]

5. Conclusions

Around vertical cylinders in the offshore environment scouring will take place. Due to changing sea conditions, the scour depth will vary with time. Hereby, also the stiffness and strength of a monopile foundation in the offshore environment will vary with time. The Horns Rev 1 Offshore Wind Farm has been used as example in a desk study to illustrate potential savings by accounting for the variation in scour depth when designing monopile foundations that are unprotected from scour development. The desk study indicated that significant savings in the amount of steel material used for the foundation can be achieved if accounting for the time variation of scour depth in FLS- and ULS-design. The design scour depths adopted in the desk

study was based on the statistical wave and current data at the Scroby Sands Offshore Wind Farm. Naturally this leads to large uncertainties since the specific site conditions affects the variation of scour depht significantly. Further, the time scale of scouring and backfilling was assumed to be zero which is is a non-conservative assumption. The actual time scale of scouring and backfilling needs to be accounted for when determining design scour depths. The study therefore do not provide guidelines for the design of monopile foundations exposed to scour. However, the desk study illustrates that further research regarding backfilling can lead to significant savings. Especially the following issues needs further investigation:

- The time scale of backfilling needs further investigation. Untill now the time scale has only been investigated for a limited variation of parameters such as the Keulegan Carpenter number, the Shields parameter, the current velocity, etc.

- Since the strength and stiffness of cohesionless materials are highly dependent on the relative density, the relative density of backfilled soil material needs to be studied comprehensively. The effect of parameters such as the Keulegan-Carpenter number, the Shields parameter, the current velocity, the grain size distribution and the time of backfilling on the relative density needs to be investigated.

- The scaling of small-scale tests on backfilling needs further investigation. The time scale of backfill found from the small-scale tests reported by Hartvig et al. (2010) deviate from the time scale found from large-scale tests reported by Sørensen et al. (2010). For the two tests the

Keulegan-Carpenter number and the Shields parameter were of similar magnitude. Whether, the deviation is due to scale effects needs further investigation.

References

API, 2000. Recommended Practice for Planning, Designing, and Constructing Fixed Offshore Platforms - Working Stress Design, API RP2A-WSD. American Petroleum Institute, Washington D.C.. 21 edition.

API, 2008. Errata and Supplement 3 for: Recommended Practice for Planning, Designing, and Constructing Fixed Offshore Platforms - Working Stress Design. American Petroleum Institute, Washington D.C.

Augustesen, A.H., Brødbæk, K.T., Møller, M., Sørensen, S.P.H., Ibsen, L.B., Pedersen, T.S., Andersen, L., 2009. Numerical modelling of large-diameter steel piles at horns rev, in: Proc. of the Twelfth Int. Conf. on Civil, Structural and Environmental Eng. Computing, Funchal, Madeira, Portugal.

den Boon, J.H., Sutherland, J., Whitehouse, R., Soulsby, R., Stam, C.J.M., Verhoeven, K., Høgedal, M., Hald, T., 2004. Scour behaviour and scour protection for monopile foundations of offshore wind turbines, in: Proc. of EWEC 2004.

Breuser, H., Nicolett, G., Shen, H., 1977. Local scour at cylindrical piers. J. of Hydraulic Research 15, 211–252.

Cox, W.R., Reese, L.C., Grubbs, B.R., 1974. Field testing of laterally loaded

piles in sand, in: Proc. of the Sixth Annual Offshore Technology Conf., Houston, Texas, USA. p. paper no. OTC 2079.

DNV, 2010. Design of Offshore Wind Turbine Structures - Offshore Standard, DNV-OS-J101. Det Norske Veritas, Norway.

DNV, 2011. Fatigue Analysis Based on S-N Data - Recommended Practice, DNV-RP-C203. Det Norske Veritas, Norway.

Fredsøe, J., Sumer, B.M., Arnskov, M.M., 1992. Time scale for wave/current scour below pipelines. Int J. of Offshore and Polar Eng. 1, 13–17.

Georgiadis, M., 1983. Development of p-y curves for layered soils, in: Proc. of the Conf. on Geotechnical Practice in Offshore Eng., ASCE, pp. 536–545.

Hartvig, P.A., Thomsen, J.M., Andersen, T.L., 2010. Experimental study of the development of scour & backfilling. Coastal Eng. J. 52, 157–194.

Høgedal, M., Hald, T., 2005. Scour assessment and design for scour for monopile foundations for offshore wind turbines, in: Proc. of Copenhagen Offshore Wind, Copenhagen, Denmark.

ISO, 2007. Petroleum and natural gas industries - Fixed steel offshore structures. Int. Organization for Standardization, ISO 19902:2007 (E).

LeBlanc, C., Houlsby, G.T., Byrne, B.W., 2010. Response of stiff piles to long-term cyclic loading. Geotechnique 60, 79–90.

Lin, C., Bennett, C., Han, J., Parsons, R.L., 2010. Scour effects on the response of laterally loaded piles considering stress history of sand. Computers and Geotechnics 37, 1008–1014.

Murchison, J.M., O'Neill, M.W., 1984. Evaluation of p-y relationships in cohesionless soils. analysis and design of pile foundations, in: Proc. of a Symp. in conjunction with the ASCE National Convention, pp. 174–191.

O'Neill, M.W., Murchison, J.M., 1983. An Evaluation of p-y Relationships in Sands. Research Report No. GT-DF02-83, Dep. of Civil Eng., University of Houston, Texas, USA.

Reese, L.C., Cox, W.R., Koop, F.D., 1974. Analysis of laterally loaded piles in sand, in: Proc. of the Sixth Annual Offshore Technology Conf., Houston, Texas, USA. p. paper no. OTC 2080.

Richardson, E.V., Davis, S.R., 2001. HEC-18. Evaluating Scour at Bridges. 18, National Highway Institute, Federal Highway Administration, U.S. Dep. of Transportation. 4 edition.

Schmertmann, J.H., 1978. Guidelines for cone penetration test, Performance and Design, Report, FHWA-TS-78-209, 145. US Federal Highway Administration, Washington, DC, USA.

Sørensen, S.P.H., Ibsen, L.B., Frigaard, P., 2010. Experimental evaluation of backfill in scour holes around offshore monopiles, in: Proc. of the Second Int. Symp. on Frontiers in Offshore Geotechnics, Perth, Western Australia, Australia. pp. 617–622.

Sumer, B.M., Christiansen, N., Fredsøe, J., 1992a. Time scale of scour around a vertical pile, in: Int. Offshore and Polar Eng. Conf., San Francisco, USA. pp. 308–315.

Sumer, B.M., Christiansen, N., Fredsøe, J., 1993. Influence of cross section on wave scour around piles. J. Waterway, Port, Coastal and Ocean Eng. 119, 477–495.

Sumer, B.M., Fredsøe, J., 2001. Scour around pile in combined waves and current. J. of Hydraulic Eng. 127, 403–411.

Sumer, B.M., Fredsøe, J., Christiansen, N., 1992b. Scour around vertical pile in waves. J. Waterway, Port, Coastal and Ocean Eng. 118, 15–31.

Ubilla, J., Abdoun, T., Zimmie, T., 2006. Application of in-flight robot in centrifuge modeling of laterally loaded stiff pile foundations, in: Proc. of the Sixth Int. Conf. on Physical Modelling in Geotechnics, London, England. pp. 259–264.

Whitehouse, R.J.S., 1998. Scour at marin structures: A manual for practical applications. Thomas Telford Publications.

Winkler, E., 1867. Die lehre von elasticzitat und festigkeit (on elasticity and fixity).

Yang, Z., Jeremic, B., 2005. Study of soil layering effects on lateral loading behavior of piles. J. of Geotechnical and Geoenvironmental Eng., ASCE 131, 762–770.

List of Figures

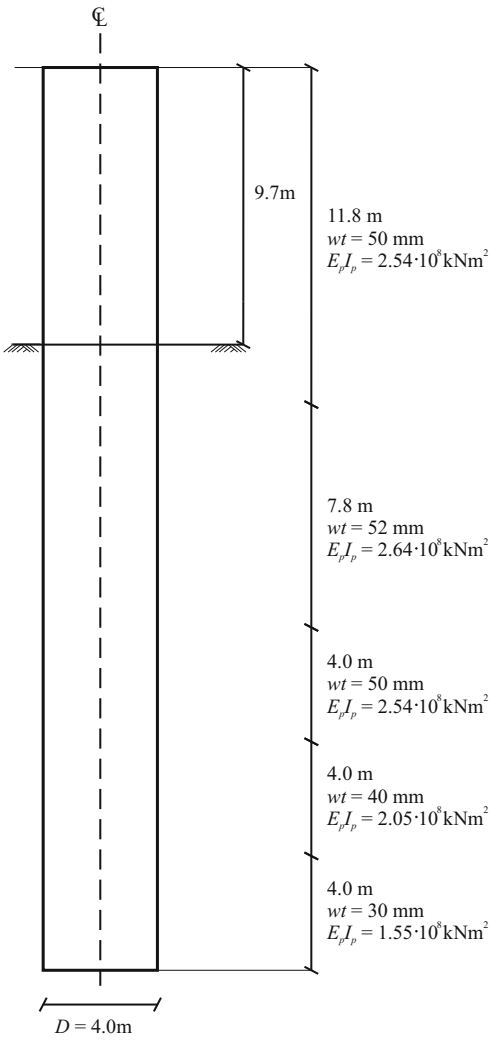

Figure 1: Details of the monopile foundation for wind turbine 14 at the Horns Rev 1 Offshore Wind Farm.

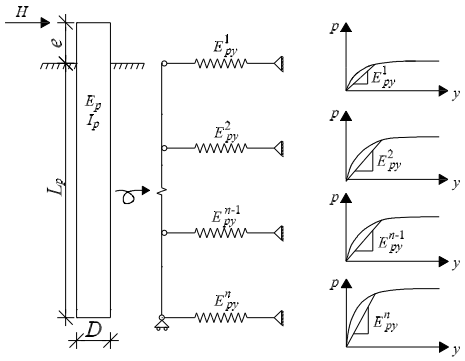

Figure 2: Winkler model approach

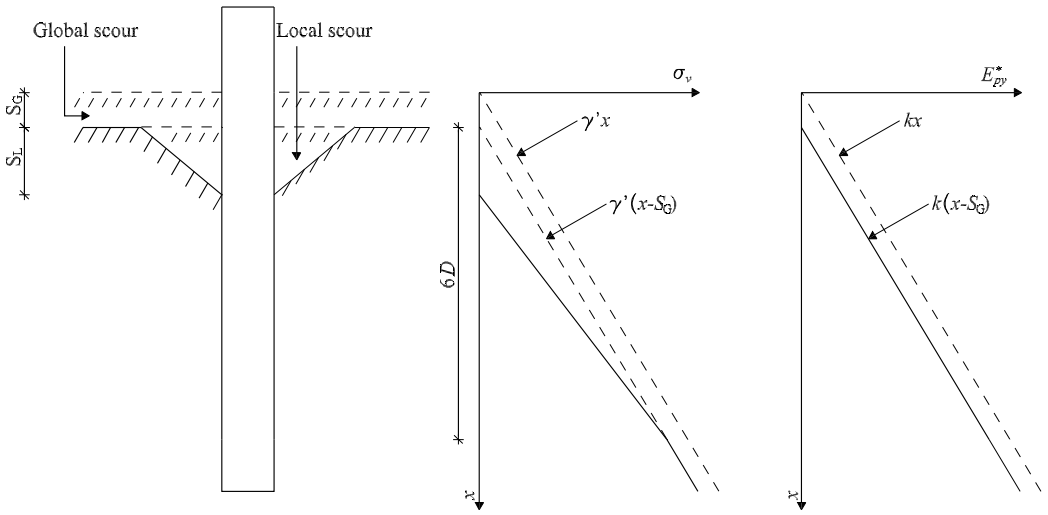

Figure 3: Reduction of effective soil stresses due to the presence of scour, after ISO (2007) and API (2008). S_G denotes the scour depth due to general scour and S_L denotes the scour depth due to local scour.

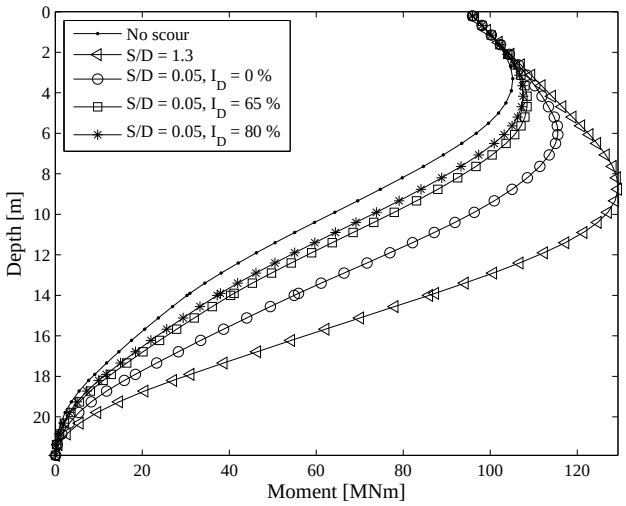

Figure 4: Distribution of bending moment, M, under ULS-load for varying scour/backfilling conditions.

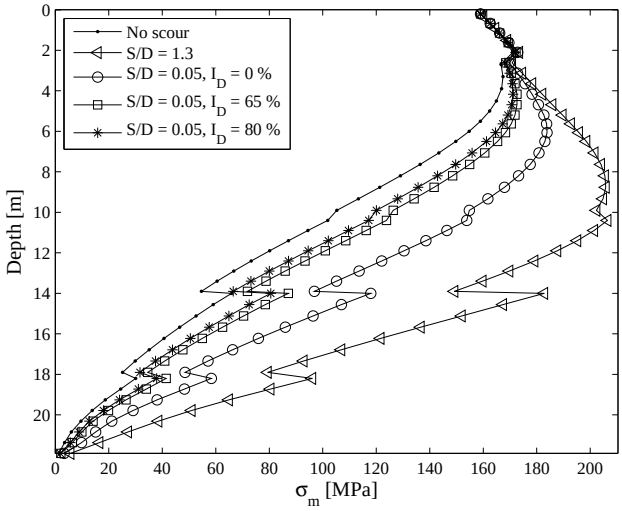

Figure 5: Distribution of maximum cross-sectional von Mises stress, σ_m, under ULS-load for varying scour/backfilling conditions.

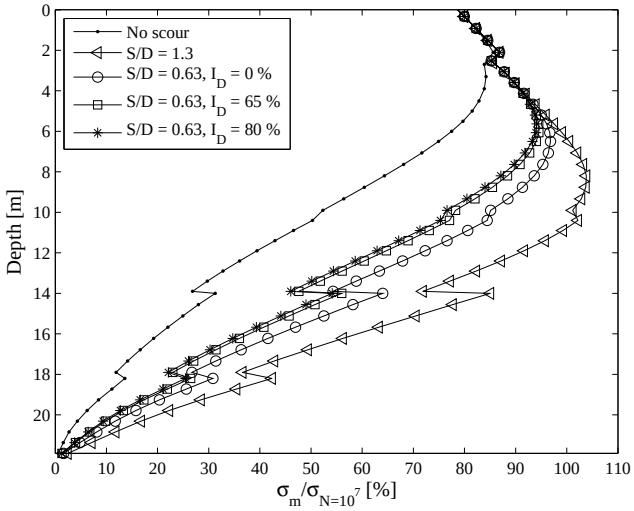

Figure 6: Variation with depth for the maximum cross-sectional von Mises stress relative to the fatigue capacity at $N = 10^7$ cycles for varying scour/backfilling conditions.

List of Tables

Table 1: Soil profile with average values of the soil parameters for each soil layer.

Soil layer	Description	Depth [m]	φ_p [°]	ψ [°]	ν [-]
1	Sand	0-4.5	45.4	15.4	0.28
2	Sand	4.5-6.5	40.7	10.7	0.28
3	Sand to silty sand	6.5-11.9	38.0	8.0	0.28
4	Sand to silty sand	11.9-14.0	36.6	6.6	0.28
5	Sand/silt/organic	14.0-18.2	27.0	0.0	0.28
6	Sand	18.2-	38.7	8.7	0.28
Backfill 1	Sand, $I_D = 0$ %		27.0	0.0	0.28
Backfill 2	Sand, $I_D = 65$ %		36.8	6.9	0.28
Backfill 3	Sand, $I_D = 80$ %		39.0	9.0	0.28

Table 2: Design loads at the seabed for wind turbine 14.

	N	M [MNm]	H [MN]	V [MN]
ULS, extreme waves	1	95.0	4.6	5.0
FLS	10^7	28.0	1.4	5.0

Table 3: The first natural frequency, $f_{n,1}$, and the change in $f_{n,1}$ due to scour/backfilling. The relative density in the table relates to the relative density of the backfilled soil material.

	$\frac{S}{D}=0$	$\frac{S}{D}=1.3$	$\frac{S}{D}=0.05$, $I_D=0$ %	$\frac{S}{D}=0.05$, $I_D=65$ %	$\frac{S}{D}=0.05$, $I_D=80$ %	$\frac{S}{D}=0.63$, $I_D=0$ %	$\frac{S}{D}=0.63$, $I_D=65$ %	$\frac{S}{D}=0.63$, $I_D=80$ %
$f_{n,1}[Hz]$	0.293	0.279	0.281	0.288	0.290	0.280	0.285	0.286
Change [%]	0.000	-5.046	-4.364	-1.671	-1.125	-4.569	-2.966	-2.591

Table 4: The second natural frequency, $f_{n,2}$, and the change in $f_{n,2}$ due to scour/backfilling. The relative density in the table relates to the relative density of the backfilled soil material.

	$\frac{S}{D} = 0$	$\frac{S}{D} = 1.3$	$\frac{S}{D} = 0.05$, $I_D = 0$ %	$\frac{S}{D} = 0.05$, $I_D = 65$ %	$\frac{S}{D} = 0.05$, $I_D = 80$ %	$\frac{S}{D} = 0.63$, $I_D = 0$ %	$\frac{S}{D} = 0.63$, $I_D = 65$ %	$\frac{S}{D} = 0.63$, $I_D = 80$ %
$f_{n,2}$ [Hz]	1.626	1.458	1.478	1.566	1.586	1.473	1.524	1.537
Change [%]	0.000	-10.357	-9.127	-3.696	-2.472	-9.410	-6.286	-5.468

Table 5: Comparison of maximum pile bending moment, M_{max}, depth to maximum pile bending moment and maximum cross-sectional von Mises stress, σ_m, under ULS-load for varying scour/backfilling conditions.

	M_{max}	Depth for M_{max}	σ_m			
			$x = 2$ m	$x = 5$ m	$x = 10$ m	$x = 15$ m
	[MNm]	[m]	[MPa]	[MPa]	[MPa]	[MPa]
No scour	105.2	3.3	171.0	162.4	105.2	52.6
$S/D = 1.3$	129.3	8.8	206.5	189.6	202.3	152.0
$S/D = 0.05$, $I_D = 0$ %	115.5	6.1	173.4	182.7	154.8	96.4
$S/D = 0.05$, $I_D = 65$ %	108.5	4.7	172.2	171.8	126.3	70.4
$S/D = 0.05$, $I_D = 80$ %	107.6	4.2	172.0	169.2	120.0	64.9

Table 6: Maximum cross-sectional von Mises stress relative to the fatigue capacity at $N = 10^7$ cycles.

	$\sigma_m/\sigma_{N=10^7}$			
	$x = 2$ m [%]	$x = 5$ m [%]	$x = 10$ m [%]	$x = 15$ m [%]
No scour	85.6	81.5	52.3	24.9
$S/D = 1.3$	86.9	95.9	101.2	70.5
$S/D = 0.63$, $I_D = 0$ %	86.9	95.0	85.1	52.5
$S/D = 0.63$, $I_D = 65$ %	86.9	94.0	78.3	45.7
$S/D = 0.63$, $I_D = 80$ %	86.9	93.8	76.6	44.1